PHOTODETECTION OF ZINC OXIDE NANOSTRUCTURES: MORPHOLOGICAL DEPENDENCE

Thesis is submitted in partial fulfilment of the requirement for the degree of

MASTERS IN LASER TECHNOLOGY

By:

SWAGATA DAS

Examination Roll No.:**M4LST22005**

Registration No.: **154560 of 2020-21**

Under the guidance of:

Prof. Chandan Kumar Ghosh and Prof. Siddhartha Bhattacharyya

School of Laser Science and Engineering

Faculty Of Interdisciplinary Studies, Law and Management

Jadavpur University

Kolkata-700032

June 2022

FACULTY OF INTERDISCIPLINARY STUDIES, LAW AND MANAGEMENT

SCHOOL OF LASER SCIENCE AND ENGINEERING

JADAVPUR UNIVERSITY

KOLKATA -700032

DECLARATION OF ORIGINALITY AND COMPLIANCE OF ACADEMIC ETHICS

I hereby declare that this thesis contains literature survey and original research work by the undersigned candidate, as part of her Masters in Laser Science and Engineering studies.

All information in this document have been obtained and presented accordance with academic rules and ethical conduct.

I also declare that, as required by these rules and conduct, I have fully cited and referred all material and results that are not original to this work.

Name: SWAGATA DAS

Examination Roll Number: M4LST22005

Registration Number: 154560 of 2020-21

Thesis Title: PHOTODETECTION OF ZINC OXIDE NANOSTRUCTURES: MORPHOLOGICAL DEPENDENCE

Signature:

Dated:

FACULTY OF INTERDISCIPLINARY STUDIES, LAW AND MANAGEMENT

JADAVPUR UNIVERSITY

KOLKATA -700032

CERTIFICATE OF APPROVAL*

This foregoing thesis is hereby approved as a credible study of an engineering subject carried out and presented in a manner satisfactory to warrant its acceptance as a prerequisite to the degree for which it has been submitted. It is understood that by this approval the undersigned do not endorse or approve any statement made, opinion expressed or conclusion drawn therein but approve the thesis only for the purpose for which it has been submitted.

Committee On Final Examination for Evaluation of Thesis

Signature:

Date:

Seal:

Signature:

Date:

Seal:

Signature:

Date:

Seal:

*Only in case the thesis is approved

FACULTY OF INTERDISCIPLINARY STUDIES, LAW AND MANAGEMENT

JADAVPUR UNIVERSITY

CERTIFICATE OF SUPERVISION

We hereby recommend that the thesis presented by Miss. SWAGATA DAS entitled **"PHOTODETECTION OF ZINC OXIDE NANOSTRUCTURES: MORPHOLOGICAL DEPENDENCE"** was under our supervision and is accepted in partial fulfilment of the degree of Masters in Laser Technology.

(Thesis Adviser)

Date:

Seal:

(Thesis Adviser)

Date:

Seal:

Countersigned by:

(Director)

(School of Laser Science and Engineering)

Date:

Seal:

(Dean)

(Faculty Of Interdisciplinary Studies, Law and Management)

Date:

Seal:

There is a crack in everything, that's how the light goes in.

-Leonard Cohen

LIST OF FIGURES

LIST OF TABLES

LIST OF FLOWCHARTS

Dedicated to My Parents, My Guides & My Little Brother

ACKNOWLEDGEMENTS

"Work" is a joint endeavour that requires togetherness not only in respect of stretching out our hands towards it but also the knowledge and experience that builds up its foundation. In this section, I am overwhelmed in all humbleness and gratefulness to acknowledge my depth to all those who have helped me to put these ideas, well above the level of simplicity and into something concrete.

I would like to express my gratitude to my guide, Professor **Chandan Kumar Ghosh** for his strong support, patience and constant availability for technical discussions. I would like to express my particular gratitude to another guide, Professor **Siddhartha Bhattacharyya** for being my well-wisher and rendering continuous support during my thesis work. I am grateful to both of my supervisors for guiding me during the entire course of research work with their valuable suggestions.

I would also like to express my sincere gratitude to Professor **Dipten Misra**, for his constant patience, guidance and ideas without which completion of this thesis would have been impossible.

I would like to thank all the faculty members of the **School of Materials Science & Nanotechnology, Jadavpur University, Kolkata**, for giving me the opportunity to carry out my MTech thesis work.

I render my heartiest thanks to the faculty members of the **School of Laser Science and Engineering, Jadavpur University, Kolkata** for giving me academic guidance throughout my M. Tech course in different subjects, the cumulative knowledge of which has helped me to complete the thesis work more effectively.

I express my thanks to **Mr. Pankaj Kr. Bhadra**, **Sk Najes Riaz, Dimitra Das, Ankita Chandra and Nibedita Halder** from the School of Materials Science & Nanotechnology for carrying out the FTIR characterization, PL characterization, DRS characterization, I-V characterization and synthesis process respectively of my sample that led to the timely completion of my thesis.

This thesis is the outcome of the kind co-operation, good-will, technical and beyond technical support extended by my dear friends **Md Rakim, Tanay Toppo, Md Imran Ansari and Manas Thakur.**

I would like to thank my **Seniors** as well as **Juniors** from the **School of Materials Science & Nanotechnology** and the **School of Laser Science and Engineering** for their moral supports throughout the duration of the project

Most of all, my deepest appreciation goes to **My Parents** for their faith, unyielding unconditional love, support, encouragement and quiet patience.

Last but not the least, I am grateful to have the most precious support system of my life **My Little Brother** whose motivation, encouragement and love has helped me to reach to this position.

ABSTRACT

The significant increase in global energy consumption and population over the last decade has prompted the development of energy-efficient, long-term and optical energy detection systems. UV photodetectors are one of the energy detection systems that has sparked interest in society, science and military defence. Due to the wide range of applications that photodetectors have in modern society; the research community is currently focusing on the development of ultraviolet (UV) photodetectors. For UV detection, a variety of wide-band gap nanomaterials were used to achieve higher photosensitivity. Wide band gap semiconductors, like ZnO, have unique optoelectronic properties that have led to a variety of sensor and optoelectronic applications. Due to their unique properties resulting from the reduction of material size from the macro to the nano scale, ZnO has become more popular for use in a variety of consumer products. The development of various methods for synthesising ZnO nanomaterials, as well as their application in various fields, has received a lot of attention in recent years. The ability to control properties, reproducibility, repeatability, low cost, short synthesis time, purity, and compliance with the eco-friendly approach are some of the advantages of using a hydrothermal process to obtain ZnO nanomaterials. The dynamic development of nano-engineering necessitates the development of ZnO nanomaterials with precisely defined properties.

Low temperature hydrothermal technique was carried out at 100°C to grow ZnO nanoparticle thin films on the conducting side of PET substrate for 3 hours with different variations in the concentration of reagents and with variation in pH. The work has been carried out considering two reagents namely Zinc nitrate hexahydrate ($Zn(NO_3)_2 \cdot 6H_2O$) and Sodium hydroxide (NaOH). The use of these specific reagents has been discussed in the thesis with some survey data. The particular work is done by taking three different concentrations of Sodium hydroxide (NaOH) as 0.75M, 1.00M and 1.25M and accordingly calculating the pH while preparing the solution with Zinc nitrate hexahydrate ($Zn(NO_3)_2 \cdot 6H_2O$). In the thin film, zinc oxide (ZnO) layer acts as a transparent conductive oxide, which is an important tool for photodetector detection.

The purpose of this thesis is to examine the state of the art in the hydrothermal synthesis of ZnO nanomaterials using different reagent concentrations. The first section of the thesis covers the introduction, properties of ZnO nanomaterials, and new applications of ZnO nanomaterials. The properties of the hydrothermal process, as well as the reactants, process parameters and synthesis mechanism, are then discussed. Gradually, it moves on to the various characterization instruments in use, defining not only the fundamental principles but also their advantages. The final section of the thesis discusses the morphology of products and divides the characterization results into three categories: i) Optical properties through FTIR (Fourier transform infrared spectroscopy), DRS (Diffuse reflectance spectroscopy) and PL (Photoluminescence spectroscopy), ii) Morphological properties through FESEM (Field emission scanning electron microscopy) and iii) Electrical properties through I-V (Current-Voltage) characterization, which describe it as a perfect material for photodetection applications.

Keywords: Photodetectors, Zinc oxide (ZnO), Hydrothermal synthesis, Optical properties, Morphological properties, Electrical properties

Table Of Contents

CHAPTER :1

INTRODUCTION WITH BRIEF IDEA ABOUT THE MATERIAL

1.1 BRIEF OVERVIEW OF THE WORK

Energy consumption has risen dramatically in recent decades as a result of increased industrialization, demand and automatic electronic appliances. As a result, focus has shifted to alternative renewable sources of energy like wind energy, solar energy, wave energy etc [1]. However, one of the most feasible approaches for supplying large amounts of power or energy is converting mechanical energy to electrical energy [2].

UV photodetectors are remarkably used in a wide range of commercial and military applications that includes pollution monitoring, proper space-to-space communications, sterilisation of water, detection of early missile plume and flames etc [3]. Zinc oxide has been a hot topic in semiconductor research for over 65 years, with publications dating back to 1945 [4]. During the 1950s and 1970s, it received increased attention in the areas of growth, doping, transport, band structure, and luminescence [5]. In recent years, ZnO has been extensively studied for its unique properties and potential applications in electronic and optoelectronic devices [6]. It has a large bandgap of 3.37 eV at room temperature, as well as strong radiation hardness, chemical stability and low cost [7].

Figure 1.1: Data survey of India's energy consumption.

ZnO has gotten more attention among the lead-free materials because of its excellent piezoelectric property and ease of synthesis [8]. ZnO nanorods are the best material for making biocompatible, non-toxic, cost-effective and flexible composites because of their low electrical resistance [9]. Zinc oxide, also known as zincite, is an inorganic compound found only in crystalline form in nature. It usually available in the form of a crystalline powder that's nearly insoluble in water.

Zinc oxide (ZnO) is a transparent semiconductor that belongs to the II-VI family. It has unique properties such as a 3.37eV direct band gap energy, a 60 meV exciton binding energy, high electron mobility, a high saturation energy, high room-temperature luminescence and a good thermal and chemical stability, making it suitable for a wide range of applications including light emitting diodes, solar cells, sensors, field emission displays and UV-laser applications [10, 11]. Synthetic ZnO accounts for the majority of commercially available ZnO.

These properties are used in liquid crystal display electrodes, energy-saving and heat-protecting windows, electronic applications of ZnO such as thin-film transistors and light-emitting diodes and ceramics plastic. Because of its unique properties and applications, it is used in transparent electronics, UV light emitters, piezoelectric devices and chemical sensors. Researchers have focused their efforts on the synthesis, characterization and device applications of ZnO nanomaterials owing to these remarkable physical properties. [12]

Low temperature hydrothermal method is a relatively new technique that has gained popularity in current years due to its unique advantages that include thermal uniformity and energy efficiency due to the rapid and homogeneous heating, low cost, high reaction rate and the ability to obtain nanoparticles of various morphologies and shapes [13].

Thin films have become a common place for a wide range of technological applications. In terms of electrical properties, they differ significantly from bulk films. They are becoming increasingly important as preparation systems advance. They have been prepared with care and attention to detail [14]. Because of the advantages of the preparation techniques, thin films have become widely used in technological applications such as optics [14], optoelectronics [15], electronics [16] and sensors [17]. The first step was to create single-layer thin films with a mono element structure. Due to technological constraints, they began to be prepared as multilayer structures and alloy forms with two or more elements after a short time.

1.2 PROPERTIES AND DEVICE APPLICATIONS

ZnO has a long history of being appreciated for its diverse set of properties [21]. In recent years, the fact that ZnO is a semiconductor with a direct band gap of 3.44 eV [19], allowing optoelectronic applications in the blue and UV regions of the spectrum, has received immense attention. The prospect of such applications has been fueled in recent years by the remarkable progress in thin-film growth [22]. ZnO can be grown on inexpensive substrates such as glass, at relatively low temperatures. The properties of ZnO that distinguish it from other semiconductors or oxides or make it useful for applications are as follows:

• Direct and wide band gap.

The band gap of ZnO is 3.44 eV at low temperatures and 3.37 eV at room temperature [19]. For comparison, the respective values for wurtzite GaN are 3.50 eV and 3.44 eV [23]. This enables applications of ZnO in blue/UV optoelectronics such as laser diodes, light-emitting diodes and photodetectors [18], as stated previously. Optically pumped lasing has been observed in a variety of ZnO thin films [20].

• Large exciton binding energy.

The binding energy of free-exciton ZnO is 60 meV [20], whereas GaN has a binding energy of 25 meV [23]. Effective excitonic emission in ZnO can be maintained at room temperature and higher due to the high exciton binding energy [23]. Because the oscillator strength of excitons is typically much higher than that of direct electron–hole transitions in direct gap semiconductors, ZnO is a promising material for optical devices based on excitonic effects [24].

• Large piezoelectric constants.

In piezoelectric materials, applied voltage causes crystal deformation, and vice versa. These materials are commonly used in sensors, transducers, and actuators. The low symmetry of the crystal structure, combined with the large electromechanical coupling of ZnO, produces strong piezoelectric and pyroelectric properties. On a variety of substrates, different deposition techniques have been used to grow ZnO films with uniform thickness and orientation [25,26].

• Strong luminescence.

Because of its strong luminescence in the green–white region of the spectrum, ZnO is a good material for phosphor applications as well. A peak at 495 nm and a half-width of 0.4 eV distinguish the emission spectrum [27]. ZnO can be used in vacuum fluorescent displays and field emission displays because of its n-type conductivity. The origin and mechanism of the luminescence centre are poorly understood, with oxygen vacancies and zinc interstitials frequently attributed without evidence [27]. Because these defects are unable to emit in the green wavelength range, it has been suggested that zinc vacancies are the more likely source of green luminescence.

• Strong sensitivity of surface conductivity to the presence of adsorbed species.

The conductivity of ZnO thin films is strongly influenced by the exposure of the surface to various gases. It can be used as a low-cost smell sensor capable of detecting the freshness of foods and drinks due to its high sensitivity to trimethylamine present in the odour [28].

• High thermal conductivity.

ZnO can be used as an additive as a result of this property (e.g., ZnO is added to rubber in order to increase the thermal conductivity of tires). It also makes ZnO more appealing as a homoepitaxy or heteroepitaxy substrate (for example, to grow GaN, which has a similar lattice constant) [29, 30]. While the device is in use, high thermal conductivity translates to high heat removal efficiency.

• Availability of large single crystals.

The availability of large area single crystals, as well as epi-ready substrates, is one of the most appealing aspects of ZnO as a semiconductor. Growth of bulk crystals can be accomplished in a variety of ways, including hydrothermal method [31, 32] and pressurised melt growth [33, 34]. To grow thin films, laser ablation [35] can be used. Epitaxial ZnO growth on native substrates could result in high-quality thin films with low extended defect concentrations. When compared to GaN, which has no natural substrates, this is especially important. Given that GaN-based devices have achieved high efficiencies despite a high concentration of extended defects, high-quality ZnO-based devices could potentially outperform GaN-based devices.

• Amenability to wet chemical etching.

It is extremely advantageous to be able to use low-temperature wet chemical etching in semiconductor device fabrication processes. Acidic, alkaline, and mixture solutions have all been reported to etch ZnO thin films. The ability to use low-temperature chemical etching to process, design, and integrate electronic and optoelectronic devices adds a lot of flexibility.

• Radiation hardness.

Radiation hardness is critical for applications at high altitudes or in space. For reasons that are still unknown, ZnO has been found to have an extremely high radiation hardness [36, 37], even higher than that of GaN. When compared to amorphous silicon or organic semiconductors, ZnO has aroused interest because of its ability to fabricate thin-film transistors on flexible substrates with high electron mobility [38].

1.3 ADVANTAGES OF ZnO

The polar surface of ZnO is extremely stable, and it has been used to create a variety of nanostructures [39]. It is a promising photonic material because of its large morphology, wide

direct band gap of 3.37 eV at 25 °C, and high excitation binding energy of 60 meV. ZnO is also tetragonally coordinated, with the positive charge centre overlapping the negative charge centre. This means that when an external force is applied, the tetrahedron's distortion causes a dipole moment, which causes its piezoelectric properties to emerge [40].

In comparison to other chemical compounds used in biosensing, such as indium oxide (In_2O_3), which has a band gap of only 2.9 eV, ZnO is a superior substitute. Because a larger band gap allows for higher breakdown voltage and offers the ability to sustain large electric fields [41]. The IEP of 9.5 is another important feature of ZnO. When compared to silicon dioxide (SiO_2), which has an IEP ranging from 1.7 to 3.5, ZnO has a higher IEP, which allows for protein absorption via electrostatic interaction [42]. Because biosensors are used in vivo, biocompatibility is another important feature. Furthermore, ZnO has demonstrated nontoxicity, chemical stability, and electrochemical activity in similar applications [43].

The field of optoelectronics is another promising application for ZnO nanostructures. Light emitting diodes (LED) and laser diodes (LD) in the green to near ultra violet range are examples [44]. The aspect ratio, length to diameter, and surface ratio of ZnO nanowires are all higher than those of bulk or thin-film photodetectors, resulting in a strong photo response. As a result, they're ideal for use as a 1D photodetector [45]. Furthermore, because of its transparency to visible light, ZnO has the potential to replace transparent conductive indium tin oxide (ITO) in transparent electronics, energy harvesting devices, and integrated sensors [46]. In addition, several experiments have shown that ZnO is highly resistant to high-energy radiation, making it a good candidate for space applications. It can be easily etched in all acids and alkalis. As a result, it can be used in the fabrication of small devices such as transparent electrodes, display window materials, and solar cells. It also has a natural substrate [47].

Figure 1.2: ZnO thin film on PET substrate

1.4 APPLICATIONS OF ZnO

Since the late 1800s, when its white powder was used in water colours and oil-based paint, ZnO has established itself as a very old technological material [48]. Because of their unique properties, ZnO nanoparticles have gotten a lot of attention. The fact that ZnO is a semiconductor with a direct band gap of approximately 3.4 eV, which in theory enables its optoelectronic applications in the blue and UV regions of the spectrum, such as light emitting diodes, laser diodes, and photodetectors, it has gotten the most attention in recent years. ZnO's efficient excitonic emission can be maintained at room temperature and higher, thanks to its free exciton binding energy of 60 meV, making it a promising material for optical devices based on excitonic effects.

ZnO is a good material for phosphor applications like vacuum fluorescent displays and field emission displays because of its strong luminescence in the green-white region of the spectrum. ZnO is useful as an additive in rubber (to increase the thermal conductivity of tyres), ceramic

processing, waste treatment, and the manufacture of sunscreens due to its high thermal conductivity and catalytic efficiency [49-53].

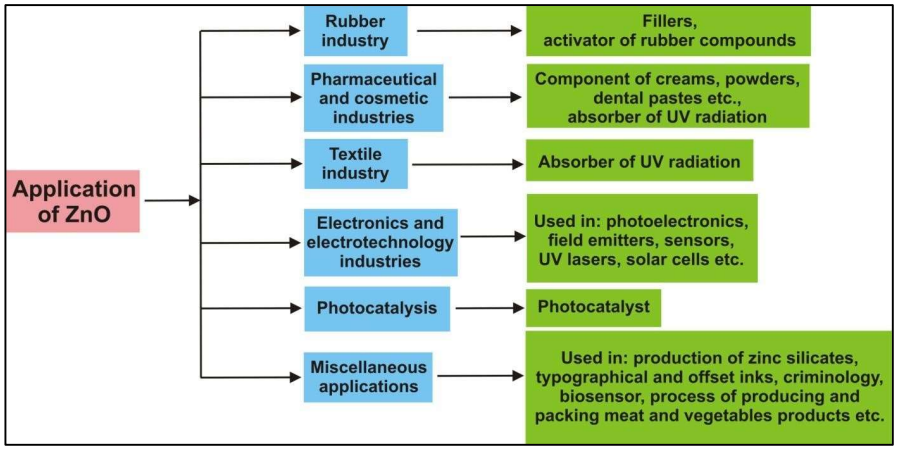

Figure 1.3: Schematic representation all the applications of ZnO.

In fact, ZnO provides better protection than TiO_2 because it can absorb both UV-A and UV-B radiation, whereas TiO_2 can only block UVB radiation. As a result, it is used in a variety of hair and skin care products, such as powders and creams, to protect the skin from harmful UV rays and promote healing. ZnO also improves the efficacy of ointments, deodorants, soaps, and anti-dandruff treatments. ZnO has been shown to have high sensitivity to the presence of adsorbed species, making it useful as a low-cost smell sensor for detecting the freshness of foods and beverages [54].

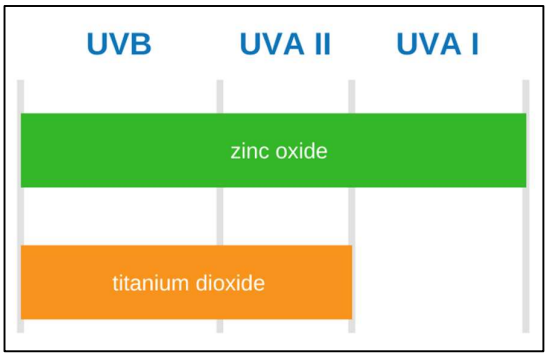

Figure 1.4: Comparison between UV spectrum of Zinc oxide and Titanium dioxide.

When compared to amorphous silicon or organic semiconductors, ZnO has also attracted attention due to its ability to make thin film transistors on flexible substrates with high electron mobility, and it is a well-known suitable candidate for the TCO layer of thin film compound solar cells [55, 56].

1.5 COMPARISON OF DIFFERENT SEMICONDUCTORS

After silicon and germanium, ZnO was one of the first semiconductors to be prepared in a relatively pure form. Due to its promising piezoelectric/acoustoelectric properties, it was extensively characterised as early as the 1950s and 1960s. Because of their potential applications as optoelectronic devices in the short wavelength and ultraviolet (UV) portions of the electromagnetic spectrum, wide band gap semiconductors have gotten a lot of attention in the last decade. The crystal structures and band gaps of these semiconductors, such as ZnSe, ZnS, SiC, GaN, SnO_2, and ZnO, are similar. Some of the important properties of these wide band gap semiconductors are summarised in the table.

Initially, blue and UV light emitting diodes, as well as injection lasers, were developed using ZnSe-based devices and GaN-based technologies. Because of the indirect band structure, SiC does not emit bright light, and ZnSe has produced some defect levels under high current drive. GaN is without any doubt the most suitable material for optoelectronic devices. ZnO, on the other hand, has significant advantages over currently used semiconductors for light emitting diodes (LEDs) and laser diodes (LDs). Because ZnO and GaN have nearly identical lattice parameters and structures, ZnO can be used as a lattice matched substrate in GaN devices or vice versa. Due to the properties similar to those of GaN, ZnO is a potential candidate for optoelectronic applications in the short wavelength range (green, blue, and ultraviolet), information storage, and sensors [66].

Among all semiconductors, ZnO has the best radiation hardness. This property allows ZnO-based devices to be used in space applications as well as high-energy radiation environments. With the alloying process, the band gap energy can be varied from 3.3 to 4.5 eV. As a result, it can be used as an active layer in quantum well lasers and doubly confined hetero-structured LEDs. These one-of-a-kind nanostructures unmistakably show that ZnO is the most diverse family of nanostructures among all materials in terms of structure and properties [58, 63].

Table1.1: Comparison of different semiconductors

Wide band gap semiconductors	Crystal structure	Lattice parameters(Å)		Effective mass (me)		Eg (eV at RT)	Melting temperature (K)	Exciton binding energy (meV)	Dielectric constant	
		a	b	m_e	m_h				ε_0	ε_∞
ZnO	Wurtzite	3.250	5.206	0.318	0.50	3.37	2248	60	8.75	3.72
GaN	Wurtzite	3.189	5.185	0.2	0.80	3.4	1973	21	9.5	5.15
ZnSe	Zinc-Blende	5.667	–	0.15	0.78	2.7	1790	20	7.1	5.3
ZnS	Wurtzite	3.824	6.261	0.34	1.76	3.7	2103	36	9.6	5.7
6H-SiC	Wurtzite	3.08	15.12	0.42	1.00	3.0	>2100	–	9.66	6.52
SnO_2	Tetragonal rutile	4.737	3.185	0.1	–	3.6	>2200	32.76	9.65	–

Because of their unique properties, such as a large surface-to-volume ratio and unique electronic properties, semiconductor nanoparticles have attracted a lot of attention in recent years. When compared to their bulk counterparts, they have unique optical properties [57]. Some of nanoparticles' unique properties may be due to their large surface to volume ratio. Transition metal oxides are a significant class of semiconductors [58–61]. Zinc oxide (ZnO) is a unique electronic and photonic semiconductor with a direct band gap of 3.37 eV and a high exciton binding energy (60meV) at room temperature among various semiconducting oxides [62, 63].

ZnO's high exciton binding energy allows for excitonic transitions even at room temperature, potentially resulting in higher radiative recombination efficiency for spontaneous emission and a lower threshold voltage for laser emission [64, 65]. Because the structure lacks a centre of symmetry and has a large electromechanical coupling, it has strong piezoelectric and

pyroelectric properties, leading to its use in mechanical actuators and piezoelectric sensors [66]. Nanogenerators, gas sensors, solar cells, photodetectors, and photocatalysts are just a few of the applications for ZnO nanoparticles [62, 66, 69]. Many recent studies have focused on the optical and electrical properties of ZnO nanomaterials synthesised using hydrothermal method [70].

1.6 ZnO MARKET PROSPECTS

It is estimated that the production of NPs of metal oxides in 2020 will be ca. 660 thousand tons, with the estimated production of ZnO NPs alone being between 45 and 56 thousand tons, i.e., ca. 7– 8% of the market [71, 72]. At present, ZnO NPs are used mainly for producing the following class of products:

- pharmaceuticals,
- cosmetics,
- paints,
- various coatings,
- antibacterial products,
- electronics,
- and in scientific research.

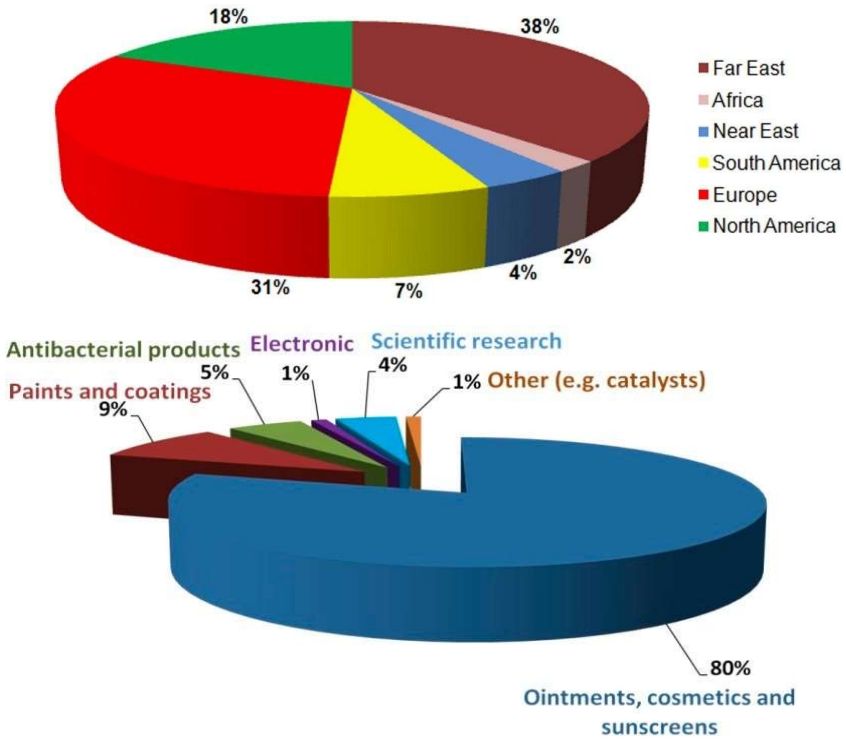

Figure 1.5. Estimated demand for ZnO NPs on the market in terms of their world-wide consumption and applications. The chart was prepared based on data from [1].

1.7 LITERATURE REVIEW

Zinc oxide (ZnO) has been studied extensively in the past. It has been the subject of thousands of research papers over the last 100 years, dating back to 1935 [73]. ZnO has penetrated far into industry, and is one of the critical building blocks in today's modern society [74]. It is valued for its ultra violet absorbance, wide chemistry, piezoelectricity, and luminescence at high temperatures. Paints, cosmetics, plastic and rubber manufacturing, electronics, and

pharmaceuticals are just a few of the industries that use it. However, ZnO has recently resurfaced in the scientific spotlight, this time due to its semiconducting properties [75].

The fabrication of high-quality single crystals and epitaxial layers was achieved thanks to advances in growth technologies and the potential for ZnO to become a suitable substrate for GaN [76, 77]. Allowing for the fabrication of ZnO-based photonic and optoelectronic devices, where it competes with GaN as a potential candidate for the next generation of light emitters for solid-state lighting applications [78, 79]. At room temperature, ZnO has a large band gap of 3.4 eV and a large exciton binding energy of 60 meV, making it ideal for blue and ultra-violet optical devices. Although GaN and GaN-based materials have previously dominated this wavelength range, ZnO has several advantages [75, 78]. The two most important of these are:

1. A higher exciton binding energy, which will allow for higher efficiency and a lower power threshold for optical pumping lasing at room temperature.

2. The ability to grow high-quality single crystal substrates at low cost and with relative ease, which GaN still lacks.

These characteristics combine to make ZnO an excellent candidate for a variety of devices, such as blue and ultraviolet laser diodes and light emitting diodes [80]. Despite the maturity of the semiconductor field and the extensive information base available for ZnO, little is actually known about this material as a semiconductor.

The thesis has been written during what could be described as the 'teenage years' of ZnO device research. The teething problems that hampered the development of ZnO devices in the past have been resolved. Growth advances, for example, have resulted in the development of repeatable high-quality epitaxial layers and single crystals [76, 77].

Surface-related and bulk-related processes govern UV photoconductivity in ZnO. When the surface area of nanocrystalline films is large, surface-related processes become more prominent. The visible photoluminescence in ZnO is thought to be caused by inherent defect centres such as oxygen vacancies and zinc interstitials.

ZnO is a popular material in research labs all over the world because of its unique properties. Researchers are increasingly focusing on ZnO in nanoform, as evidenced by the search results in the ScienceDirect scientific paper search engine. The terms "zinc oxide" and "nano zinc oxide" received 264,763 and 38,999 hits, respectively. The overall share of publications about "nano zinc oxide" among all ZnO papers previously published was 14.7 percent.

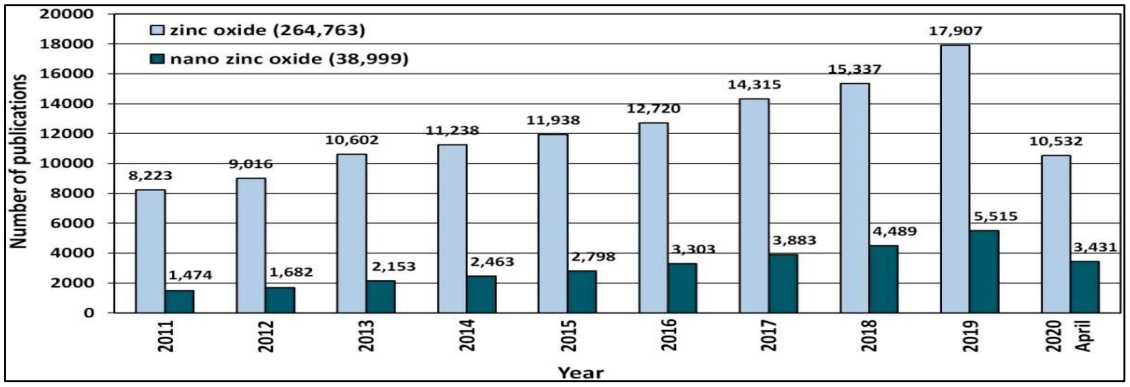

Figure 1.6. The number of scientific publications referring to the search of "zinc oxide" and "nano zinc oxide" phrases published in the period of 2011–2020. Source: ScienceDirect (accessed on 19th April 2020).

The number of publications on nano ZnO has been steadily increasing year after year, with the annual share of publications on nano ZnO reaching 32.6 percent in 2020. The number of scientific publications relating to nano ZnO has increased by 400% in the last ten years. The growing popularity of nano ZnO is due, among other things, to technological advancements in the production of ZnO nanostructures, which have novel physical properties that allow previously unimagined applications and possibilities [81–83].

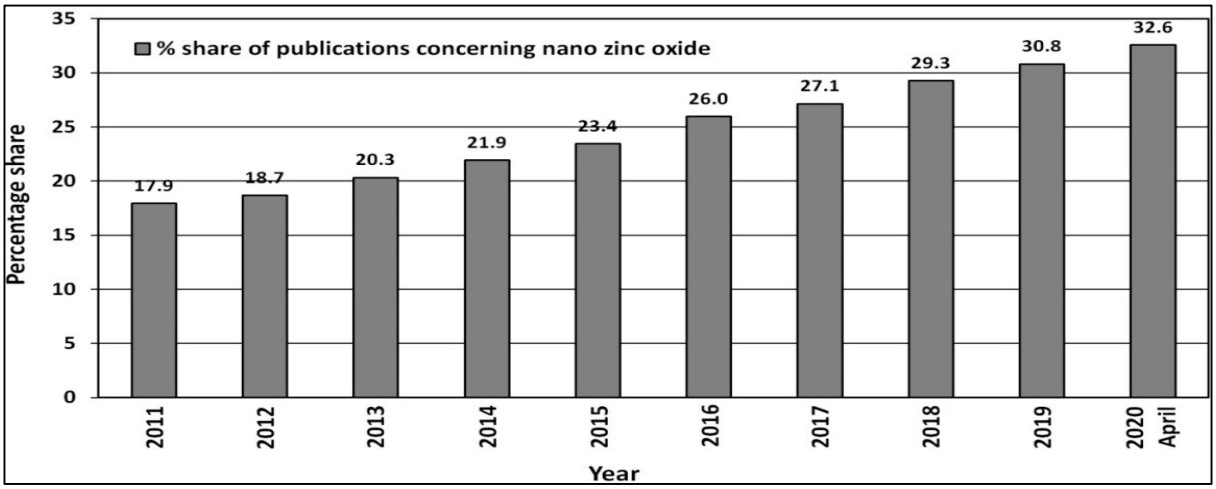

Figure 1.7. Percentage share of publications concerning "nano zinc oxide" among all publications concerning "zinc oxide" published in the period 2011–2020. Source: ScienceDirect (accessed on 19th April 2020).

Nano ZnO is considered a safe material [84] that performs admirably as an ultraviolet (UV) radiation filter because it allows for the creation of protective layers that are imperceptible to the naked eye. Long-term protection and broadband protection (UV-A (315–380 nm) and UV-B (280–315 nm)) are two other advantages of using ZnO nanoparticles (NPs) as a UV filter in the area of personal hygiene and sun protection [85]. The effects of ZnO NPs coming into contact with human skin are still being studied [86]. Deodorants, medical and sanitary materials, glass, ceramics, and self-cleaning materials all use ZnO NPs [85, 87].

Various ZnO nanostructures are used in optoelectronics to make lasers, UV detectors, and UV diodes [88–91]. ZnO nanostructures could be used to make gas sensors for things like steam (humidity, H_2O) [96], ammonia (NH_3) [92–94, 104], nitrogen (N_2) [94], nitrogen monoxide (NO) [92, 93, 102], nitrogen dioxide (NO_2) [92, 94, 97–99], hydrogen (H_2) [92–95, 105], ozone (O_3) [94, 100], hydrogen sulphide (H_2S) [92]

For the time being, the use of ZnO nanostructures in the commercial development of new gas sensors is severely limited, owing to, above all, the ageing effect [106]. Transparent electrodes, transparent windows, flat panel displays, and other flexible and transparent devices commonly use thin films of nano ZnO as inorganic conductors [107, 108].

Various ZnO nanostructures are currently being used in the development of new light-emitting diodes [109], lasers [110], solar cells [111], liquid crystals [112], food packaging materials [113], photoluminescent NPs [114], supercapacitors [108], flexible and transparent thin-film transistors [107, 108], batteries [115, 116], water treatment [117], water filters [118], and other devices.

According to the literature, various techniques are being developed to achieve the desired properties of these nanostructures in a suitable and simple manner. As a result, choosing an efficient synthesis process is critical, as it is a key factor that has a significant impact on the efficacy of synthesised nanocrystalline materials. The current development of appropriate

reaction conditions that could be used in four chemical synthesis methods (hydrothermal, solvothermal (microwave-assisted), sol-gel, and hybrids to achieve the desired features of zinc oxide nanoparticles for its specific application is critically examined in this thesis.

Details of other research papers concerning the microwave hydrothermal synthesis of ZnO without any additional heat treatment are presented in Table listed below [119-132].

Table 1.2. Summary of hydrothermal synthesis of ZnO.

SUBSTRATES	CONDITIONS DURING PREPARATION	PROPERTIES
$Zn(NO_3)_2 \cdot 6H_2O$ (0.1, 0.5 and 2 M), NaOH, H_2O	pH: 8–12; T: 100– 190 °C; P: 1–13 bar, duration: 2 min–2 h; microwave reactor	particles, sub-micrometre grains and star-like morphology
$Zn(NO_3)_2 \cdot 6H_2O$ (0.1 M), NaOH (2M),H_2O	P: 9–39 bar, duration: 3–7 min; power: 70– 100%; microwave reactor (750 W)	heterogeneous nano and microstructures; particles size: 10–300 nm
$Zn(NO_3)_2 \cdot 6H_2O$ (0.43 M),NaOH (0.43M), H_2O	duration: 15 min; T: 75–170 °C; power: 40–450 W; Teflon cell in microwave oven; pulsed mode	crystallite size: 30–45 nm
$Zn(NO_3)_2 \cdot 6H_2O$, NaOH, H_2O	duration: 20 min; T: 100–180 °C; power: 0–1000 W; microwave reactor	nanorods; nanowires; nano-thruster vanes; nano-dandelions; nano-spindles
$Zn(NO_3)_2 \cdot 6H_2O$ (1.6 M), NaOH(3.2 M),H_2O	pH: 8.3; duration: 1–5 min; microwave oven	nanorods (diameter: 100–200 nm) and flower structures
$Zn(NO_3)_2 \cdot 6H_2O$, NaOH (different concentrations), H_2O	duration: 1 h; T: 110 °C; microwave oven	submicron starshaped structures, chrysanthemum flower structures, nanoflakes
$Zn(NO_3)_2 \cdot 6H_2O$ (different concentrations), NaOH, H_2O	pH: 7–13.1; duration: 20; power: 180 W; microwave oven	nanoparticles in clusters, nanoplates in flower-like clusters, and spear-shaped particles in flower-like clusters
$Zn(NO_3)_2 \cdot 6H_2O$, NaOH, H_2O	duration: 15–50 min; power: 120– 420 W; microwave reactor (700 W)	nanostructures consisted of flower-like, sword-like, needle-like and rods-like structures
$Zn(NO_3)_2 \cdot 6H_2O$ (0.005 M), KOH (4 M), H_2O	pH: 12; T: 120 °C; duration: 4 h; microwave oven	nanowires with diameter of 80 nm and lengths of up to 10 μm
$Zn(NO_3)_2 \cdot 6H_2O$ (0.01 M), urea (0.1 M), H2O	T: 120 °C; duration: 10–24 min; power: 150 W; microwave oven	javelins, length: 14–17 μm, width: 0.9–1.4 μm
$Zn(NO_3)_2 \cdot 6H_2O$ (0.005 M), hexamethylenetetramine ($C_6H_{12}N_4$) (0.005 M), H_2O	T: 90 °C; duration: 2 min; microwave reactor	ZnO rods (e.g., bipods, tripods, tetrapods and multipods); diameter: 160–220 nm; length: 1.25–1.3 μm
$Zn(NO_3)_2 \cdot 6H_2O$ (0.13 M), NaOH (1.3 M), 1-n-butyl-3-methyl imidazolium tetrafluoroborate, H_2O	T: 90–125 °C; duration: 2–10 min; microwave reactor	morphology: flower-like + needle-like, from 60 to 450 nm and lengths up to several micrometres

$Zn(NO_3)_2 \cdot 6H_2O$ (0.005 M), hexamethylenetetramine ($C_6H_{12}N_4$) (0.010 M), NaOH (3 M)	pH: 9 and 13; T: 96 °C; duration: 60 min;	flower-like ZnO microstructures (2–3 μm) of hexagonal prisms (length: 1–2 μm, diameter: 50–130 nm) with planar and hexagonal pyramid tips (length: 1.5 μm, diameter: 300 nm)

1.8 MOTIVATION AND OBJECTIVE OF THE WORK

It could be argued that modern research and technology development should include more than just new devices, methods, or device improvements. Researchers should continue to flesh out fundamental physics, optics, and materials principles that are still unknown in their entirety. Much has been learned and much progress has been made in these fields, particularly in the areas of electronics and semiconductor devices; however, it would be foolish of the scientific community to abandon further research into fundamental physics principles, or even to abandon questioning established scientific principles.

Although the interaction of light with matter is a fundamental interaction that is at the heart of many semiconductor technologies, there are still aspects of this reaction that have yet to be fully explored. Even a complete understanding of the nature of light and what it is has yet to be achieved. The goal of this study is to uncover new findings that will spur further experimentation and contribute to our current understanding of light and its interactions with materials and devices.

The goal of this study is to learn more about the properties of ZnO nanocrystalline materials made by the hydrothermal method. Initially, a series of samples were prepared using the hydrothermal technique on PET substrate under various concentration and pH conditions. As a result, various structural and microstructural properties, as well as different surface morphologies of nanostructures, were obtained. The optical properties of ZnO are also known to be sensitive to the structural quality of the material.

Following are the main goals:

1. Characterization of the structural, microstructural, and photoluminescence properties of the synthesized material.

2. Correlation of key technological parameters with material properties.

3. A general conclusion on the potential and applicability of the technique used to prepare nanocrystalline ZnO, as well as the potential applications of the low-sized structures obtained.

PET is thought to be the substrate best suited for ZnO growth because of its good electrical and thermal conductivity, low cost, high crystal quality, and large size availability. The concentration of NaOH has a significant impact on the properties of ZnO. The effect of different concentrations on ZnO properties should be revealed by examining a series of ZnO samples deposited at 0.75M, 1.00M, and 1.25M at 100°C.

A second goal of this research is to uncover photodetector properties that could be used in the future as a flexible, low-cost solar cell that replaces Si and can be used to store renewable energy. In terms of the current nanotechnological trend, the structure, microstructure, and optical emitting properties of such nanosized heterostructures are of great interest for optoelectronic applications.

The following appropriate characterization techniques have been used:

1. The optical properties of ZnO were investigated via FTIR analysis, DRS analysis and PL analysis for all the three samples.

2. The microstructure of ZnO nanocrystalline material has been investigated by Field Emission Scanning Electron Microscope (FESEM): the top-view images of the surface were obtained at different magnifications for the three samples.

3. The electrical properties of ZnO has been investigated by I-V characterization which is the basic application part of this thesis that has been carried out to determine the functionality of a Photodetector.

References

1. S. Priya, D.J. Inman, Energy Harvesting Technologies, 2009, pp. 1-517, https://doi.org/10.1007/978-0-387-76464-1.
2. J.H. Jung, M. Lee, J. Hong, Y. Ding, C. Chen, L. Chou, Z.L. Wang, Lead-free NaNbO3 Nanowires for a High Output Piezoelectric, 2011, pp. 10041-10046, https://doi.org/10.1021/nn2039033
3. Monroy, E.; Calle, F.; Pau, J.L.; Munoz, E.; Omnes, F.; Beaumont, B.; Gibart, P. AlGaN-Based UV Photodetectors. J. Cryst. Growth 2001, 230, 537-543.
4. Brubaker DG, Fuller ML (1945) J Appl Phys 16:128
5. Klingshirn C, Hauschild R, Priller H, Zeller J, Decker M, Kalt H (2006) Adv Spectrosc Lasers Sens 231:277
6. Özgür, Ü.; Alivov, Y.A.; Liu, C.; Teke, A.; Reshchikov, M.A.; Doğan, S.; Avrutin, V.; Cho, S.J.; Morkoç, H. A Comprehensive Review of ZnO Materials and Devices. J. Appl. Phys. 2005, 98, 041301.
7. Look, D.C. Recent Advances in ZnO Materials and Devices. Mater. Sci. Eng. B 2001, 80, 383-387.
8. K. Batra, N. Sinha, S. Goel, H. Yadav, A.J. Joseph, B. Kumar, Enhanced dielectric, ferroelectric and piezoelectric performance of Nd-ZnO nanorods and their application in flexible piezoelectric nanogenerator, J. Alloy. Compd. 767 (2018) 1003e1011, https://doi.org/10.1016/j.jallcom.2018.07.187
9. S. Goel, N. Sinha, H. Yadav, S. Godara, A.J. Joseph, B. Kumar, Ferroelectric Gddoped ZnO nanostructures: enhanced dielectric, ferroelectric and piezoelectric properties, Mater. Chem. Phys. 202 (2017) 56e64, https://doi.org/10.1016/j.matchemphys.2017.08.067
10. Angshuman Deka and Karuna Kar Nanda, A comparison of ZnO films deposited on indium tin oxide and soda lime glass under identical conditions, AIP ADVANCES 3, 062104 (2013), http://dx.doi.org/10.1063/1.4811091.
11. D. Nunes, A. Pimentel, A. Gonçalves, S. Pereira, R. Branquinho, P. Barquinha, E Fortunato and R Martins, Metal oxide nanostructures for sensor applications, Semiconductor Science and Technology 34[4] 043001 (2019), https://doi.org/10.1088/1361-6641/ab011e
12. Jayanta Kumar Behera.Synthesis and Characterization of Nano-particles.M.Tech Thesis, NIT Rourkela.
13. V. Musat, A. Filip, N. Tigau, R. Dinica, E. Herbei, C. Romanitan, I. Mihalache, Munizer Purica, 1D Nanostructured ZnO Layers by Microwave-Assisted Hydrothermal Synthesis, Revista de chimie 69[10] (2018), 2788-2793.
14. D. E. Aspnes, "Optical properties of thin films,"Thin Solid Films, vol. 89, no. 3, pp. 249–262, 1982.
15. G. Eda and M. Chhowala, "Chemically derived graphene oxide: towards large-area thin-film electronics and optoelectronics," Advanced Materials, vol. 22, no. 22, pp. 2392–2415, 2010.
16. M. S. Boon, W. P. S. Saw, and M. Mariatti, "Magnetic, dielectric and thermal stability of NiZn ferrite-epoxy composite thin films for electronic applications," Journal of Magnetism and Magnetic Materials, vol. 324, no. 5, pp. 755–760, 2012.
17. G. Sberveglieri, "Recent developments in semiconducting thin film gas sensors," Sensors and Actuators B, vol. 23, no. 2-3, pp. 103–109, 1995.
18. Nickel N H and Terukov E (ed) 2005 Zinc Oxide—A Material for Micro- and Optoelectronic Applications (Netherlands: Springer)
19. Mang A, Reimann K and Rubenacke St 1995 ¨ Solid State Commun. 94 251

20. Bagnall D M, Chen Y F, Zhu Z, Yao T, Koyama S, Shen M Y and Goto T 1997 Appl. Phys. Lett. 70 2230
21. Brown M E (ed) 1957 ZnO—Rediscovered (New York: The New Jersey Zinc Company)
22. Look D C, Reynolds D C, Litton C W, Jones R L, Eason D B and Cantwell G 2002 Appl. Phys. Lett. 81 1830
23. Madelung O (ed) 1996 Semiconductors—Basic Data 2nd Revised Edn (Berlin: Springer)
24. Yu P Y and Cardona M 2005 Fundamentals of Semiconductors 3rd edn (Berlin: Springer)
25. Kamalasanan M N and Chandra S 1996 Thin Solid Films 288 112
26. Paraguay F D, Estrada W L, Acosta D R N, Andrade E and Miki-Yoshida M 1999 Thin Solid Films 350 192
27. Shionoya S and Yen W H (ed) 1997 Phosphor Handbook By Phosphor Research Society (Boca Raton, FL: CRC Press)
28. Nanto H, Sokooshi H and Usuda T 1991 Solid-State Sensors and Actuators 24–27 596
29. Florescu D I, Mourokh L G, Pollak F H, Look D C, Cantwell G and Li X 2002 J. Appl. Phys. 91 890
30. Ozg ¨ ur¨ U, Gu X, Chevtchenko S, Spradlin J, Cho S-J, ¨ Morkoc¸ H, Pollak F H, Everitt H O, Nemeth B and Nause J E 2006 J. Electr. Mater. 35 550
31. Suscavag M et al 1999 MRS Internet J. Nitride Semicond. Res. 4S1 G3.40
32. Ohshima E, Ogino H, Niikura I, Maeda K, Sato M, Ito M and Fukuda T 2004 J. Cryst. Growth 260 166
33. Reynolds D C, Litton C W, Look D C, Hoelscher J E, Claflin B, Collins T C, Nause J and Nemeth B 2004 J. Appl. Phys. 95 4802
34. Nause J and Nemeth B 2005 Semicond. Sci. Technol. 20 S45
35. Ardakani H K 1996 Thin Sol. Films 287 280
36. Tuomisto F, Saarinen K, Look D C and Farlow G C 2005 Phys. Rev. B 72 085206
37. Look D C, Hemsky J W and Sizelove J R 1999 Phys. Rev. Lett. 82 2552
38. Nomura K, Hiromichi O, Takagi A, Kamiya T, Hirano M and Hosono H 2004 Nature 432 488
39. Fryar J, McGlynn E, Henry MO, Cafolla AA, Hanson CJ (2004) Nanotechnology 15:1797
40. Wang ZL, Gao PX (2004) J Phys Chem B 108:7534
41. Gomez JL, Tigli O (2011) In: IEEE NMDC, Jeju
42. Carcia PF, McLean RS, Reilly MH, Crawford MK, Blanchard EN, Kattamis AZ, Wagner S (2007) J Appl Phys 102: 074512
43. Ozgur U, Alivov YI, Liu C, Teke A, Reshchikov MA, Dogan S, Avrutin V, Cho SJ, Morkoc H (2005) J Appl Phys 98: 041301
44. Klingshirn C, Fallert J, Zhou H, Sartor J, Thiele C, Maier-Flaig F, Schneider D, Kalt H (2010) Phys Status Solid B-Basic Solid-State Phys 247:1424
45. Hsueh TJ, Hsu CL, Chang SJ, Lin YR, Lin TS, Chen IC (2007) J Electrochem Soc 154:H153
46. Hahn YB (2011) Korean J Chem Eng 28:1797 J Mater Sci (2013) 48:612–624 623
47. S. Priya, D.J. Inman, Energy Harvesting Technologies, 2009, pp. 1e517, https:// doi.org/10.1007/978-0-387-76464-1.
48. K. Ellmer and A. Klein, “Zinc Oxide and its Applications,” in Transparent Conductive Zinc Oxide-Basics and Applications, K. Ellmer, A. Klein and B. Rech, Eds., New York, Springer, pp. 1-33, 2008

49. A. Janotti and C. Van de Walle, “Fundamentals of Zinc Oxide as a Semiconductor,” Reports on Progress in Physics, vol. 72, no. 12, pp. 1-29, 2009.
50. A. Janotti, J. Varley, J. Lyons and C. Van de Walle, “Controlling the Conductivity in Oxide Semiconductors,” in Functional Metal Oxide Nanostructures, vol. 6, J. Wu, J. Cao, W. Han, A. Janotti and H. Kim, Eds., Santa Barbara, Springer, pp. 23-35, 2012.
51. A. Janotti and C. Van de Walle, “Native Point Defects and Doping in ZnO,” in Zinc Oxide Materials for electronic and optoelectronic device applications, C. Litton, D. Reynolds and T. Collins, Eds., West Sussex, Wiley, pp. 113-134, 2011
52. C. Van de Walle, “Oxides as Semiconductors,” Santa Barbara, 2014.
53. C. Jagadish and S. Pearton, Zinc Oxide Bulk,Thin Films and Nanostructures: Processing, Properties and Applications, Amsterdam: Elsevier, 2006.
54. C. Wang, L. Zhang, D. Xiang and R. Gao, “Metal Oxide Gas Sensors: Sensitivity and Influencing Factors,” Sensors, vol. 10, no. 3, pp. 2088-2106, 2010.
55. Q. Peng and Y. Qin, “ZnO Nanowires and their Application for Solar Cells,” in Nanowires-Implementations & Applications, Nanchang, InTech, pp. 157-178, 2011.
56. S. Gunalan, R. Sivaraj and V. Rajendran, “Green synthesis of ZnO nanoparticles against bacterial and fungal pathogens,” Progress in Natural Science: Materials International, vol. 22, no. 6, pp. 693–700, 2012.
57. Abou El-Nour KMM, Eftaiha A, Al-Warthan A, Ammar RAA. Synthesis and applications of silver nanoparticles. Arab J Chem 2010; 3:135–40.
58. Nirmala JNS, Sagayaraj P. The influence of capping by TGA and PVP in modifying the structural, morphological, optical and thermal properties of ZnS nanoparticles. Appl Sci Res 2012;4(2):1079–90.
59. Alabi AB, Coppede N, Vilani M, Calestani D, Zappetini A, Babalola O, et al. Photocatalytic activity of nanostructured copper (II) oxide particles. Ife J Sci 2013;15(2):409–14.
60. Rao CNR, Rao GVS. Transition metal oxide, crystal chemistry phase transition and related aspects, NSRDS-NBS 49. Washington DC: U.S. Government Printing Office; 1974.
61. Mark TG, Zheng HL. Thin-film metal oxides in organic semiconductor devices: their electronic structures, work functions and interfaces. NPG Asia Mater 2013;5: e55, http://dx.doi.org/10.1038/am.2013.29.
62. Li D, Hu J, Fan F, Bai S, Luo R, Chen A, et al. Quantum-sized ZnO nanoparticles synthesized in aqueous medium for toxic gases detection. J Alloys Compd 2012; 539:205–9.
63. Wang ZH, Geng DY, Han Z, Zhang ZD. Characterization and optical properties of ZnO nanoparticles obtained by oxidation of Zn nanoparticles. Mater Lett 2009;63: 2533–5.
64. Samuel SM, Bose L, George KC. Optical properties of ZnO nanoparticles. SB Acad Rev 2009;1(2):57–65.
65. Karami H, Fakoori E. Synthesis and characterization of ZnO nanorods based on a new gel pyrolysis method. J Nanomater 2011, http://dx.doi.org/10.1155/2011/628203 [Article ID 628203; 11 pp.].
66. Xudong W, Jinhui S, Zhong LW. Nanowire and nanobelt arrays of zinc oxide from synthesis to properties and to novel devices. J Mater Chem 2007; 17:711–20.
67. Lupan O, Pauporte T, Chow L, Viana B, Pelle F, Ono LK, et al. Effects of annealing on properties of ZnO thin films prepared by electrochemical deposition in chloride medium. Appl Surf Sci 2010; 256:1895–907.

68. Chen R, Zou C, Yan X, Alyamani A, Gao W. Growth mechanism of ZnO nanostructures in wet-oxidation process. Thin Solid Films 2011; 519:1837–44.
69. Ma Y, Wang WL, Liao KJ, Kong CY. Study on sensitivity of nano-grain ZnO gas sensors. J Wide Bandgap Mater 2002; 10:113–20.
70. Urgessa ZN, Oluwafemi OS, Botha JR. Hydrothermal synthesis of ZnO thin-films and its electrical characterization. Mater Lett 2012; 79:266–9, http://dx.doi.org/10.1016/j.matlet.2012.04.065.
71. Future Markets, Inc. The Global Market for Zinc Oxide Nanoparticles; Future Markets: Rockville, MD, USA, 2015; p. 68.
72. The Global Market for Metal. Oxide Nanoparticles to 2020; Future Markets: Rockville, MD, USA, 2013; p. 322.
73. C. W. Bunn, "The lattice-dimensions of zinc oxide," Proc. Phys. Soc. London 47: 835,1935.
74. D. R. Lide (editor), CRC Handbook of Chemistry and Physics, CRC Press, New York, 73rd edition, 1992.
75. D. C. Look, "Recent advances in ZnO materials and devices," Mat. Sci. Eng. B. 80: 383, 2001.
76. D. C. Look, D. C. Reynolds, J. R. Sizelove, R. L. Jones, C. W. Litton, G. Cantwell and W. C. Harsch, "Electrical properties of bulk ZnO," Solid State Commun. 105: 399, 1998.
77. Y. Segawa, A. Ohtomo, M. Kawasaki, H. Koinuma, Z. K. Tang, P. Yu and G. K. L. Wong, "Growth of ZnO thin films by laser-MBE: Lasing of excitons at room temperature," Phys. Stat. Sol. 202: 669, 1997.
78. J. E. Nause, "ZnO broadens the spectrum," III-Vs Review 12: 28, 1999.
79. J. E. Nause, "Fluorescent substrate offers route to phosphor-free LEDs," Comp. Semicond. 11: 29, 2005.
80. S. J. Pearton, D. P. Norton, K. Ip, Y. Heo and T. Steiner, "Recent advances in processing of ZnO," J. Vac. Sci. Technol. B 22: 932, 2004.
81. Klingshirn, C.F.; Waag, A.; Hoffmann, A.; Geurts, J. Zinc Oxide, 1st ed.; Springer: Berlin, Germany, 2010; ISBN 978-3-642-10576-0.
82. Theerthagiri, J.; Salla, S.; Senthil, R.A.; Nithyadharseni, P.; Madankumar, A.; Arunachalam, P.; Maiyalagan, T.; Kim, H.-S. A review on ZnO nanostructured materials: Energy, environmental and biological applications. Nanotechnology 2019, 30, 392001, doi:10.1088/1361-6528/ab268a.
83. Ealias, A.E.; Saravanakumar, M.P. A review on the classification, characterisation, synthesis of nanoparticles and their application. IOP Conf. Ser.: Mater. Sci. Eng. 2017, 263, 032019, doi:10.1088/1757- 899X/263/3/032019.
84. Schilling, K.; Bradford, B.; Castelli, D.; Dufour, E.; Nash, J.F.; Wolfgang Pape, W.; Schulte, S.; Tooley, I.; van den Bosch, J.; Schellauf, F. Human safety review of "nano" titanium dioxide and zinc oxide. Photochem. Photobiol. Sci. 2010, 9, 495–509, doi:10.1039/b9pp00180h.
85. Future Markets, Inc. The Global Market for Zinc Oxide Nanoparticles; Future Markets: Rockville, MD, USA, 2015; p. 68.
86. Newman, M.D.; Stotland, M.; Ellis, J.I. The safety of nanosized particles in titanium dioxide- and zinc oxidebased sunscreens. J. Am. Acad. Dermatol. 2009, 61, 685–692, doi: 10.1016/j.jaad.2009.02.051.
87. The Global Market for Metal. Oxide Nanoparticles to 2020; Future Markets: Rockville, MD, USA, 2013; p. 322.

88. Djurišić, A.B.; Ng, A.M.C.; Chen, X.Y. ZnO nanostructures for optoelectronics: Material properties and device applications. Prog. Quantum Electron. 2010, 34, 191–259, doi: 10.1016/j.pquantelec.2010.04.001.
89. Boscarino, S.; Filice, S.; Sciuto, A.; Libertino, S.; Scuderi, M.; Galati, C.; Scalese, S. Investigation of ZnOdecorated CNTs for UV Light Detection Applications. Nanomaterials 2019, 9, 1099, doi:10.3390/nano9081099.
90. Chen, C.; Zhou, P.; Wang, N.; Ma, Y.; San, H. UV-assisted photochemical synthesis of reduced graphene oxide/ZnO nanowires composite for photoresponse enhancement in UV photodetectors. Nanomaterials 2018, 8, 26, doi:10.3390/nano8010026.
91. Look, D.C. Recent advances in ZnO materials and devices. Mater. Sci. Eng. B-Adv. 2001, 80, 383–387, doi:10.1016/S0921-5107(00)00604-8.
92. Bhati, V.S.; Hojamberdiev, M.; Kumar, M. Enhanced sensing performance of ZnO nanostructures-based gas sensors: A review. Energy Rep. 2019, 6, 46–62, doi: 10.1016/j.egyr.2019.08.070.
93. Praveenkumar, S.; Manikandan, S.; Lingaraja, D.; Sugapriya, T. A review of doped and undoped ZnO nanoparticles for fabrication of gas sensor. Sens. Lett. 2018, 16, 889–900, doi:10.1166/sl.2018.4049.
94. Zhu, L.; Zeng, W. Room-temperature gas sensing of ZnO-based gas sensor: A review. Sens. Actuators APhys. 2017, 267, 242–261, doi: 10.1016/j.sna.2017.10.021.
95. Weber, M.; Kim, J.-Y.; Lee, J.-H.; Kim, J.-H.; Iatsunskyi, I.; Coy, E.; Miele, P.; Bechelany, M.; Sub Kim, S. Highly efficient hydrogen sensors based on Pd nanoparticles supported on boron nitride coated ZnO nanowires. J. Mater. Chem. A 2019, 7, 8107–8116, doi:10.1039/C9TA00788A.
96. Park, S.; Lee, D.; Kwak, B.; Lee, H.-S.; Lee, S.; Yoo, B. Synthesis of self-bridged ZnO nanowires and their humidity sensing properties. Sens. Actuators B-Chem. 2018, 268, 293–298, doi: 10.1016/j.snb.2018.04.118.
97. Kumar, R.; Al-Dossary, O.; Kumar, G.; Umar, A. Zinc oxide nanostructures for NO2 gas–sensor applications: A review. Nano-Micro Lett. 2015, 7, 97–120, doi:10.1007/s40820-014-0023-3.
98. Hjiri, M.; El Mir, L.; Leonardi, S.G.; Donato, N.; Neri, G. CO and NO2 selective monitoring by ZnO-based sensors. Nanomaterials 2013, 3, 357–369, doi:10.3390/nano3030357.
99. Procek, M.; Stolarczyk, A.; Pustelny, T. Impact of temperature and UV irradiation on dynamics of NO2 sensors based on ZnO nanostructures. Nanomaterials 2017, 7, 312, doi:10.3390/nano7100312.
100. Wu, C.-H.; Jiang, G.-J.; Chang, K.-W.; Deng, Z.-Y.; Li, Y.-N.; Chen, K.-L.; Jeng, C.-C. Analysis of the sensing properties of a highly stable and reproducible ozone gas sensor based on amorphous In-Ga-Zn-O thin film. Sensors 2018, 18, 163, doi:10.3390/s18010163.
101. Shewale, P.S.; Yu, Y.S.; Kim, J.H.; Bobade, C.R.; Uplane, M.D. H2S gas sensitive Sn-doped ZnO thin films: Synthesis and characterization. J. Anal. Appl. Pyrol. 2015, 112, 348–356, doi: 10.1016/j.jaap.2015.01.001.
102. Gupta, S.K.; Joshi, A.; Kaur, M. Development of gas sensors using ZnO nanostructures. J. Chem. Sci. 2010, 122, 57–62, doi:10.1007/s12039-010-0006-y.
103. Kanaparthi, S.; Singh, S.G. Chemiresistive sensor based on zinc oxide nanoflakes for CO2 detection. ACS Appl. Nano Mater. 2019, 2, 700–706, doi:10.1021/acsanm.8b01763.

104. Dighavkar, C. Characterization of nanosized zinc oxide-based ammonia gas sensor. Arch. Appl. Sci. Res. 2013, 5, 6–101.
105. Lu, Y.; Hsieh, C.; Su, G. The Role of ALD-ZnO seed layers in the growth of ZnO nanorods for hydrogen sensing. Micromachines 2019, 10, 491, doi:10.3390/mi10070491.
106. Kwoka, M.; Lyson-Sypien, B.; Kulis, A.; Maslyk, M.; Borysiewicz, M.A.; Kaminska, E.; Szuber, J. Surface properties of nanostructured, porous ZnO thin films prepared by direct current reactive magnetron sputtering. Materials 2018, 11, 131, doi:10.3390/ma11010131.
107. Zhang, Y.H.; Mei, Z.X.; Liang, H.L.; Du, X.L. Review of flexible and transparent thin-film transistors based on zinc oxide and related materials. Chin. Phys. B 2017, 26, 047307, doi:10.1088/1674-1056/26/4/047307.
108. Rong, P.; Ren, S.; Yu, Q. Fabrications and applications of ZnO nanomaterials in flexible functional devices— A review. Crit. Rev. Anal. Chem. 2019, 49, 336–349, doi:10.1080/10408347.2018.1531691.
109. Ding, M.; Guo, Z.; Zhou, L.; Fang, X.; Zhang, L.; Zeng, L.; Xie, L.; Zhao, H. One-dimensional zinc oxide nanomaterials for application in high-performance advanced optoelectronic devices. Crystals 2018, 8, 223, doi:10.3390/cryst8050223.
110. Jamadi, O.; Reveret, F.; Disseix, P.; Medard, F.; Leymarie, J.; Moreau, A.; Solnyshkov, D.; Deparis, C.; Leroux, M.; Cambril, E.; et al. Edge-emitting polariton laser and amplifier based on a ZnO waveguide. Light Sci. Appl. 2018, 7, 82, doi:10.1038/s41377-018-0084-z.
111. Jamalullail, N.; Salwani Mohamad, I.; Norizan, M.N.; Mahmed, N.; Taib, B.N. Recent improvements on TiO2 and ZnO nanostructure photoanode for dye sensitized solar cells: A brief review. Web Conf. 2017, 162, 01045, doi:10.1051/epjconf/201716201045.
112. Omelchenko, M.M.; Wojnarowicz, J.; Salamonczyk, M.; Lojkowski, W. Lyotropic liquid crystal based on zinc oxide nanoparticles obtained by microwave solvothermal synthesis. Mater. Chem. Phys. 2017, 192, 383– 391, doi: 10.1016/j.matchemphys.2017.02.001.
113. Kim, I.; Viswanathan, K.; Kasi, G.; Thanakkasaranee, S.; Sadeghi, K.; Seo, J. ZnO nanostructures in active antibacterial food packaging: Preparation methods, antimicrobial mechanisms, safety issues, future prospects, and challenges. Food Rev. Int. 2020, doi:10.1080/87559129.2020.1737709.
114. Zhang, Z.-Y.; Xiong, H.-M. Photoluminescent ZnO nanoparticles and their biological applications. Materials 2015, 8, 3101–3127, doi:10.3390/ma8063101.
115. Wang, S.; Gao, F.; Ma, R.; Du, A.; Tan, T.; Du, M.; Zhao, X.; Fan, Y.; Wen, M. ZnO nanoparticles anchored on a N-doped graphene-coated separator for high performance lithium/sulfur batteries. Metals 2018, 8, 755, doi:10.3390/met8100755.
116. Fernando, J.F.S.; Zhang, C.; Firestein, K.L.; Nerkarb, J.Y.; Golberg, D.V. ZnO quantum dots anchored in multilayered and flexible amorphous carbon sheets for high performance and stable lithium-ion batteries. J. Mater. Chem. A 2019, 7, 8460–8471, doi:10.1039/C8TA12511B.
117. Dimapilis, E.A.S.; Hsu, C.S.; Mendoza, R.M.O.; Lu, M.-C. Zinc oxide nanoparticles for water disinfection. Sustain. Environ. Res. 2018, 28, 47–56, doi: 10.1016/j.serj.2017.10.001.
118. Huang, J.; Huang, G.; An, C.; He, Y.; Yao, Y.; Zhang, P.; Shen, J. Performance of ceramic disk filter coated with nano ZnO for removing Escherichia coli from

water in small rural and remote communities of developing regions. Environ. Pollut. 2018, 238, 52–62, doi: 10.1016/j.envpol.2018.03.008.
119. Pulit-Prociak, J.; Banach, M. Effect of process parameters on the size and shape of nano- and micrometric zinc oxide. Acta Chim. Slov. 2016, 63, 317–322, doi:10.17344/acsi.2016.2245322
120. Komarneni, S.; Bruno, M.; Mariani, E. Synthesis of ZnO with and without microwaves. Mater. Res. Bull. 2000, 35, 1843–1847, doi:10.1016/S0025-5408(00)00385-8.
121. Pulit-Prociak, J.; Banach, M. Effect of process parameters on the size and shape of nano- and micrometric zinc oxide. Acta Chim. Slov. 2016, 63, 317–322, doi:10.17344/acsi.2016.2245322.
122. Shaporev, S.; Ivanov, V.K.; Baranchikov, A.E.; Tret'yakov, Y.D. Microwave-assisted hydrothermal synthesis and photocatalytic activity of ZnO. Inorg. Mater. 2007, 43, 35–39, doi:10.1134/S0020168507010098.
123. 51. Huang, J.; Xia, C.; Cao, L.; Zeng, X. Facile microwave hydrothermal synthesis of zinc oxide one-dimensional nanostructure with three-dimensional morphology. Mater. Sci. Eng. B 2008, 150, 187–193, doi: 10.1016/j.mseb.2008.05.014.
124. Sadhukhan, P.; Kundu, M.; Rana, S.; Kumar, R.; Das, J.; Sil, P.C. Microwave induced synthesis of ZnO nanorods and their efficacy as a drug carrier with profound anticancer and antibacterial properties. Toxicol. Rep. 2019, 6, 176–185, doi: 10.1016/j.toxrep.2019.01.006.
125. Marzouqi, F.; Al Adawi, H.; Qi, K.; Liu, S.Y.; Kim, Y.; Selvaraj, R. A green approach to the microwave assisted synthesis of flower-like ZnO nanostructures for reduction of Cr(VI). Toxicol. Environ. Chem. 2019, 101, 1–21, doi:10.1080/02772248.2019.1635602.
126. Thongtem, T.; Phuruangrat, A.; Thongtem, S. Characterization of nanostructured ZnO produced by microwave irradiation. Ceram. Int. 2010, 36, 257–262, doi: 10.1016/j.ceramint.2009.07.027.
127. Kondawar, S.B.; Acharya, S.A.; Dhakate, S.R. Microwave assisted hydrothermally synthesized nanostructure zinc oxide reinforced polyaniline nanocomposites. Adv. Mater. Lett. 2011, 2, 362–367, doi:10.5185/amlett.2011.9107am2011.
128. Min, C.; Shen, X.; Sheng, W. Microwave-assisted aqueous synthesis of ultralong ZnO nanowires: Photoluminescence and photovoltaic performance for dye-sensitized solar cell. Appl. Phys. A. 2009, 96, 799– 803, doi:10.1007/s00339-009-5299-7.
129. Padmanabhan, S.C.; Ledwith, D.; Pillai, S.C.; McCormack, D.E.; Kelly, J.M. Microwave-assisted synthesis of ZnO micro-javelins. J. Mater. Chem. 2009, 19, 9250–9259, doi:10.1039/B912537J.
130. Hu, Z.-L.; Zhu, Y.-J.; Wang, S.-W. Sonochemical and microwave-assisted synthesis of linked singlecrystalline ZnO rods. Mater. Chem. Phys. 2004, 88, 421–426, doi: 10.1016/j.matchemphys.2004.08.010.
131. Wang, W.-W.; Zhu, Y.-J. Shape-controlled synthesis of zinc oxide by microwave heating using an imidazolium salt. Inorg. Chem. Commun. 2004, 7, 1003–1005, doi: 10.1016/j.inoche.2004.06.014
132. Phuruangrat, A.; Thongtem, T.; Thongtem, S. Controlling morphologies and growth mechanism of hexagonal prisms with planar and pyramid tips of ZnO microflowers by microwave radiation. Ceram. Int. 2014, 40, 9069–9076, doi: 10.1016/j.ceramint.2014.01.120.

CHAPTER :2

NANOTECHNOLOGY AND NANO MATERIALS

2.1 INTRODUCTION

The study of manipulating matter on an atomic and molecular scale is known as nanotechnology [1]. Nanotechnology, in general, is concerned with structures whose sizes range from 1 to 100 nm in at least one dimension, and it entails the development of materials with at least one dimension falling within that range. It covers a wide range of topics, from traditional device physics to completely new approaches based on molecular self-assembly, from nanoscale materials to determining whether we can control matter at the atomic level. It can make a variety of new materials with a wide range of applications, including medicine, biomaterials, electronics, and energy production. However, nanotechnology raises numerous concerns about the toxicity of nanomaterials, their impact on the environment, and their implications for global economics.

When nanoparticles are used to make traditional materials, their properties change. This is usually due to the fact that nanoparticles have a higher surface area per weight than larger particles, making them more reactive to other molecules. Nanoparticles are used in a variety of fields, or are being evaluated for use in a variety of fields. Nanoparticles are fascinating to scientists because they act as a link between bulk materials and atomic or molecular structures. A bulk material should have constant physical properties regardless of size, but size-dependent properties are frequently observed at the nanoscale. As a result, as a material's size approaches the nanoscale and the percentage of atoms on its surface begins to become significant, its properties change.

The percentage of atoms at the surface of bulk materials larger than one micrometre (or micron) is insignificant in comparison to the number of atoms in the bulk of the material [2]. The large surface area of the material, which dominates the contributions made by the small bulk of the material, is thus largely responsible for the interesting and sometimes unexpected properties of nanoparticles. Because nanoparticles are small enough to confine their electrons and produce quantum effects, they often have unexpected optical properties.

2.2 PROPERTIES OF NANOPARTICLES

- A bulk material should have constant physical properties regardless of size, but size-dependent properties are frequently observed at the nanoscale. As a result, as a material's size approaches the nanoscale and the percentage of atoms on its surface becomes significant, its properties change.
- The percentage of atoms at the surface of bulk materials larger than one micrometre (or micron) is insignificant in comparison to the number of atoms in the bulk of the material. The large surface area of the material, which dominates the contributions made by the small bulk of the material, is thus largely responsible for the interesting and sometimes unexpected properties of nanoparticles.
- Nanoparticles of yellow gold and grey silicon are red in colour; gold nanoparticles melt at much lower temperatures (nearly 300°C for 2.5 nm size) than gold slabs (1064°C); and solar absorption in photovoltaic cells is much higher in nanoparticle-based materials than in thin films of continuous sheets of material; the smaller the particles, the greater the solar absorption.
- Nanoparticle suspensions are possible because the particle surface's interaction with the solvent is strong enough to overcome density differences, which would otherwise result in a material sinking or floating in a liquid.
- Nanoparticles often have unexpected optical properties because they are small enough to confine their electrons and produce quantum effects. In solution, gold nanoparticles for example, appear deep red to black.

- Furthermore, nanoparticles have been discovered to impart additional properties to a variety of everyday products. The presence of titanium dioxide nanoparticles, for example, causes a self-cleaning effect and because the particles are so small, they cannot be seen. When compared to its bulk substitute, zinc oxide particles have been found to have superior UV blocking properties. This is one of the reasons why it is frequently used in the formulation of sunscreen lotions and it is completely photosensitive.
- Nanoparticles have a large surface area to volume ratio, which provides a powerful driving force for diffusion, especially at high temperatures.

2.3 APPLICATIONS OF NANOTECHNOLOGY

Nanotechnology is being used in a variety of fields of research, with a variety of unique applications. When a particle is shrunk to the nanoscale, the material's properties change in proportion to its size. As a result, it opens up new possibilities in a variety of fields. Because the surface to volume ratio increases as the size decreases, there is more surface area to react. The diameter or size of particles has an impact on a number of optical and mechanical properties.

• **Energy Sector**: Lithium-ion batteries have a higher capacity and a faster rate of discharge than traditional batteries. As an energy storage device, PV solar cells, photo capacitors and supercapacitors are used [3].

• **Electronics**: Nano-sensors based on silver, copper and a variety of other nanowires are used in space, automobiles and robotics applications [4].

• **Biological and medicinal science**: Near infrared-laser-heated gold-silica nanosheets are being used to destroy tumours in prostate cancer patients. Different types of nanoparticles are also being developed for targeted drug delivery in cancer therapy.

• **Defence and Security**: Nanotechnology will improve future combat soldiers' protection, lethality, endurance, and self-supporting capabilities. Threat detection, novel electronic display and interface systems, as well as a key role in the development of miniaturised unmanned combat vehicles and robotics are all expected to be significant benefits

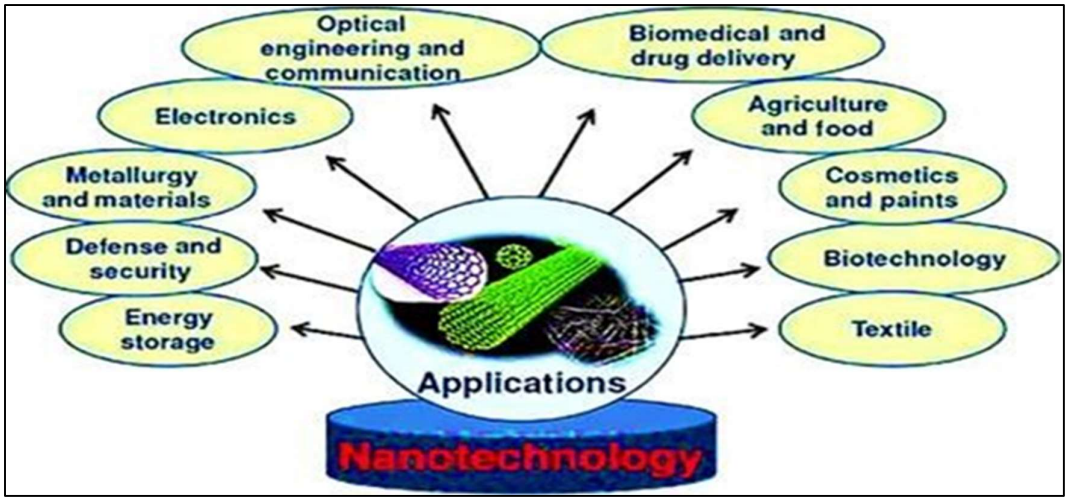

Figure 2.8: Applications of Nanotechnology.

References

1. http://www.aadet.com/article/nanoparticle, Nanoparticle Data.
2. http://www.reachinformation.com/define/nanoparticle.aspx Nanoparticles.
3. Application of Nanotechnologies in the Energy Sector Volume 9 of the series Aktionslinie Hessen- Nanotech of the Hessian Ministry of Economy, Transport, Urban and Regional Development.
4. Electrochemical Supercapacitors B.E. Conway Fellow of the Royal Society of Canada, University of Ottawa.

CHAPTER :3

FUNDAMENTAL PROPERTIES OF ZnO

3.1 ELECTRONIC BAND STRUCTURE

The band structure of any semiconductor is very important because it determines many important properties such as the band gap and effective electron and hole masses. Because the band structure determines the relationship between the energy and momentum of the carrier, a clear understanding of the band structure is important to explain the electrical properties and many other phenomena because it determines the most suitable semiconductor among all his family members for ultraviolet lasing at room temperature, device application, as well as possibilities to engineer the band gap.

The most important thing is to understand the band gap between occupied and empty bands. This is the difference in energy between the full and empty states. The valence band is made up of these filled states, and the energy at the top of the valence band is usually zero, referred to as the valence band edge. The conduction band refers to the empty states above the gap. The conduction band edge is the lowest point in the conduction band. For ZnO, the conduction band edge is at k= 0, which is also the valence band edge's k-value. The material is known as a direct band gap semiconductor because the valence band and conduction band edges occur at the same k-values in ZnO [1, 2].

3.2 OPTICAL PROPERTIES

Both intrinsic and extrinsic effects are linked to a semiconductor's optical properties. Between electrons in the conduction band and holes in the valence band, intrinsic optical transitions occur, including excitonic effects. The main requirement for exciton formation is that the electron and hole have the same group velocity. Excitons are divided into two categories: free and bound excitons. The free exciton can exhibit excited states in addition to ground-state transitions in high-quality samples with low impurity concentrations. Extrinsic properties are associated with dopants or defects, which create discrete electronic states in the band gap and thus affect both optical absorption and emission processes [9].

Zinc oxide [3] is transparent to visible light but absorbs ultra violet light below 3655 A very strongly. White pigments absorb more light than other white pigments. Zinc oxide is photoconductive when exposed to ultra violet light. Solar cells require a transparent conductive coating, and the best materials are indium tin oxide and zinc oxide. The photoluminescence spectra of ZnO nanorods have revealed excitonic emissions. These findings suggest that ZnO nanostructures could be useful components in integrated optoelectronic circuits [4].

3.3 THERMAL CONDUCTIVITY

The kinetic nature of thermal conductivity (k) is determined by vibration, rotation, and electronic degrees of freedom. When semiconductors are used in high-power, high-temperature, or optoelectronic devices, this property is extremely important. The electronic thermal conductivity is very low, with a negligible light carrier concentration. The thermal conductivity of a ZnO material is affected by point defects such as vacancies, impurities, and isotope fluctuations.

At temperatures ranging from room temperature to 1000°C, the thermal conductivity of fully sintered ZnO is measured. As the temperature rises from room temperature to 1000 °C, the

thermal conductivity drops from 37 to 4 W/m K. Resistive phonon-phonon interactions are the most common scattering mechanism [5].

3.4 ELECTRICAL PROPERTIES

A device made of a material with a larger band gap, for example, may have a higher breakdown voltage, lower noise generation, and be able to operate at higher temperatures while consuming more power. At low and high electric fields, electron transport in semiconductors performs differently. The energy distribution of electrons in ZnO is unaffected by low electric fields because the electrons can't get much energy from the applied electrical field compared to their thermal energy. Because the scattering rate, which determines electron mobility, does not change much, the electron mobility will remain constant.

The energy of the electrons from the applied electrical field is equal to the thermal energy of the electron when the electrical field is increased. The electron distribution function deviates from its equilibrium value significantly. These electrons become hot electrons, whose temperature exceeds that of the lattice. As a result, there is no energy loss to the lattice during a critical period. It is possible to make a higher frequency device when the electron drift velocity is greater than its steady-state value [9]. Higher breakdown voltages, the ability to sustain large electric fields, and high-temperature and high-power operations are all advantages of a large band gap [6].

3.5 PROPERTIES OF ZnO

The basic physical parameters for ZnO are listed in the table below [7, 8].

Table 3.3: Basic physical properties of ZnO

Property	Value
Lattice parameters at 300 K	
a_0	0.324 95 nm
c_0	0.520 69 nm
a_0/c_0	1.602 (ideal hexagonal structure shows 1.633)
u	0.345
Density	5.606 g cm^{-3}
Stable phase at 300 K	Wurtzite
Bond length	1.977µm
Melting point	1975 ◦C
Thermal conductivity	0.6, 1–1.2
Linear expansion coefficient (/C)	a_0: 6.5 × 10^{-6}
	c_0:3.9 x 10^{-6}
Static dielectric constant	8.656
Refractive index	2.008, 2.029
Energy gap	3.4 eV, direct
Intrinsic carrier concentration	<106 cm^{-3}
Breakdown voltage (10^6 V cm^{-1})	5.0
Saturation velocity (10^7 cms^{-1})	3.0
Exciton binding energy	60 meV
Electron effective mass	0.24
Electron Hall mobility at 300 K for low n-type conductivity	200 cm^2 V−1 s^{-1}
Hole effective mass	0.59
Hole Hall mobility at 300 K for low p-type conductivity	5–50 cm^2 V−1 s^{-1}
Knoop hardness	0.5N/cm^2
Minimum pressure at melting point	7.82atm
Ionicity	62%
Heat capacity Cp	9.6 cal/molK
Heat of crystallization ΔHls	62KJ/mol
Young's modulus E (bulk ZnO)	111.2±4.7 GPa
Bulk modulus, B (Polycrystalline ZnO)	142.2 Gpa
dB/dP	3.6
Spontaneous polarization (C/m^2)	-0.057
Born effective charge*	2.10

References

1. Ivanov and J. Pollmann, Phys. Rev. B 24. 7273-7276 (1981).
2. W. Göpel, J. Pollmann, I. Ivanov and B. Reihl, Phys. Rev. B 26 (1982) 3144-3150.
3. Ü. Özgür, Ya. I. Alivov, C. Liu, A. Teke, M. A. Reshchikov, S. Doğan, V. Avrutin, S.J. Cho and H. Morkoçd, journal of applied physics **98**,041301(2005).
4. http://www.scribd.com/doc/43567667/Next-Generation-Technology-1
5. T. Olorunyolemi, A. Birnboim, Y. Carmel, O. C. Wilson, Jr., and I. K. Lloyd, J. Am. Ceram. Soc. 85, 1249 (2002).
6. http://www.aadet.com/article/nanoparticle, Nanoparticle Data.
7. S.J. Pearton, D.P. Norton, K. Ip, Y.W. Heo, T. Steinerb, Superlattices and Microstructures 3429–32 (2003).
8. www.semiconducators.co.uk
9. http://www.znoxide.org/properties.html Physical Properties of Zinc Oxide - CAS 1314-13-2 International Zinc Association.

CHAPTER :4

ZnO AS PHOTODETECTOR

4.1 INTRODUCTION

Measurement and monitoring of ultraviolet (UV) radiation in various military and civil situations are extremely important. UV detectors have found applications in missile warning systems, UV astronomy, ozone layer monitoring, environmental monitoring, high-temperature flame and fire detection etc [1].

Currently, the development of ultraviolet (UV) photodetectors (PDs) has attracted the attention of the research community because of the vast range of applications of photodetectors in modern society. A variety of wide-band gap nanomaterials have been utilized for UV detection to achieve higher photosensitivity. Specifically, zinc oxide (ZnO) nanomaterials have attracted significant attention primarily due to their additional properties such as piezo-phototronic and pyro-phototronic effects, which allow the fabrication of high-performance and low power consumption-based UV PDs.

A photodetector is a device which converts the energy of photons to electrical energy, usually expressed as a photocurrent or photovoltage. Depending upon the material properties of the photodetectors, it can be used for the detection of optical signals over a range of the electromagnetic spectrum. However, a detector is usually selected based on the requirements of a particular application

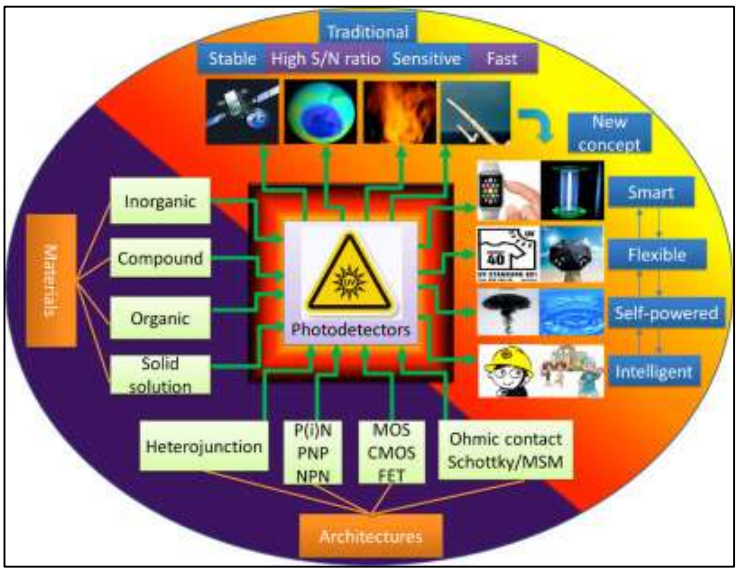

Figure 4.9. A technology roadmap leading to next generational UV photodetectors.

4.2 ZnO AS A POTENTIAL MATERIAL FOR PHOTODETECTOR

ZnO, which is a promising environmentally friendly material, has widely been deployed in the fabrication of UV photodetectors. It is well known that ZnO is a wide-bandgap semiconductor with a direct bandgap of 3.37 eV at 300 K, a high exciton binding energy of 60 meV, an excellent radiation hardness and a large photo response [2].

The general requirements include wavelength of light to be detected, sensitivity level and the response speed of the detector. Most of the photodetectors respond uniformly within a specific range of the electromagnetic radiation. Therefore, the wavelength of light to be detected determines the selection of a photodetector material and the target application. The various applications where the photodetectors play an important role are such as sensing, biological research, detection and missile launch etc.

The nanomaterials as an active light collection region in photodetectors have become an attractive research topic due to their high surface-to-volume ratio and also more freedom in the design of material properties. However, there are a number of photodetector materials depending upon the applications but ZnO based photodetectors have become popular in recent years particularly due to its low cost, non-toxicity and stability against photo corrosion.

Furthermore, ZnO nanostructures have very high internal photoconductivity gain due to the surface-enhanced electron-hole separation efficiency. The interest is also because it is a rich family of nanostructures, versatile and low-cost synthesis processes large excitonic binding energy. The ZnO as a photodetector is used in the form of single crystals ZnO, polycrystalline ZnO films, and nanostructures of ZnO. Generally, the performance of ZnO based photodetector depends upon the deposition techniques, growth conditions, measurement ambient, structure, porosity, presence of defects and orientation of the crystallites etc.

One of the most promising semiconductor materials is ZnO because of its wide band gap (≈ 3.3 eV), restricts its performance to UV region. To expand its performance to visible region, many strategies have been reported such as creation of oxygen vacancy defects, doping with metals and nonmetals, cations, anions and combining with another semiconductor material. However, most of these methods often need a higher process temperature and pressure, complicated and expensive equipment. Among these strategies, the creation of oxygen defects states in the synthesized ZnO nanostructures is an efficient way to fabricate ZnO nanostructure-based photodetector.

Once the oxygen defects are created, the ZnO nanostructures due to their high surface area exhibit higher photo response due to extended absorption in the visible region. We know that the oxygen vacancy defects are kind of self-doping without addition of external impurities which enhances the visible photocatalytic activity by narrowing the bandgap. Identifying the importance of oxygen vacancy defects, it is important to find a simple method to create oxygen vacancies inside synthesized ZnO nanostructures in order to work them in the visible region.

The undoped ZnO is an n-type semiconductor due to the presence of donor centers like zinc interstitials and oxygen vacancies. The dangling bonds due to a breaking of the periodicity of ZnO lattice on its surface induce acceptor-type surface states which serve as charge traps and electron barriers. Therefore, the surface states of ZnO nanostructures play a crucial role in the optical properties of ZnO nanostructures. In many reported studies, the ZnO has been used as a visible-light photodetector by doping with some suitable dopant material or combining it with a material having low band gap. However, to the best of our knowledge, there are few studies which report the photodetection property of ZnO in visible range without modifications. The high sensitivity in the short-wavelength spectral range, linearity of the dependence of the photocurrent on the incident power density, fast response, and compatibility with integrated-circuit technology make them especially attractive for such applications.

Here in this thesis, we investigated visible-light photo response of nano structural morphologies of ZnO synthesized by a Hydrothermal method. The oxygen vacancy defects effectively extend the absorption of ZnO nanostructures to the visible light range. The distinct and fast photo response of the device is a direct result of enhanced charge transfer between surface defects and ZnO nanostructures in visible region. This work will provide a new perspective on preparation and utilization of ZnO semiconductor for energy applications in visible region.

References

1. E. Monroy, F. Omne` s, and F. Calle, B Wide-bandgap semiconductor ultraviolet photodetectors, [Semicond. Sci.Technol., vol. 8, no. 4, pp. R33–R51, Mar. 2003.
2. U¨. O¨zgu¨ r, Y. I. Alivov, C. Liu, A. Teke, M. A. Reshchikov, S. Doan, V. Avrutin, S. J. Cho, and H. Morkoc¸, BA comprehensive review of ZnO materials and devices, J. Appl. Phys., vol. 98, no. 4, pp. 041 301-1–041 301-103, Aug. 2005.

CHAPTER :5

PET SUBSTRATE

5.1 INTRODUCTION

Polyester is one of the most important classes of polymers in use today. Hundreds of polyesters exist although only about a dozen are of commercial significance. Although there are many types of polyester, the term "polyester" as a specific material most commonly refers to polyethylene terephthalate (PET). Polyethylene terephthalate, commonly abbreviated as PET, PETE or the obsolete PETP or PET-P, is a thermoplastic polymer resin of the polyester family. The applications of Polyethylene terephthalate (PET) can be divided into three major categories: fiber, bottles, and industrial use. It can be used in synthetic fibers; beverage, food and other liquid containers; film, plastic and engineering resins often in combination with glass fiber. The two widely used applications are PET fabrics and PET bottles.

5.2 PROPERTIES OF POLYETHYLENE TEREPHTHALATE (PET)

5.2.1 INTRODUCTION

Polyethylene terephthalate (PET) exists both as an amorphous (transparent) and a semi-crystalline (opaque and white) thermoplastic. Generally, it has good resistance to mineral oils, solvents and acids but not to bases. The semi-crystalline PET has good strength, ductility, stiffness and hardness while the amorphous PET has better ductility. PET also has good process ability and can be recycled for other applications.

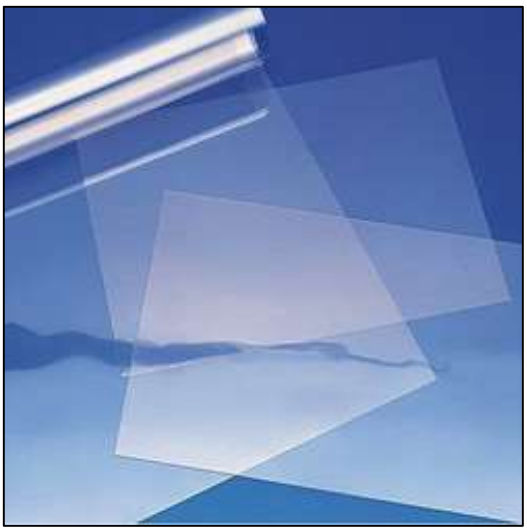

Figure 5.10: PET Substrate

5.2.2 TYPICAL PROPERTIES OF PET

- High hardness, stiffness and strength in thermoplastic
- Low friction and high abrasion resistance
- High dimensional stability
- Service temperature range, from -40°C to 100°C
- In the semi-crystalline state, it is white
- In the amorphous state it is transparent (glass clear)
- High tracking resistance
- Physiologically acceptable

• Resistant to water at room temperature, dilute acids, neutral and acidic salts, alcohol, ethers, oils, fats, aromatic and aliphatic hydrocarbons.

• Not resistant to alkalis, superheated steam, phenols, esters, oxidizing acids and chlorinated hydrocarbons

• Resistant to stress cracking

• Amorphous PET has slightly lower hardness, stiffness and heat resistance than crystalline PET, but has higher toughness.

5.3 APPLICATIONS OF POLYETHYLENE TEREPHTHALATE (PET)

5.3.1 OVERVIEW

The majority of the world's PET production is for synthetic fibers (in excess of 60%) with bottle production accounting for around 30% and production for industrial use accounting for around 10% of global demand. The polyester industry makes up about 18% of world polymer production. PET Fabrics can have a synthetic feel when compared to fabrics made from natural materials. However, polyester does have the advantage of better wrinkle resistance and is often spun together with natural fibers such as cotton and wool to produce a fabric with blended properties. Polyester is the largest synthetic fiber used in the world.

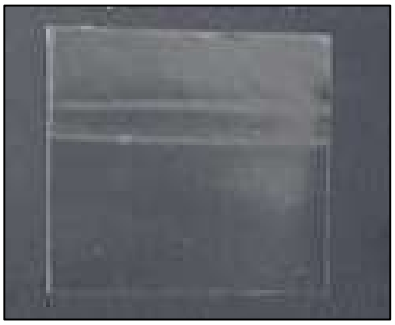

Figure 5.11: PET Films

5.3.2 PET BOTTLES

PET has taken market share in the bottled water market due to its good clarity and not leaving any taste in the water. PET has good barrier properties against oxygen and carbon dioxide. Its chemical inertness and physical properties made it particularly suitable in food packaging applications, especially in beverages and drinking water. It has also found applications in more niche markets such as sports drinks and fruit juices, and is used to make bottles for cooking and salad oils, sauces and dressings.

PET packaging markets have seen very strong growth over the last 20 years. It first penetrated the carbonated soft drinks market because it is lightweight and strong. PET bottles are virtually unbreakable while a typical 1.5 litre bottle weighs about 40-45 gm, about one-tenth the weight of glass.

5.3.3 PET FILMS

Polyethylene terephthalate or PET film is a thermoplastic polymer commonly referred to as polyester film. Polyester film is one of the most common substrates used in the converting industry because of its balance of properties in relation to other thermoplastic polymers. Additionally, polyester film is available in many variations, engineered for specific applications, this combined with the processing tolerance of PET films makes it a good substrate for a variety of applications.

5.3.4 ENGINEERING PLASTIC

PET also as engineering plastics is used in electronic, electrical and other fields, such as instrument case, hot air masks.

5.4 MARKET PERSPECTIVES OF PET INDUSTRY

5.4.1 WORLD MARKET

Market perspectives look good for Polyethylene Terephthalate in middle-term period. World PET capacity will increase slower than demand bringing the market to balance. With average annual growth of 3.5% global capacity will reach 24.4mln tons/year.

The Global PET Market is expected to grow in the Forecast Period after Recovery from Economic Slowdown. The global demand for PET was growing fast over the last decade. The effect of the economic slowdown has adversely affected the consumption of various commodities in many countries globally. Hence, demand for PET has also slowed down over the past two years. The global PET market in 2009 was 15.3 million tons. As the economies recover from the slowdown, the consumption of commodities will rise again and the global demand for PET will grow by 4.9%.

Not considering the fabrics production, the largest PET consuming markets are Carbonated Soft Drinks and Bottled Water. CSD is the largest market for PET globally. Because of its light weight, toughness and clarity, PET is the most preferred material for CSD bottles. Bottled water is the second biggest PET consuming market globally. However, the packaged food segment is also a very important and growing market for PET. The beer market is largely untapped but has strong potential for growth with regard to PET applications.

5.4.2 ASIAN MARKET

Asia is the Largest Consumer of PET followed by Europe. The demand for PET is highest in Asia. China is driving the majority of the demand for PET in the world. The demand in advanced countries like Japan has largely stabilized. With the large population in countries such as India and China, there is a huge consumption potential in these countries. The Asian demand by volume for PET in 2009 was nearly 4.7 million tons. The unparalleled growth of carbonated soft drinks and bottled water industries and thus the packaging industry can be primarily attributed to the changing lifestyles of people in the developing countries. Taking into account that India and China are heavily populated, it does not come as a surprise that these economies are key regional drivers for the global polyethylene terephthalate demand.

References

1. John Scheirs, Timothy E. Long, “Modern polyesters: chemistry and technology of polyesters and copolyesters”, John Wiley and Sons, 2003.
2. Tony Yu Long River, Xu Chi polyester fiber Manual (2nd edition), Textile Industry Press, 1995.08.

CHAPTER: 6

PROCESS AND SYNTHESIS

6.1 HYDROTHERMAL PROCESS

6.1.1 INTRODUCTION

The hydrothermal synthesis was defined in the literature [1] as a process in a closed system, in which chemical reactions take place exclusively in a water solvent at increased temperatures, at a pressure that is higher than atmospheric pressure (P > 101,325 Pa). This definition is often modified by scholars, e.g., Byrappa and Yoshimura [2] proposed a definition of the "hydrothermal reaction" as any heterogeneous chemical reaction in the presence of a solvent (whether aqueous or non-aqueous) above the room temperature and at a pressure greater than 1 atm in a closed system. For the purposes of this review, we assume that the "hydrothermal synthesis" is a process occurring in an aqueous environment (where $mH_2O > 50\%$), with the pressure equal to or higher than atmospheric pressure. In hydrothermal processes, reaction products are mainly oxides and salts due to the properties of water as a solvent.

Solvothermal synthesis is a method for preparing a variety of materials such as metals, semiconductors, ceramics, and polymers. The process involves the use of a solvent under moderate to high pressure (typically between 1 atm and 10,000 atm) and temperature (typically between 100 °C and 1000 °C) that facilitates the interaction of precursors during synthesis. If water is used as the solvent, the method is called 'hydrothermal synthesis'. The synthesis under hydrothermal conditions is usually performed below the supercritical temperature of water (374 °C). The process can be used to prepare structures wth various morphologies including thin films, bulk powders, single crystals, and nanocrystals.

In addition, the morphology (sphere (3D), rod (2D), or wire (1D)) of the crystals formed is controlled by manipulating the solvent supersaturation, concentration of chemical of interest, and kinetic control. The method can be used to prepare thermodynamically stable and metastable states including novel materials that cannot be easily formed from other synthetic routes [3]. An example of a hydrothermal reaction is the synthesis of zinc oxide as proposed by Chen et al. [4], using the reagents $ZnCl_2$ and NaOH in a ratio of 1:2, in an aqueous environment.

A hydrothermal process was also used by Ismail et al. [5] using $Zn(CH_3COO)_2$ and NaOH carried out in the presence of hexamethylenetetramine (HMTA), at room temperature. The shape of the particles is also affected by the time and temperature of the hydrothermal process. With an increase in time, temperature and surfactant concentration, the size of the particles increases. Musić et al. [6] determined the effect of chemical synthesis on the size and properties of ZnO particles. A suspension obtained from a solution of $Zn(CH_3COO)_2 \cdot 2H_2O$ and neutralized using different quantities of a solution of NH_4OH underwent hydrothermal treatment in an autoclave at a temperature of 160 °C. A number of studies [7-9] have shown that the use of microwave reactors in hydrothermal synthesis processes brings significant benefits.

ABOUT THE THESIS PRESENTED HERE

I have looked upon the basic synthesis procedures of nanoparticles. Having my first laboratory experience carried out, I have concentrated upon the basic synthesis process for synthesizing Zinc oxide nanoparticles i.e., the Hydrothermal synthesis. Various characterizations were also carried out in order to know the optical properties and surface morphologies as well as ohmic characteristics of the samples.

6.1.2 ADVANTAGES OF THE HYDROTHERMAL METHOD

I. Possible to precipitate powders directly from solution
II. Ability to synthesize crystals of substances which are unstable near melting point
III. Suitable when it is difficult to dissolve precursors at room or lower temperatures
IV. Can be hybridised with other processes like microwave, ultrasound etc [10].

6.1.3 DISADVANTAGES OF THE HYDROTHERMAL METHOD

I. High cost of equipment e.g., the need of expensive autoclaves.

II. Inability to observe the crystals in the process of their growth [11, 12].

6.2 REACTANTS

The most popular reactants of the "Zn^{2+}" zinc cation precursor used for ZnO synthesis according to the data derived from the literature review [13–46] are Zn $(NO_3)_2 \cdot 6H_2O$, $Zn(CH_3COO)_2 \cdot 2H_2O$, $ZnCl_2$, $ZnSO_4 \cdot 7H_2O$ and ZnO respectively. The popularity of these reactants stems from their low price and easy availability. Reactants being a source of "Zn^{2+}" ions are commonly produced at a large scale mostly by several producers in each developed country.

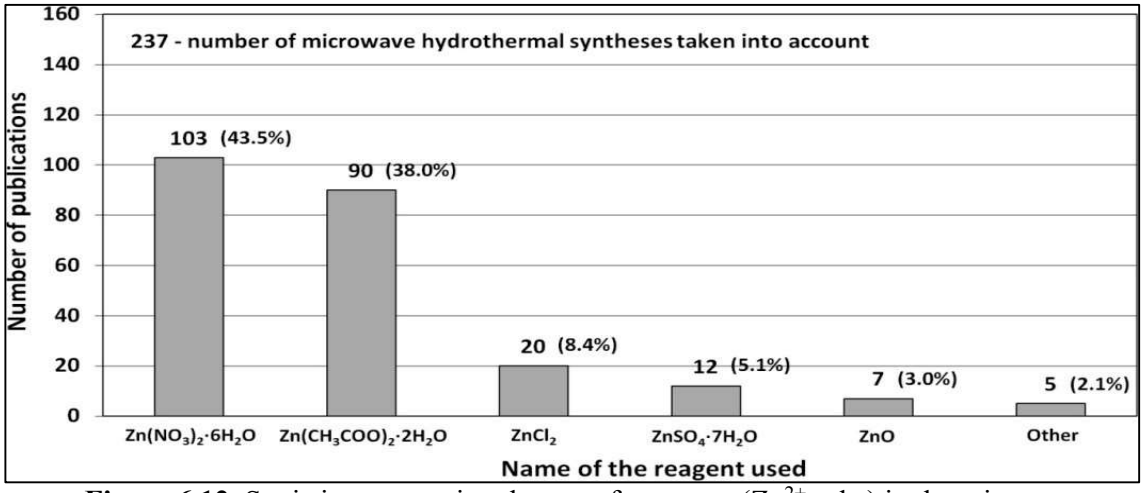

Figure 6.12. Statistics concerning the use of reactants (Zn^{2+} salts) in the microwave hydrothermal synthesis of ZnO.

It should be emphasised that $ZnCl_2$ is one of the problematic reactants, which arises from the possibility that during the ZnO synthesis a stable by-product (impurity), called simonkolleite ($Zn_5(OH)_8Cl_2 \cdot H_2O$), is formed. If $Zn(NO_3)_2 \cdot 6H_2O$ is used as the reactant and if the temperature of the ZnO synthesis is too low (below 100 °C), one of the synthesis by-products (impurity) may be the salt $Zn_5(OH)_8(NO_3)_2 \cdot 2H_2O$ [14]. It must be borne in mind that ZnO obtained by the hydrothermal method, depending on the parameters employed (T, P, pH), may contain impurities being hydroxides, oxide hydroxides or basic salts.

The most popular reactants being hydroxide anion precursor chemicals "OH^-" used for the ZnO synthesis according to the data derived from the literature review [13-46] are sodium hydroxide (NaOH), ammonia water ($NH_3 \cdot H_2O$, $NH_4(OH)$), potassium hydroxide (KOH) etc.

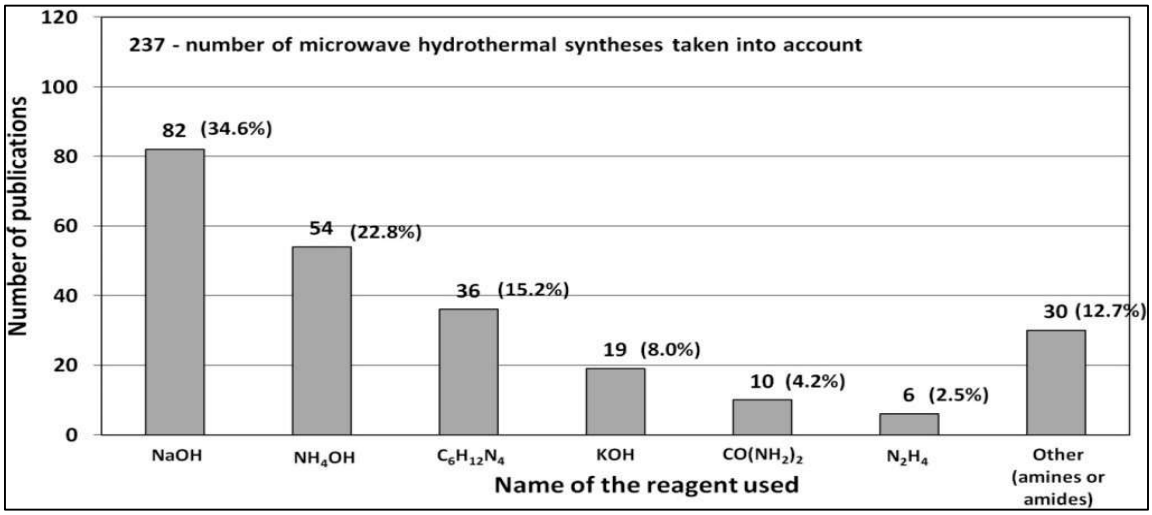

Figure 6.13. Statistics concerning the use of reactants (OH−) in the microwave hydrothermal synthesis of ZnO

Figure 6.14: Reactants used in my thesis

6.3 GROWTH TECHNIQUES

There are various techniques that have been adopted for the growth of ZnO layers.According to literatures, ZnO epitaxial films have been achieved by molecular beam epitaxy (MBE), having the main advantage of this technique is the precise control over the deposition parameters and capability of layer-by layer growth with excellent control of the purity and crystalline quality of the film. However, the growth speed is very slow and for this reason, growth of ZnO single crystal is very difficult.

Magnetron sputtering (DC sputtering, RF magnetron sputtering and reactive sputtering), as compared to the Sol-gel and Chemical vapor deposition, has been known as a perfect method because of its low cost, simplicity and low operating temperature. Pulsed laser deposition (PLD) is the most attractive one among these features that it has the ability to create high energy source particles, permitting the growth of high-quality material up to a point in a wide range of substrate temperatures typically ranging from 2000 to 8000 C.

However, this technique is not easily adaptable to a large area substrate. In some papers pulsed laser deposition (PLD) with different variants like electron cyclotron resonance assisted PLD, femtosecond and nanosecond PLD, UV assisted or radical assisted PLD has been used for the growth of ZnO layers [47,48]. Although spray pyrolysis is a low-cost method used for deposition of highly orientated ZnO films that may be useful for laser applications.

In this process plane orientation determines the epitaxial relationship between film and substrate, which means that in-plane orientations of the ZnO unit cells in the film are probably different from place to place. But in epitaxial growth, it is necessary that unit cells have the same in-plane orientation along the growth direction. To gain the high quality of ZnO film a lot of different techniques like, close spaced vapor transport (CSVT), post annealing of zinc implanted silica, thermal oxidation of ZnS or Zn, hydrothermal method, screen printing, radical beam getter epitaxy, plasma-assisted or electron cyclotron resonance-assisted, seed vapor phase (SVP) has been used so for.

6.4 TWO TYPES OF HYDROTHERMAL SYNTHESIS PROCESS

ZnO NRs prepared by the LT-HM can be a good choice in other applications where recombination is important such as OLEDS or mechanical energy harvesting (piezoelectric) devices.

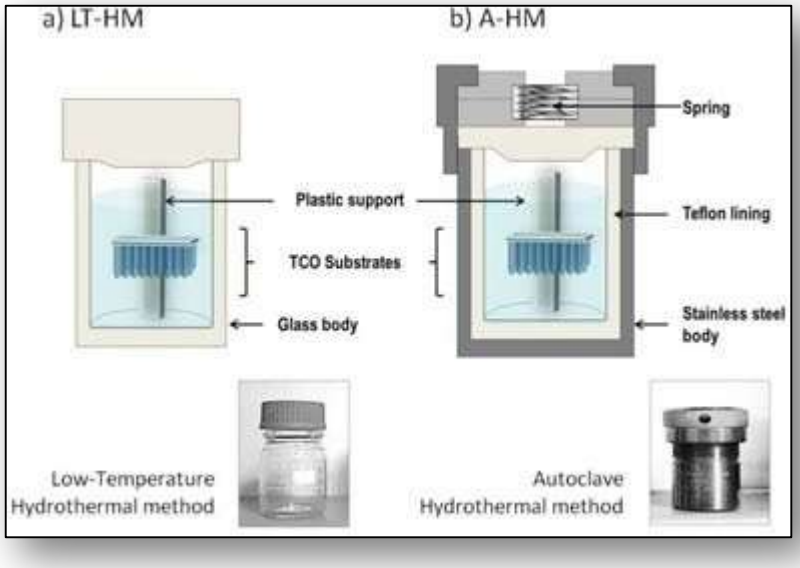

Figure 6.15: Schematic representation of both hydrothermal reactors and their images from a) the low-temperature hydrothermal method (LT-HM) and b) the autoclave hydrothermal method (A- HM).

Figure 6.16. Low temperature hydrothermal reactor vessel

6.5 SYNTHESIS OF ZnO NANOSTRUCTURES

ZnO nanostructures were prepared using different concentrations of sodium hydroxide (NaOH) (0.75M i.e., 0.75 gm, 1.00M i.e., 1.00 gm and 1.25M i.e., 1.25 gms) with zinc nitrate hexahydrate (Zn $(NO_3)_2.6H_2O$) (0.04M) using hydrothermal method. At first, the ITO coated PET substrate was dipped in 40 ml of DI water and sonicated for 30 mins to remove the coating of ITO. Then, zinc nitrate hexahydrate (Zn $(NO_3)_2.6H_2O$) of 0.04M i.e., 0.2975 gm was dissolved into deionized (DI) water of 25ml concentration. An alkaline aqueous solution prepared by mixing different concentrations of NaOH into 25 ml of DI water, that was added dropwise in the zinc nitrate hexahydrate solution, followed by vigorous stirring. Then, by removing the ITO coating, the substrate was dipped into the solution by checking the conducting side and was wrapped by Teflon. Finally, the whole mixture was subjected to a hydrothermal reaction at 100°C for 3hours. After reaction, ZnO nanoparticles are formed on the PET substrate.

$$Zn(NO_3)_2 .6H_2O \overset{H_2O}{\longleftrightarrow} Zn^{2+} + 2NO_3^-$$

$$NaOH \overset{H_2O}{\longleftrightarrow} Na^+ + OH^-$$

$$Zn^{2+} + 4OH^- \overset{H_2O}{\longleftrightarrow} Zn(OH)_4^{2-}$$

$$Zn(OH)_4^{2-} \overset{MH}{\longleftrightarrow} ZnO + H_2O + 2OH^-$$

Table 6.4: Parameters for the synthesis of ZnO nanostructures.

PRECURSORS	REACTANT'S AMOUNT	pH VARIATIONS	STIRRING TIME
Zn $(NO_3)_2.6H_2O$ NaOH	0.04M in 25ml DI 0.75M in 25ml DI	11	15 mins
Zn $(NO_3)_2.6H_2O$ NaOH	0.04M in 25ml DI 1.00M in 25ml DI	12	20 mins
Zn $(NO_3)_2.6H_2O$ NaOH	0.04M in 25ml DI 1.25M in 25ml DI	13 or tends to 14	25 mins

Figure 6.17: Stirring machine

Figure 6.18: Ultra sonicate machine

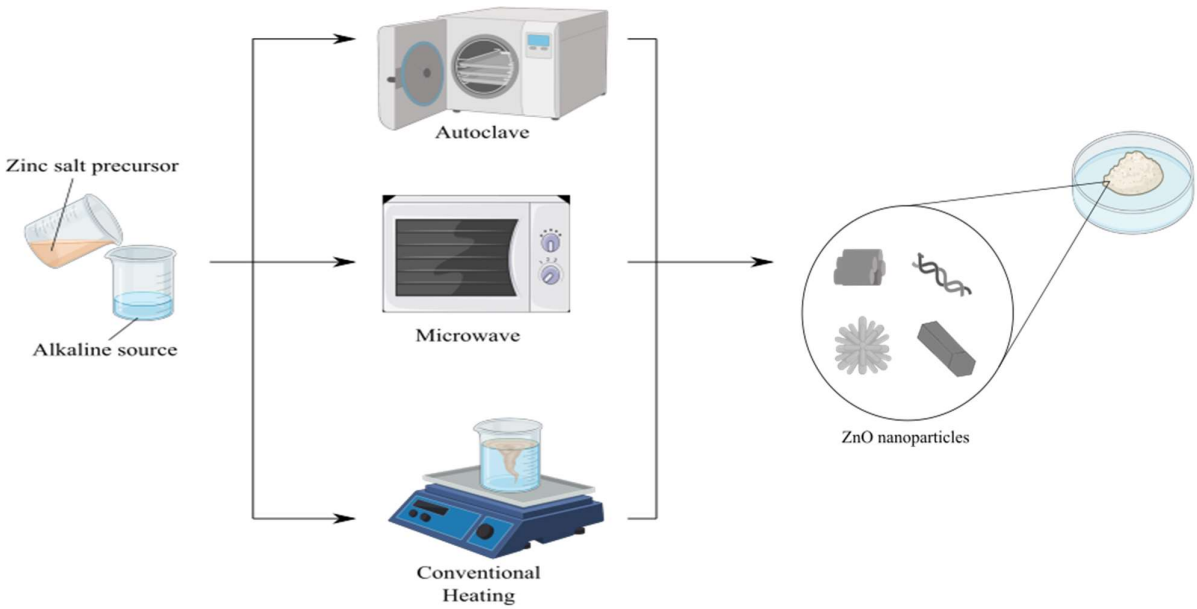

Figure 6.19: Pictorial representation of ZnO formation

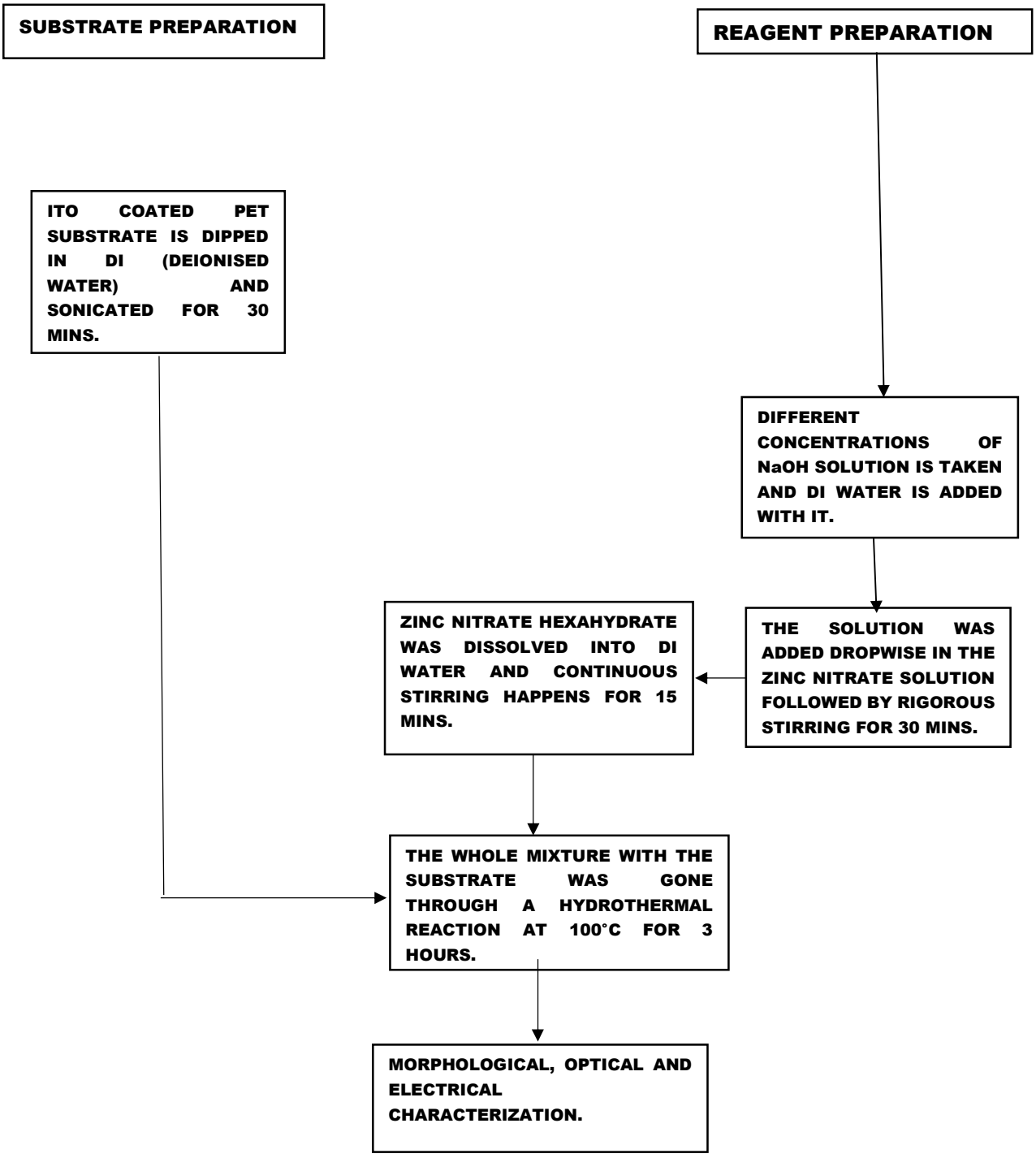

Flowchart 6.1: Synthesis procedure of ZnO formation

References

1. Byrappaa, K.; Adschirib, T. Hydrothermal technology for nanotechnology. Prog. Cryst. Growth Ch. Mater. 2017, 53, 117–166, doi: 10.1016/j.pcrysgrow.2007.04.001.
2. Byrappa, K.; Yoshimura, M. Handbook of Hydrothermal Technology, 1st ed.; Noyes Publications: Norwich, NJ, USA, 2001.
3. B. Djuri cić, X. Y. Chen and Y. H. Lung, Recent Pat. Nanotechnol., 2012, 6, 124.
4. D. Chen, X. Ciao and G. Cheng, Solid State Commun., 2000, 113, 363.
5. A. A. Ismail, A. El-Midany, E. A. Abdel-Aal and H. El-Shall, Mater. Lett., 2005, 59, 1924.
6. S. Musić, D. Dragčević, S. Popović and M. Ivanda, Mater. Lett., 2005, 59, 2388.
7. S. J. Chen, L. H. Li, X. T. Chen, Z. Xue, J. M. Hong and X. Z. You, J. Cryst. Growth, 2003, 252, 184.
8. J. Zhang, J. Wang, S. Zhou, K. Duan, B. Feng, J. Weng, H. Tang and P. Wu, J. Mater. Chem., 2010, 20, 9798.
9. J. Ma, J. Liu, Y. Bao, Z. Zhu, X. Wang and J. Zhang, Ceram. Int., 2013, 39, 2803.
10. A. Sengupta and C. Sarker, Eds., Introduction to Nano: Basics to Nanoscience and Nanotechnology, Berlin: Springer, 2015.
11. "Hydrothermalsynthesis,"[Online]Available: https://en.wikipedia.org/wiki/Hydrothermal_synthesis. [Accessed 17 May 2016].
12. "Hydrothermal synthesis," [Online]. Available: http://eng.thesaurus.rusnano.com/wiki/article729. [Accessed 26 August 2016].
13. Pulit-Prociak, J.; Banach, M. Effect of process parameters on the size and shape of nano- and micrometric zinc oxide. Acta Chim. Slov. 2016, 63, 317–322, doi:10.17344/acsi.2016.2245322.
14. Strachowski, T.; Grzanka, E.; Palosz, B.F.; Presz, A.; Ślusarski, L.; Łojkowski, Ł. Microwave driven hydrothermal synthesis of zinc oxide nanopowders. Solid State Phenom. 2003, 94, 189–192, doi: 10.4028/www.scientific.net/SSP.94.189.
15. Lu, C.-H.; Hwang, W.-J.; Godbole, S.V. Microwave-hydrothermal synthesis and photoluminescence characteristics of zinc oxide powders. J. Mater. Res. 2005, 20, 464–471, doi:10.1557/JMR.2005.0067.
16. Shaporev, S.; Ivanov, V.K.; Baranchikov, A.E.; Tret'yakov, Y.D. Microwave-assisted hydrothermal synthesis and photocatalytic activity of ZnO. Inorg. Mater. 2007, 43, 35–39, doi:10.1134/S0020168507010098.
17. Huang, J.; Xia, C.; Cao, L.; Zeng, X. Facile microwave hydrothermal synthesis of zinc oxide one-dimensional nanostructure with three-dimensional morphology. Mater. Sci. Eng. B 2008, 150, 187–193, doi: 10.1016/j.mseb.2008.05.014.
18. Ma, M.G.; Zhu, Y.J.; Cheng, G.F.; Huang, Y.H. Microwave synthesis and characterization of ZnO with various morphologies. Mater. Lett. 2008, 62, 507–510, doi: 10.1016/j.matlet.2007.05.072.
19. Chen, L.; Xie, H. Synthesis of ZnO microcrystals with controllable morphology by microwave reaction. In 2009 Symposium on Photonics and Optoelectronics; IEEE: Piscataway, NJ, USA, 2009; pp. 1–3.
20. Krishnakumar, T.; Jayaprakash, R.; Pinna, N.; Singh, V.N.; Mehta, B.R.; Phani, A.R. Microwave-assisted synthesis and characterization of flower shaped zinc oxide nanostructures. Mater. Lett. 2009, 63, 242–245, doi: 10.1016/j.matlet.2008.10.008.
21. Padmanabhan, S.C.; Ledwith, D.; Pillai, S.C.; McCormack, D.E.; Kelly, J.M. Microwave-assisted synthesis of ZnO micro-javelins. J. Mater. Chem. 2009, 19, 9250–9259, doi:10.1039/B912537J.

22. Phuruangrat, A.; Thongtem, T.; Thongtem, S. Microwave-assisted synthesis of ZnO nanostructure flowers. Mater. Lett. 2009, 63, 1224–1226, doi: 10.1016/j.matlet.2009.02.049.
23. Zhu, J.Y.; Zhang, J.X.; Zhou, H.F.; Qin, W.Q.; Chai, L.Y.; Hu, Y.H. Microwave-assisted synthesis and characterization of ZnO-nanorod arrays. Trans. Nonferrous Met. Soc. China 2009, 19, 1578–1582, doi:10.1016/S1003-632660073-X.
24. Wu, S.S.; Jia, Q.M.; Sun, Y.L.; Shan, S.Y.; Jiang, L.H.; Wang, Y.M. Microwave-hydrothermal preparation of flower-like ZnO microstructure and its photocatalytic activity. Trans. Nonferrous Met. Soc. China 2012, 22, 2465–2470, doi:10.1016/S1003-6326(11)61486-6.
25. Boudjadar, S.; Achour, S.; Boukhenoufa, N.; Guerbous, L. Microwave hydrothermal synthesis and characterization of ZnO nanosheets. Int. J. Nanosci. 2010, 9, 585–590, doi:10.1142/S0219581X10007307.
26. Lee, Y.C.; Yang, C.S.; Huang, H.J.; Hu, S.Y.; Lee, J.W.; Cheng, C.F.; Huang, C.C.; Tsai, M.K.; Kuang, H.C. Structural and optical properties of ZnO nanopowder prepared by microwave-assisted synthesis. J. Lumin. 2010, 130, 1756–1759, doi: 10.1016/j.jlumin.2010.04.005.
27. Shojaee, N.; Ebadzadeh, T.; Aghaei, A. Microwave assisted hydrothermal synthesize of ZnO nanorods and their characterization. Int. J. Mod. Phys. Conf. Ser. 2012, 148, 72–78, doi:10.1142/S2010194512001869.
28. Thongtem, T.; Phuruangrat, A.; Thongtem, S. Characterization of nanostructured ZnO produced by microwave irradiation. Ceram. Int. 2010, 36, 257–262, doi: 10.1016/j.ceramint.2009.07.027.
29. Zhu, Z.; Yang, D.; Liu, H. Microwave-assisted hydrothermal synthesis of ZnO rod-assembled microspheres and their photocatalytic performances. Adv. Powder Technol. 2011, 22, 493–497, doi: 10.1016/j.apt.2010.07.002.
30. Klofac, J.; Munster, L.; Bazant, P.; Sedlak, J.; Kuritka, I. Preparation of Flower-Like ZnO Microparticles by Microwave Assisted Synthesis; NanoCon: Brno, Czech, 2012.
31. Sahoo, S.; Barik, S.K.; Gaur, A.P.S.; Correa, M.; Singh, G.; Katiyar, R.K.; Puli, V.S.; Liriano, J.; Katiyar, R.S. Microwave assisted synthesis of ZnO nano-sheets and their application in UV-detector. ECS J. Solid State Sci. Technol. 2012, 1, 140–143, doi: 10.1149/2.023206jss.
32. Xavier, C.S.; de Moura, A.P.; Li, M.S.; Varela, J.A.; Longo, E.; Cava, S. Microwave-assisted hydrothermal synthesis of ZnO powders with different reagents. TechConnect Briefs 2012, 1, 405–408.
33. Tseng, C.C.; Chou, Y.H.; Liu, C.M.; Liu, Y.M.; Ger, M.D.; Shu, Y.Y. Microwave-assisted hydrothermal synthesis of zinc oxide particles starting from chloride precursor. Mater. Res. Bull. 2012, 47, 96–100, doi: 10.1016/j.materresbull.2011.09.027.
34. Barreto, G.P.; Morales, G.; Quintanilla Ma, L.L. Microwave assisted synthesis of ZnO nanoparticles: Effect of precursor reagents, temperature, irradiation time, and additives on nano-ZnO morphology development. J. Mater. 2013, 2013, 478681, doi:10.1155/2013/478681.
35. Liu, D. Technical study on microwave method for the preparation of flower-like ZnO. Adv. Mater. Res. 2013, 750, 344–347, doi: 10.4028/www.scientific.net/AMR.750-752.344.
36. Majithia, R.; Speich, J.; Meissner, K.E. Mechanism of generation of ZnO microstructures by microwave assisted hydrothermal approach. Materials 2013, 6, 2497–2507, doi:10.3390/ma6062497.
37. Tong, L.; Liu, Y.; Rong, H.; Gong, L. Microwave-assisted synthesis of hierarchical ZnO nanostructures. Mater. Lett. 2013, 112, 5–7, doi: 10.1016/j.matlet.2013.08.119.

38. Tan, S.T.; Umar, A.A.; Yahaya, M.; Yap, C.C.; Salleh, M.M. Ultrafast formation of ZnO nanorods via seedmediated microwave assisted hydrolysis process. J. Phys. Conf. Ser. 2013, 431, 012001, doi:10.1088/1742- 6596/431/1/012001.
39. Yu, H.; Fan, H.; Wang, X.; Wang, J. Synthesis and characterization of ZnO microstructures via microwaveassisted hydrothermal synthesis process. Optik 2014, 125, 1461–1464, doi: 10.1016/j.ijleo.2013.09.009.
40. Barreto, G.; Morales, G.; Cañizo, A.; Eyler, N. Microwave assisted synthesis of ZnO tridimensional nanostructures. Procedia Mater. Sci. 2015, 8, 535–540, doi: 10.1016/j.mspro.2015.04.106.
41. Hasanpoora, M.; Aliofkhazraeia, M.; Delavaria, H. Microwave-assisted synthesis of zinc oxide nanoparticles. Procedia Mater. Sci. 2015, 11, 320–325, doi: 10.1016/j.mspro.2015.11.101.
42. Ocakoglu, K.; Mansour, S.A.; Yildirimcan, S.; Al-Ghamdi, A.A.; El-Tantawy, F.; Yakuphanoglu, F. Microwave- assisted hydrothermal synthesis and characterization of ZnO nanorods. Spectrochim. Acta— Part. A Mol. Biomol. Spectrosc. 2015, 148, 362–368, doi: 10.1016/j.saa.2015.03.106.
43. Gray, R.J.; Jaafar, A.H.; Verrelli, E.; Kemp, N.T. Method to reduce the formation of crystallites in ZnO nanorod thin-films grown via ultra-fast microwave heating. Thin Solid Films 2018, 662, 116–122, doi: 10.1016/j.tsf.2018.07.034.
44. Ridwan, M.; Fauzia, V.; Roza, L. Synthesis and characterization of ZnO nanorods prepared using microwave-assisted hydrothermal method. IOP Conf. Ser. Mater. Sci. Eng. 2019, 496, 012018, doi:10.1088/1757-899X/496/1/012018.
45. Thamima, T.; Karuppuchamy, S. Microwave assisted synthesis of zinc oxide nanoparticles. Int. J. Chem. Tech. Res. 2015, 8, 250–256.
46. Ou, M.; Ma, L.; Xu, L.; Li, X.; Yang, Z.; Lan, Z. Microwave-assisted synthesis of hierarchical ZnO nanostructures and their photocatalytic properties. MATEC Web Conf. 2016, 67, 02005, doi:10.1051/matecconf/20166702005.
47. William L.Hughes “Synthesis and characterization of ZnO for piezoelectric applications”, PhD thesis, School of materials science & engineering, Georgia institute of technology USA, (2006).
48. Ü. Özgür, Ya. I. Alivov, C. Liu, A. Teke, M. A. Reshchikov, S. Do÷an, V. Avrutin, S.J. Cho and H. Morkoçd, journal of applied physics 98,041301(2005).

CHAPTER :7

INSTRUMENTS AND TECHNIQUES

7.1 FOURIER TRANSFORM INFRA-RED SPECTROSCOPY (FTIR)

For studying the vibrational properties of synthesised materials, FTIR spectroscopy is a very useful tool. The band positions and absorption peak of thin films are influenced not only by their chemical composition and structure, but also by their morphology [1].

The preferred method of infrared spectroscopy is known as Fourier Transform InfraRed (FT-IR). Infrared spectroscopy involves passing IR radiation through a sample. The sample absorbs some of the infrared radiation and passes some of it through (transmitted). The resulting spectrum depicts the sample's molecular absorption and transmission, resulting in a molecular fingerprint. No two unique molecular structures produce the same infrared spectrum, just like a fingerprint. As a result, infrared spectroscopy can be used for a variety of purposes.

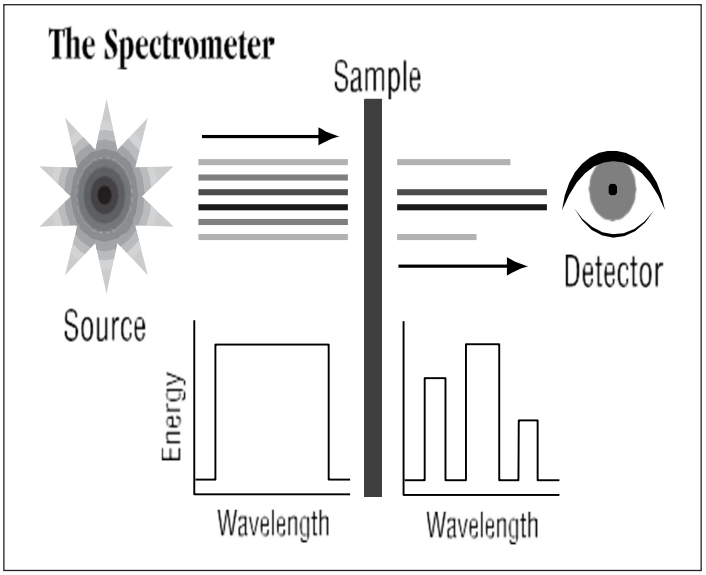

Figure 7.20: Spectrometer

So, what kind of information can FT-IR give you?

• It can determine the quality or consistency of a sample

• It can determine the number of components in a mixture

• It can identify unknown materials

7.1.1 WHY INFRARED SPECTROSCOPY?

For over seventy years, infrared spectroscopy has been a workhorse technique in the laboratory for materials analysis. An infrared spectrum is a sample's fingerprint, with absorption peaks corresponding to the frequencies of vibrations between the bonds of the material's atoms. Because each material is made up of a different set of atoms, no two compounds have the same infrared spectrum. As a result, infrared spectroscopy can be used to positively identify (qualitatively analyse) any type of material. Furthermore, the size of the peaks in the spectrum indicates the amount of material present. Infrared is an excellent tool for quantitative analysis thanks to modern software algorithms.

7.1.2 OLDER TECHNOLOGY

The first infrared instruments were dispersive in nature. Individual frequencies of energy emitted from the infrared source were separated using these instruments. A prism or grating was used to accomplish this. A visible prism separates visible light into its colours, and an

infrared prism does the same (frequencies). A grating is a more modern dispersive element that separates infrared energy frequencies better. The detector counts the amount of energy that has passed through the sample at each frequency. As a result, a spectrum is created, which is a plot of intensity against frequency.

For several reasons, Fourier transform infrared spectroscopy is preferred to dispersive or filter methods of infrared spectral analysis:

• It is a non-destructive technique

• It provides a precise measurement method that does not require external calibration

• It can increase speed, collecting a scan every second

• It can increase sensitivity – one second scans can be co-added together to ratio out random noise

• It has greater optical throughput

7.1.3 WHY FT-IR?

In order to overcome the limitations of dispersive instruments, Fourier Transform Infrared (FT-IR) spectrometry was developed. The slow scanning process was the main issue. It was necessary to develop a method for measuring all infrared frequencies simultaneously rather than individually. An interferometer, a very simple optical device, was used to develop a solution. The interferometer generates a unique signal that contains all of the infrared frequencies "encoded." The signal can be measured very quickly, usually in a fraction of a second. As a result, the time element per sample is reduced from several minutes to a few seconds. A beam splitter is used in most interferometers to divide the incoming infrared beam into two optical beams.

Figure 7.21: An interferogram signal

A flat mirror, which is fixed in place, reflects one beam. The other beam reflects off a flat mirror that moves a very short distance (typically a few millimetres) away from the beam splitter thanks to a mechanism. When the two beams meet again at the beam splitter, they reflect off their respective mirrors and are recombined. The signal that exits the interferometer is the result of these two beams "interfering" with each other because one beam's path is fixed and the other's is constantly changing as its mirror moves.

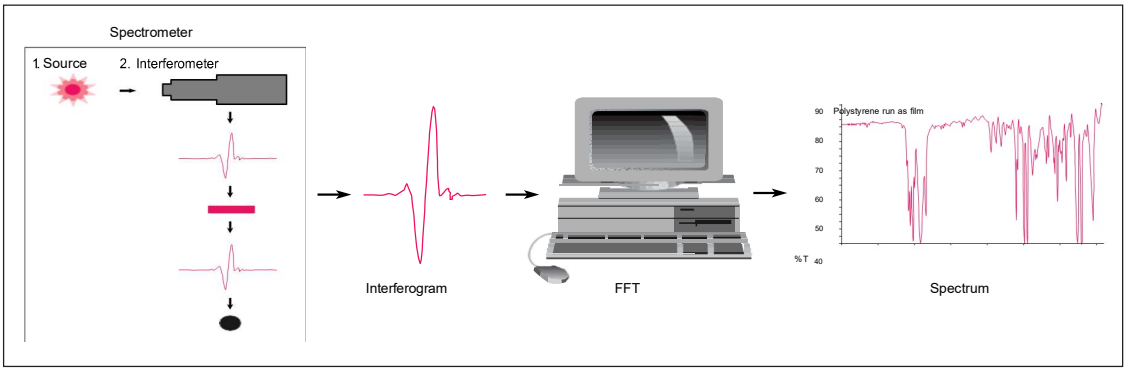

Figure 7.22: Process of generating an FTIR spectra

The resulting signal is known as an interferogram, and it has the unique property of having information about each infrared frequency that comes from the source in every data point (a function of the moving mirror position) that makes up the signal. This means that all frequencies are measured simultaneously as the interferogram is measured. As a result of the interferometer's use, measurements are extremely quick. The measured interferogram signal cannot be interpreted directly because the analyst requires a frequency spectrum (a plot of the intensity at each individual frequency) in order to make an identification. It's necessary to have a way of "decoding" the individual frequencies. The Fourier transformation, a well-known mathematical technique, can be used to accomplish this. The computer performs this transformation and then presents the user with the desired spectral information for analysis.

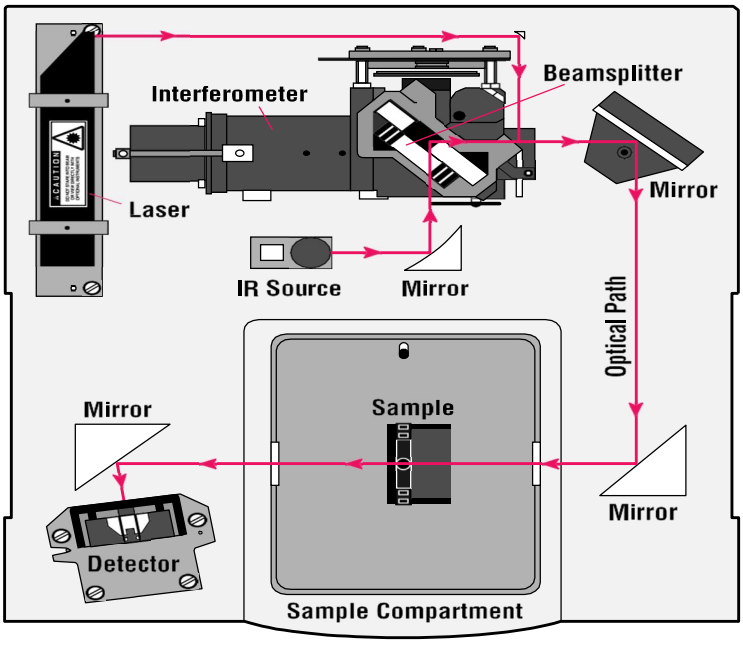

Figure 7.23: A simple spectrometer layout

7.1.4 THE SAMPLE ANALYSIS PROCESS

The standard instrumental procedure goes like this [2]:

1. **The Source**: A glowing black-body source emits infrared energy. This beam passes through an aperture that regulates how much energy is delivered to the sample (and, ultimately, to the detector).

2. **The Interferometer**: The beam passes through the interferometer, which performs "spectral encoding." The interferogram signal is then output from the interferometer.

3. **The Sample**: Depending on the type of analysis being performed, the beam enters the sample compartment and is transmitted through or reflected off the surface of the sample. This is where the sample's specific frequencies of energy, which are unique to it, are absorbed.

4. **The Detector**: The beam finally reaches the detector, where it is measured. The detectors used were created specifically to measure the interferogram signal.

5. **The Computer**: The measured signal is digitised and sent to the computer, which performs the Fourier transformation. The user is then presented with the final infrared spectrum for interpretation and any further manipulation.

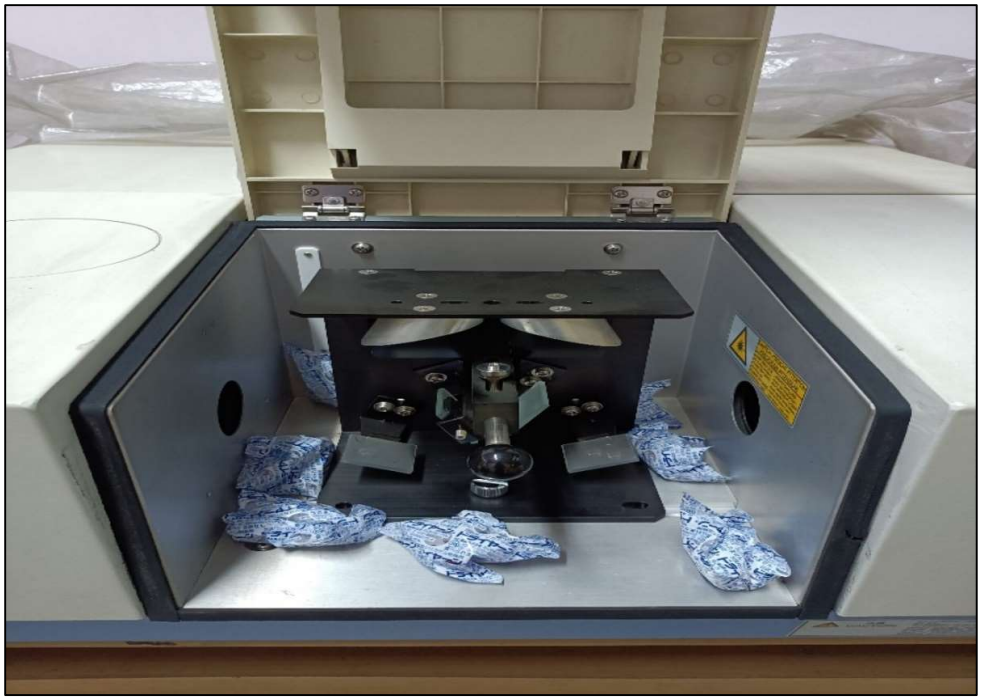

Figure 7.24: Internal components of FTIR instrument.

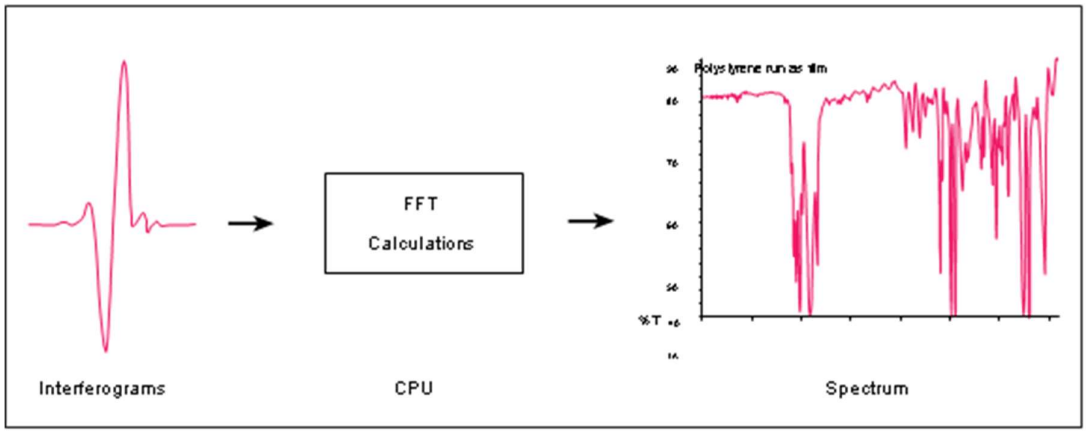

Figure 7.25: Internal Process for the formation of FTIR spectra

Because the absorption intensity must be measured on a relative scale, a background spectrum must also be measured. Normally, this is a measurement without a sample in the beam. This can be compared to the "percent transmittance" measurement taken with the sample in the beam. This method yields a spectrum that is devoid of all instrumental characteristics. As a

result, all spectral features present are solely due to the sample. Because the instrument's spectrum is characteristic, a single background measurement can be used for multiple sample measurements.

7.1.5 ADVANTAGES OF FT-IR

The following are some of the major advantages of FT-IR over the dispersive technique:

• **Speed**: Because all of the frequencies are measured at the same time, most FT-IR measurements are completed in seconds rather than minutes.

• **Sensitivity**: FT-IR dramatically improves sensitivity for a variety of reasons. The detectors used are much more sensitive, the optical throughput is much higher resulting in much lower noise levels, and the fast scans allow the co-addition of multiple scans to reduce random measurement noise to any desired level.

• **Mechanical Simplicity**: The interferometer's moving mirror is the instrument's only continuously moving part. As a result, mechanical failure is extremely unlikely.

• **Internally calibrated**: A HeNe laser is used as an internal wavelength calibration standard in these instruments (referred to as the Connes Advantage). These instruments are self-calibrating and do not require user calibration.

These advantages, along with a number of others, make FT-IR measurements extremely precise and repeatable. As a result, it's a very reliable technique for positively identifying almost any sample. The sensitivity benefits allow even the tiniest contaminants to be detected. As a result, whether it's batch-to-batch comparisons to quality standards or analysis of an unknown contaminant, FT-IR is an invaluable tool for quality control and quality assurance applications.

Furthermore, the sensitivity and accuracy of FT-IR detectors, as well as a wide range of software algorithms, have greatly expanded the practical application of infrared for quantitative analysis. Quantitative methods are simple to develop and calibrate, and they can be incorporated into routine analysis procedures. As a result, infrared spectroscopy has benefited greatly from the Fourier Transform Infrared (FT-IR) technique. It has paved the way for the development of a slew of new sampling techniques aimed at tackling problems that older technology couldn't handle. It has virtually unrestricted the use of infrared analysis.

Figure 7.26: FTIR Machine -Shimadzu IR Prestige, (Japan) used in my thesis

7.2 DIFFUSE REFLECTANCE SPECTROSCOPY (DRS)

7.2.1. UV-VIS NEAR INFRARED SPECTROSCOPY

UV-Vis near Infrared (UV-Vis-NIR) Spectrophotometer measures Optical transmittance, absorbance and reflectance in the ultraviolet-visible spectral region. UV-Vis near Infrared (UV-Vis-NIR) Spectrophotometer measures Optical transmittance, absorbance and reflectance in the ultraviolet visible spectral region [3].

UV-VIS absorption spectroscopy measures the percentage of radiation that is absorbed or transmitted or reflected at each wavelength. This is usually accomplished by scanning the wavelength range and measuring the absorption [4].

Light absorption can be described by two fundamental laws as:

Lambert's Law -The proportion of incident light absorbed by a transparent medium is independent of the intensity of the light (provided that there is no other physical or chemical change to the medium). Therefore, successive layers of equal thickness will transmit an equal proportion of the incident energy.

Lambert's law can be expressed by

$$\frac{I}{I_0} = T$$

Where I is defined as the intensity of the transmitted light, I_0 is the intensity of the incident light, and T is the Transmittance.

Beer's Law-The absorption of light is directly proportional to both the concentration of the absorbing medium and the thickness of the medium in the light path.

A combination of the two laws (known jointly as the Beer-Lambert Law) defines the relationship between absorbance (A) and transmittance (T).

$$A = log\frac{I_0}{I} = log\frac{100}{T} = \varepsilon cb$$

where, A is absorbance (no unit of measurement), ε is molar absorptivity ($dm^3mol^{-1}cm^{-1}$), c is molar concentration (mol dm^{-3}), and b is path length (cm).

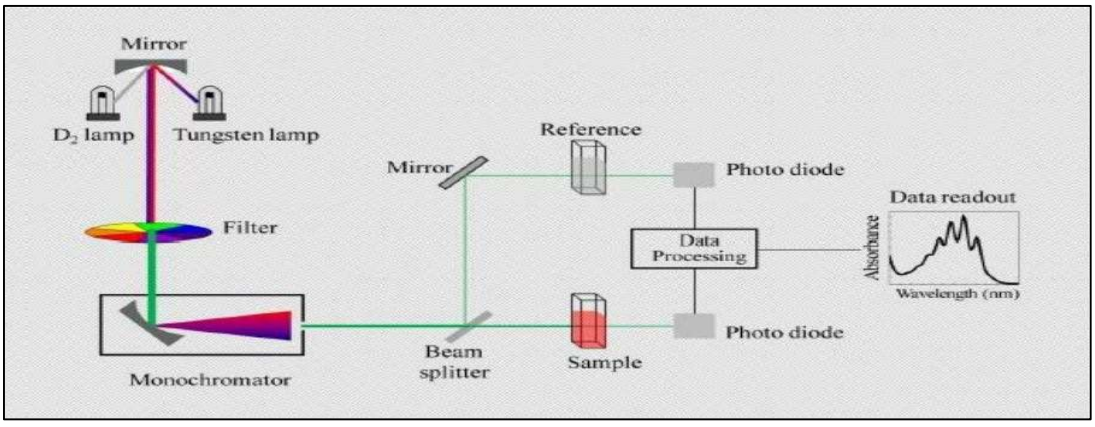

Figure 7.27: Basic Principles of UV-VIS Spectroscopy

7.2.2 LIGHT REFLECTION AND REFLECTANCE SPECTRA

The spectrometer beam is directed into the sample, where it is reflected, dispersed, and transmitted through the sample material, resulting in diffuse reflectance (shown on the right).

The accessory collects the back reflected, diffusely dispersed light (part of which is absorbed by the sample) and directs it to the detector optics. Diffuse reflection refers to the portion of a beam that is dispersed within a sample and returns to the surface [6,7].

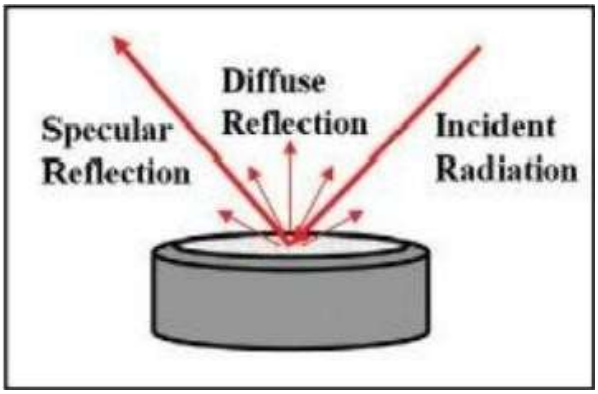

Figure 7.28: Diffuse and Specular Reflectance

Particle size, refractive index, homogeneity, and packing are further parameters that contribute to excellent spectral quality in diffuse reflectance sampling. The raw diffuse reflectance spectra will seem different from its transmission counterpart despite all of these sample preparation techniques (stronger than expected absorption from weak IR bands) [8,9].

To correct for these discrepancies, a Kubelka-Munk conversion can be performed to a diffuse reflectance spectrum.

Kubelka-Munk Function:

$$F(R) = \frac{(1-R)^2}{R} = \frac{k}{s}$$

R stands for the sampled layer's absolute reflectance, k for the molar absorption coefficient, and s for the scattering coefficient.

In material sciences and industry, diffuse reflectance spectroscopy (DRS) of (nano-scaled) powders is a widely used and powerful tool [5–7]. The scattered intensity of an incident light beam is scanned over the sample as a function of wavelength, and the data set is analysed in terms of its macroscopic optical properties, such as overall reflectivity.

Furthermore, DRS has the potential to determine the absorption characteristics of the particles themselves, even at sub-micron length scales. The absorption coefficient's absolute values as well as its dispersive characteristics are important for a variety of materials with high commercial potential, such as pigments or phosphors [10,11,12]. Absorption properties play a large role in determining the macroscopic optical properties of dielectric powders, but they also play a role in the losses of internally emitted light. As a result, the application of DRS frequently falls short of its capabilities, and it is primarily used to determine macroscopic optical parameters [13].

This method has several advantages, including

1) high quality reflectance spectra,

2) high reproducibility in determining absorption features, and

3) easy identification of signal artefacts, which allows for their subsequent reduction.

7.2.3 MEASUREMENT SETUP

7.2.3.(a) REQUIREMENTS AND PROCEDURES

For accurate and repeatable measurements of diffuse reflectance spectra, a specific optical setup is required. While it is possible to assemble it from scratch and obtain acceptable results, several dedicated spectrometers are commercially available for higher precision measurements at the time of writing this paper. Naturally, depending on their specifications and measurement options, successor or predecessor models are also suitable [14,15].

7.2.3.(b) COMPONENTS OF DIFFUSE REFLECTANCE SPECTROPHOTOMETER

Spectrophotometer consists of the following components

- A source of radiation of appropriate wavelengths
- Monochromator and optical geometry
- Filter Sample compartment
- Detector, Photomultiplier, Measuring system, Computer

Because double-beam spectrometers measure both the sample and the white standard at the same time, determining the diffuse reflectance of non-luminescent samples is simple, quick, and accurate [16]. Extraneous light emission at wavelengths other than the excitation creates spurious additional signals in fluorescence, making an unfiltered diffuse reflectance spectrum inaccurate. Instead, using a fluorescence spectrometer has the distinct advantage of allowing you to easily perform diffuse reflectance measurements on any material.

In favour of a collimated (or, optionally, defocused) beam, such a scenario is now omitted. A setup with two individual monochromators is required for fluorescent samples: The excitation monochromator chooses a wavelength for sample illumination, while the emission monochromator transmits the sample's linear diffuse reflectance, cancelling out any additional fluorescence emission [18].

As a result, this mode of operation is commonly referred to as synchronous scanning, in which both monochromators are set to the same wavelength. Additional spectral filters, in addition to monochromators, remove potential higher diffraction orders transmitted through grating-based monochromators, as well as sample fluorescence [19]. If only monochromatic illumination is required, a suitable laser or bandpass filtering behind a broadband emission source can be used to replace the light source/monochromator combination.

Figure 7.29: UV-VIS-NIS (SHIMADZU UV-3600) Spectrophotometer

It is recommended to split a small portion of the excitation light into a low-drift reference detector if intensity fluctuations are a significant factor, such as due to lamp power drifts or ambient temperature changes. The majority of the remaining material will be used to illuminate the samples. The signal of the reference detector can then be used to scale the measured diffuse reflectance intensities [21]. It should be noted, however, that any additional detector will inevitably increase overall electronic noise and should therefore be used with caution.

When compared to vertically placed samples, which are common in integrating spheres where an additional cover window is often used to keep the sample in place [17,18], a horizontal alignment of the sample has the distinct advantage of eliminating potential contamination of the spectrometer due to material gliding off of the (brittle) surface.

Even without a cover window, the horizontal alignment ensures that the sample is preserved throughout the measurement and that contamination of its surroundings is avoided. A parallel excitation/emission beam geometry also eliminates specular reflection losses caused by a slight tilt of the incident light direction relative to the sample surface normal. This significantly reduces the impact of sample surfaces that aren't perfectly Lambertian. The beam path requires at least one additional mirror to reflect the excitation beam downwards onto the sample to account for this geometry. This mirror also relays the emission beam towards the detection arm in an optimised setup. The sample's diffusely reflected light is directed into the optical detection path and then recorded by a detector within the spectrometer, such as a photomultiplier tube (PMT).

7.2.4 WHITE STANDARDS

Experimenting with precise, absolute values for diffuse reflectance of a sample is difficult in general. It invariably necessitates a thorough understanding of the used spectrometer, particularly its optical transfer function. The use of reference materials with well-documented diffuse reflectance is a common method for investigating the peculiarities of spectrometers and for calibration purposes. The diffuse reflectance of such white standards is characteristic over a wide spectral range [3,5,17,20,22–24].

7.3 PHOTOLUMINESCENCE SPECTROSCOPY (PL)

7.3.1 INTRODUCTION

Photoluminescence (PL) spectroscopy is a simple, contactless and non-destructive method. It can be used to determine the band gap, impurity level and defect detection, recombination mechanism, surface structure, fluorescence property of materials and excited states of a material. The non-contact mode of photoluminescence spectroscopy is used. It is a non-destructive method of examining the electronic structure of a material. In simple words it can be defined as an instrument which interacts light with matter [25].

7.3.2 BASIC PRINCIPLE

When light strikes a sample, it is absorbed by the material by imparting its excess energy. This is known as photo-excitation. Light emission, or luminescence, is one method by which the sample dissipates this excess energy [26]. Photoluminescence refers to luminescence that occurs as a result of photo-excitation. When a material is excited, its electrons occupy the allowed excited states. These excited electrons dissipate the extra energy in the form of light (radiative process) or any non-radiative process to return to their stable, i.e., equilibrium or ground state [27]. The energy difference in the two electronic states participating in the transition between the excited and equilibrium states is linked to the emitted light energy

(photoluminescence). The quantity of light emitted is determined by the portion of the radiative process [28].

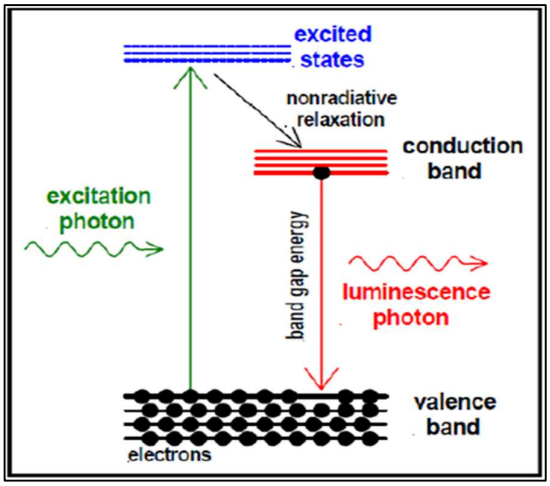

Figure 7.30: Basic Principle of Photoluminescence

7.3.3 PHOTOLUMINESCENCE DIFFERENT MODES

• **Resonant radiation**: In this process, a specific wavelength photon gets absorbed with the immediate emission of equivalent photon. This process does not involve any appreciable internal energy transitions between absorption and emission, further the time scales of the process is of the order of 10 nanoseconds.

• **Fluorescence**: The chemical substrate, when it is undergoing the internal energy transition by emitting photon before returning to its ground state, certain joule of absorbed energy gets liberated such that the emitted light has lower energy in comparison to the absorbed. Fluorescence is the one of the known mechanisms whose lifetime is about 10^{-8} to 10^{-4} s.

• **Phosphorescence**: It is a radiation-based transition, wherein the absorbed energy experiences electronic transition having different spin states, i.e., intersystem crossing (ISC). Phosphorescence phenomena lifespan is typically from 10^{-4} - 10^{-2} s which is considerably lengthier in comparison to Fluorescence lifespan. Thus, phosphorescence phenomena occur rarely when compared to fluorescence, as the molecule in its triplet state has a more chance of experiencing intersystem crossing to lower energy state before the occurrence of phosphorescence.

7.3.4 SPECTROSCOPY

Photo excitation allows electrons within a material to migrate into permitted excited states when light is focused onto it. The surplus energy is released when these electrons return to their equilibrium states, which may or may not entail the emission of light (a radiative process or a non-radiative process). The difference energy levels between the two electron states involved in the transition between the excited state and the equilibrium state determines the energy of the produced light (photoluminescence). The amount of light emitted is in proportional to the radiative process' proportionate contribution. In most situations, the released light has a longer wavelength than the absorbed radiation, and so has less energy.

When the absorbed electromagnetic radiation is strong enough, one electron can absorb two photons; this two-photon absorption can result in the emission of light with a shorter wavelength than the absorbed energy. Resonance fluorescence occurs when the released radiation has the same wavelength as the absorbed light. When radiation is absorbed in the

ultraviolet part of the spectrum, which is invisible to the human eye, and the released light is in the visible range, photoluminescence occurs. The ground state of a fluorophore (fluorescent molecule) is designated S_0, while the first (electronically) excited state is named S_1. S_1 is a molecule that may relax in a variety of ways.

It can go through a process known as 'non-radiative relaxation, in which the excitation energy is transferred to the solvent as heat (vibrations). Organic molecules that have been excited can also relax by converting to a triplet state, which can then relax by phosphorescence or a secondary nonradiative relaxation process. Interaction with a second molecule via fluorescence quenching can also cause an S_1 state to relax. Because of its unique triplet ground state, molecular oxygen (O_2) is a highly effective fluorescence quencher [29].

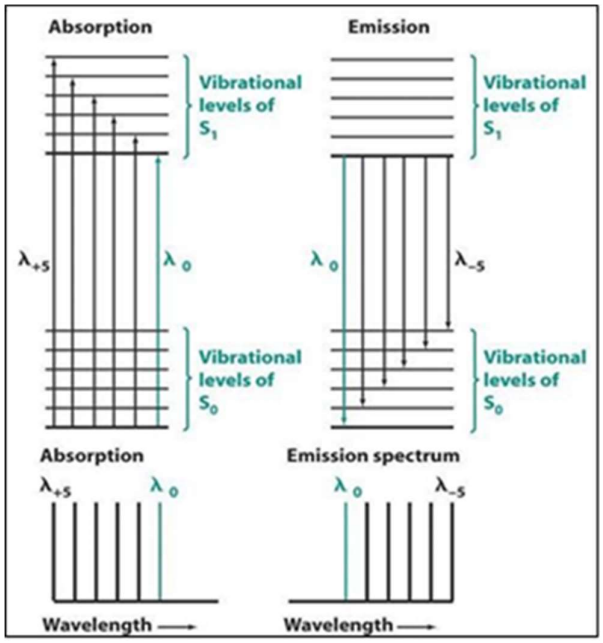

Figure 7.31: Representing the energy-level diagrams which mentions that why structure is seen in the absorption as well as emission spectrum also why the spectra are roughly mirror images of each other.

7.3.5 RELATION BETWEEN ABSORPTION AND EMISSION SPECTRUM

At lower energy, chance of fluorescence and phosphorescence is more than absorption (the energy of excitation). As presented, in case of absorption, $\lambda_{0\ \text{wavelength}}$ means transition from the ground state of vibration i.e., S_0 to S_1. When absorbing radiation, S_1 molecule which excited vibrationally goes to lower vibrational level before emitting any radiation. $\lambda_{0\ \text{wavelength}}$ corresponds to transition of very high energy, cascade of peaks occurs at higher wavelength. Both emission as well as absorption spectrum are likely to have mirror image relation if spacing of vibrational levels are approximately equivalent and if the probability of transition is alike. λ_0 transitions do not overlap completely.

A radiation absorbing molecule which is primarily in its ground state, S_0; have a firm geometry in addition to solvation. The transitions in the electronic states are rapid in comparison to atoms vibrational movement or the solvent molecules 'translational movement, once the radiation is absorbed, the S_1 excited molecule yet have its geometry as well as solvation S_0 state.

Geometry in addition to solvation is modified to an utmost appropriate amount soon after the excitation. This rearrangement lowers the energy of excited molecule. When an S_1 molecule fluoresces, it returns back to the S_0 state having S_1 geometry and solvation. This unbalanced

arrangement must have a higher energy than that of an S_0 molecule having S_0 geometry and solvation. The net outcome has been shown in Figure in which excitation energy is higher than the emission energy [30].

7.3.6 INSTRUMENTATION OF PHOTOLUMINESCENCE

The fluorescence from a sample is recorded and measured by an analytical device known as spectrofluorometer. Scanning of the excitation, emission or both wavelengths is done in order to record the fluorescence. Through extra attachments, study of signal deviation with respect to time, temperature, concentration, polarization, or other variables is observed [31].

Block diagram of fluorescence spectrometer is represented below. Fluorescence spectrometers use laser sources, which has monochromator (wavelength selectors), laser source (sample illumination), detectors and corrected spectrum

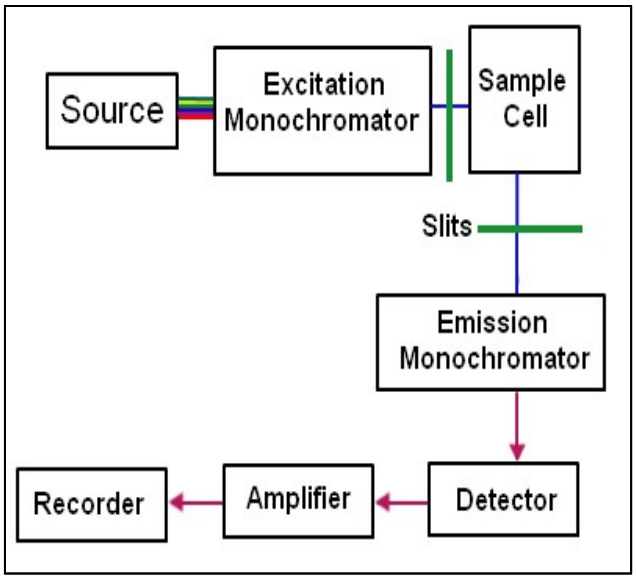

Figure 7.32: Block diagram of fluorescence spectrometer

- **Source of Illumination**:

The source of light used is a continuous type, 150 W ozone free xenon arc lamp. Lamps' light is accumulated by a diamond turned elliptical shaped mirror, which is then focused onto the excitation monochromators 'entrance slit.

A quartz-based window is used to isolate excitation monochromator from the housing of lamp, which vents heat out of the device, and shields against the unlikely occurrence of failure of lamp. Resolution over the complete spectrum stretches and reduces spherical aberrations and re-diffraction.

- **Monochromators:**

There are two types of monochromators, i.e., Excitation and Emission monochromators. Entire reflective optics is used by it in order to keep great resolution over the full range of spectrum as well as to reduce aberrations (spherical) and re-diffraction.

- **Gratings:**

Reflection Grating is the crucial part of a monochromator, whose purpose is to disperse striking (incident) light through grooves which are positioned vertically. Spectra are acquired by

gratings rotation which contain 1200 grooves per mm, and are blazed at 330 nm (excitation) at 500 nm (emission).

- **Slits**:

Very flexible slits are used at the entrance and exit points of the monochromator. Bandpass of the incident light is determined by the slit's width on the excitation monochromator whereas fluorescence intensity signal is controlled (recorded by signal detector) by the emission monochromator's slits.

When setting slit width, the trade-off is intensity of signal versus spectral resolution. In a case where slit width is wider, shows decrease in resolution because extra light falls on the sample as well as on the detector whereas when narrower slits are used, higher resolution is obtained but at the cost of signal.

- **Shutters**:

Beneath the excitation monochromator's exit slit an excitation shutter is placed and its purpose is to shield sample from photo bleaching or photo degradation by long exposure to the light. The detector is protected from the bright light through an emission shutter which is positioned just prior to the entrance of the emission monochromator.

- **Sample compartment**:

In sample compartment, several optional attachments are present and bundles of fibre optic to take the excitation beam to the sample which is placed remotely and bring back the emission beam to the emission monochromator.

- **Detectors**:

There are 2 types of detectors i.e. Signal and reference detector. The signal detector is based on photon counting, which is an R928P photomultiplier tube that directs the signal to a photon counting module. The reference detector's purpose is to monitor the xenon lamp for correction of wavelength and time dependent output of the lamp. This detector is based on UV which enhances silicon photodiode, placed just prior to the compartment of sample.

Figure 7.33: Horiba Jobin Yvon Fluromax spectrofluorometer

7.3.7 PHOTOLUMINESCENCE SPECTROSCOPY LIMITATIONS

In spite of the fact that this technique is not qualitative in nature, it can be used to detect low concentration of optical centres. The major scientific PL limitation is that several optical

centres might possess numerous excited states that are vacant at low temperatures. Another major limitation of PL is that the luminescent signal gets disappeared.

7.3.8 APPLICATIONS

- **Determination of Band gap**

Band gap represents the energy difference among the conduction band (top) and valence band (bottom) in semiconductors exhibiting radiative transitions. The range of PL spectrum of a semiconductor is used for non-destructive analysis of bandgap. Through this mode it is possible to quantify the composition of the element of a semiconductor compound as well as it is crucially significant material specification influencing the device efficacy such as solar cell.

- **Identification of level of Impurity as well as defect**

Some localized defects levels are created when radiative transition occurs in semiconductors. Particular defects related to these levels can be recognized by the photoluminescence energy whereas their concentration can be ascertained by the PL amount. The Photoluminescence spectra of the sample at low temperatures often reveals peaks of the spectra linked with the impurities present inside the material of the host. Highly sensitive Fourier transform photoluminescence micro spectroscopy have potential for recognizing very small concentrations of intended and unintended impurities which strongly influence the quality of material as well as performance of the device.

- **Recombination phenomena**

Both the radiation and non-radiation-based processes involve the mechanism known as "recombination". The emitted PL quantity of a material is straight away linked with the relative quantity of radiative and nonradiative recombination rates. The quantity of PL and impurities are commonly linked with the nonradiative rates and it is dependent on the photo-excitation level plus temperature which are directly associated to the dominant recombination process.

- **Surface structure and excited states**

Some broadly utilized conventional techniques like XRD, IR spectroscopy are very frequent non- sensitive for catalysts which are oxide supported with less concentrations of metal oxide. PL, on the other hand, is too sensitive to surface effects or semiconductor-based particles adsorbed species therefore, it is utilized as a probe of electron hole surface processes.

Figure 7.34: Photoluminescence analysis carried out by Horiba Jobin Yvon Fluromax spectrofluorometer

7.4 FIELD EMISSION SCANNING ELECTRON MICROSCOPE (FESEM)

7.4.1 PRINCIPLE

7.4.1.1 WHAT DOES THE WORD FESEM MEAN?

FESEM is the abbreviation of Field Emission Scanning Electron Microscope. A FESEM is microscope that works with electrons (particles with a negative charge) instead of light. These electrons are liberated by a field emission source.

7.4.1.2 WHAT CAN BE DONE WITH A FESEM?

A FESEM is used to visualize very small topographic details on the surface or entire or fractioned objects. Researchers apply this technique to observe structures that may be as small as 1 nanometre (= billion of a millimetre).

7.4.1.3 HOW DOES A FESEM FUNCTION?

Electrons are liberated from a field emission source and accelerated in a high electrical field gradient. Within the high vacuum column these so-called primary electrons are focussed and deflected by electronic lenses to produce a narrow scan beam that bombards the object. As a result, secondary electrons are emitted from each spot on the object. The angle and velocity of these secondary electrons relates to the surface structure of the object. A detector catches the secondary electrons and produces an electronic signal. This signal is amplified and transformed to a video scan-image that can be seen on a monitor or to a digital image that can be saved and processed further.

7.4.2 COMPONENTS OF FESEM

Electron Guns

Modern SEM systems require a steady electron beam from the electron gun with a high current, small spot size, tunable energy, and low energy dispersion. Several types of electron guns are used in a SEM system, and the quality of the electron beam produced by each differs significantly.

Electron Lenses

Electron beams can be concentrated by electrostatic or magnetic fields. The SEM system, on the other hand, only uses a magnetic field because an electron beam controlled by a magnetic field has less aberration.

Condenser Lens

The electron beam will diverge after passing through the anode plate from the emission source. The electron beam is converged and collimated by the condenser lens into a nearly parallel stream. A magnetic lens is made up of two rotationally symmetric iron pole pieces that are connected by a copper winding to create a magnetic field. The electron beam can pass through a hole in the middle of the pole pieces. Through a lens-gap that separates the two pole components, the magnetic field influences (focuses) the electron beam. The condenser lens current can be changed to change the focus point location.

Scan Coils

The scan coils deflect the electron beam in a zigzag pattern as it passes over the item. The movement of the scanner is timed to coincide with the creation of the image on the display.

The scan velocity determines the screen refresh rate and the amount of noise in the image. In scan coils, upper and lower coils are commonly used to prevent the formation of a circular shadow at low magnification.

The Objective Lens

The electron beam will diverge below the condenser aperture. The electron beam is focused into a probe point on the specimen surface using objective lenses, which also provide additional demagnification. The diameter of the electron beam on the specimen surface (spot size) is reduced as the aperture and fundamentals of the microscopy are increased, which improves picture resolution.

The Stigmator Coil

The stigmator coils are used to correct x and y deflection inconsistencies in the beam, resulting in a perfectly round beam.

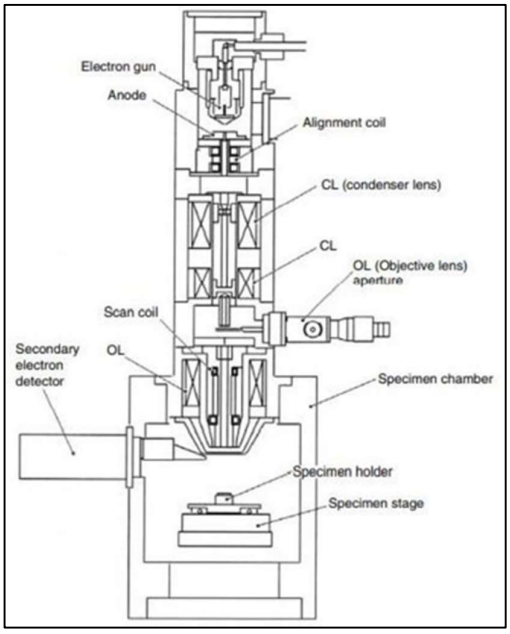

Figure 7.35: Schematic diagram of FESEM **Figure 7.36:** FESEM (Hitachi S-4800)

Object Chamber

After being coated with a conductive coating, the item is placed on a specific holder. Through an exchange chamber, the item is introduced into the microscope's high vacuum section and anchored on a movable stage. The secondary electron emission detector (scintillator) is located at the back of the object holder in the chamber.

Image Formation

Complex interactions occur when an electron beam in a SEM impinges on a specimen surface and excites different signals for SEM inspection. Secondary electrons, back scattered electrons (BSEs), transmitted electrons, and specimen current can all be collected and displayed on a computer monitor. The composition of the specimen is determined by examining the excited x-ray. The interactions of the electron beam with the specimen surface, as well as the principle of picture creation using various signals, will be covered in this section.

7.5 I-V CHARACTERIZATION

The techniques for the measurement of the electrical behaviour of laminated composites are the two- probe method and four probe methods. The two-probe method is based on the definition of resistance when two electrodes are used to measure the electrical resistance. Figure below shows a specimen, on which a pair of contacts (probe 1 and probe 2) with conductive wires is attached. Two probes are used for the electrical current input, as well as for the voltage measure. The resistance of the segment between the voltage contacts can be calculated through Ohm's law:

$$V = I * R$$

where, V and I are the voltage and current from the voltage and current contacts, respectively.

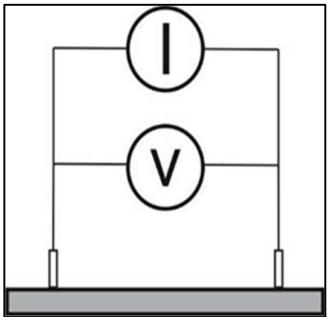

Figure 7.37: Electrical resistivity measurement by two probe method

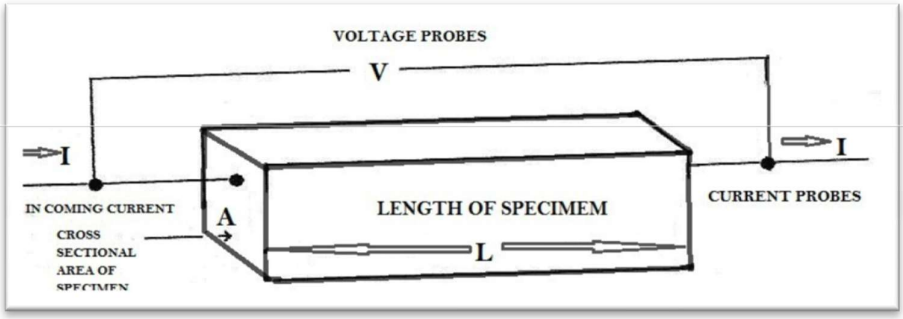

(a)

(b)

Figures 7.38 (a, b): Two probe device (Keysight-model no. B2902A)

Reference:

1. Z. Yang, Z. Z. Ye, Z. Xu and B. H. Zhao, "Effect of the Morphology on the Optical Properties of ZnO Nanostructured," Physica E: Low-Dimensional Systems and Nanostructures, Vol. 42, No. 2, December 2009, pp. 116- 119. doi: 10.1016/j.physe.2009.09.010.
2. Thermo Nicolate, Introduction to Fourier Transform Infrared Spectrometry, © 2001 Thermo Nicolet Corporation.
3. Kortüm, G. Reflectance Spectroscopy: Principles, Methods, Applications; Kortüm, G., Ed.; Springer: Heidelberg/Berlin, Germany, 1969.
4. Frei, R.W.; Frodyma, M.M.; Lieu, V.T. Diffuse reflectance spectroscopy. In Instrumentation for Spectroscopy. Analytical Atomic Absorption and Fluorescence Spectroscopy. Diffuse Reflectance Spectroscopy; Svehla, G., Ed.; Wilson & Wilson's Comprehensive Analytical Chemistry; Elsevier Scientific Publishing Company: Amsterdam, The Netherlands, 1975; Volume 4, Chapter 3, pp. 263–345.
5. Höpe, A. Diffuse Reflectance and Transmittance. In Spectrophotometry: Accurate Measurement of Optical Properties of Materials; Germer, T.A., Zwinkels, J.C., Tsai, B.K., Eds.; Experimental Methods in the Physical Sciences; Academic Press Elsevier Inc.: Amsterdam, The Netherlands, 2014; Volume 46, Chapter 6, pp. 179–219.
6. Lambert, J.H. Lambert's Photometrie. Photometria Sive De Mensura Et Gradibus Luminis, Colorum et Umbrae (1760); Anding, E., Ed.; Ostwald's Klassiker der exakten Wissenschaften; Verlag von Wilhelm Engelmann: Leipzig, Germany, 1892; Volume 31.
7. Bouguer, P. Traité d'optique sur la gradation de la lumiere; I'Abbé de la Caille, M., Ed.; De l'Imprimerie de H.L. Guerin & L.F. Delatour: Paris, France, 1760.
8. Ångström, K. Ueber die Diffusion der strahlenden Wärme von ebenen Flächen. Ann. Phys. 1885, 262, 253–287. [CrossRef]
9. Messerschmitt, J.B. Ueber diffuse Reflexion. Ann. Phys. 1888, 270, 867–896. [CrossRef]
10. Seeliger, H. Zur Photometrie zerstreut reflectirender Substanzen. In Sitzungsberichte der Mathematisch-Physikalischen Classe der k. b. Akademie der Wissenschaften zu München; Franz, G., Ed.; Verlag der K. Akademie: Munich, Germany, 1888; Volume 18, pp. 201–248.
11. Lommel, E. Die Photometrie der diffusen Zurückwerfung. Ann. Phys. 1889, 272, 473–502. [CrossRef]
12. Uljanin, W. Ueber das Lambert'sche Gesetz und die Polarisation der schief emittirten Strahlen. Ann. Phys. 1897, 298, 528–542. [CrossRef]
13. Wright, H. Die diffuse Reflexion des Lichtes an matten Oberflächen. Ann. Phys. 1900, 306, 17–41. [CrossRef]
14. Pokrowski, G.I. Zur Theorie der diffusen Lichtreflexion. Z. Phys. 1924, 30, 66–72. [CrossRef]
15. Schulz, H. Untersuchungen über die Reflexion a teilweise lichtzerstreuenden Flächen. Z. Phys. 1925, 31, 496–506. [CrossRef]
16. Harrison, V.G.W. The light-diffusing properties of magnesium oxide. Proc. Phys. Soc. 1946, 58, 408–419. [CrossRef]
17. Torrent, J.; Barrón, V. Diffuse Reflectance Spectroscopy. In Methods of Soil Analysis Part 5–Mineralogical Methods; Number 5 in the Soil Science Society of America Book Series; Ulery, A.L., Drees, L.R., Eds.; Soil Science Society of America Inc.: Madison, WI, USA, 2008; Volume 5, Chapter 13, pp. 367–385.
18. Blake, T.A.; Johnson, T.J.; Tonkyn, R.G.; Forland, B.M.; Myers, T.L.; Brauer, C.S.; Su, Y.F.; Bernacki, B.E.; Hanssen, L.; Gonzalez, G. Methods for quantitative infrared

directional-hemispherical and diffuse reflectance measurements using an FTIR and a commercial integrating sphere. Appl. Opt. 2018, 57, 432–446. [CrossRef]
19. Clarke, F.J.J.; Compton, J.A. Correction Methods for Integrating-Sphere Measurement of Hemispherical Reflectance. Color Res. Appl. 1986, 11, 253–262. [CrossRef]
20. Kortüm, G.; Braun, W.; Herzog, G. Prinzip und Meßmethodik der diffusen Reflexionsspektroskopie. Angew. Chem. 1963, 75, 653–661. [Cross Ref]
21. Hanssen, L. Integrating-sphere system and method for absolute measurement of transmittance, reflectance, and absorptance of specular samples. Appl. Opt. 2001, 40, 3196–3204. [CrossRef] [PubMed]
22. Jacquez, J.A.; McKeehan, W.; Huss, J.; Dimitroff, J.M.; Kuppenheim, H.F. An Integrating Sphere for Measuring Diffuse Reflectance in the Near Infrared. J. Opt. Soc. Am. 1955, 45, 781–785. [Cross Ref]
23. Goebel, D.G.; Caldwell, B.P.; Hammond, H.K. Use of an Auxiliary Sphere with a Spectro reflectometer to Obtain Absolute Reflectance. J. Opt. Soc. Am. 1966, 56, 783–788. [CrossRef]
24. Adams, J.B. Interpretation of Visible and Near-Infrared Diffuse Reflectance Spectra of Pyroxenes and other Rock-Forming Minerals. In Infrared and Raman Spectroscopy of Lunar and Terrestrial Minerals; Karr, C., Ed.; Academic Press Inc.: London, UK, 1975; Chapter 4, pp. 91–115.
25. Photoluminescence Spectroscopy, Physics U600, Adv Lab I – Physics of Waves and Optics – Summer 2004, D. Heiman, North eastern University, 6/1/2004.
26. J. Reichman, Handbook of Optical Filters for Fluorescence Microscopy (Chroma Technology, Brattleboro, 2010).
27. C. Ronda, Luminescence from Theory to Applications (Wiley-VCH, New York, 2008).
28. I. Parreu, J.J. Carvajal, X. Solans, F. Díaz, M. Aguiló, Chem. Mater. 18, 221 (2006).
29. Y. Hong, J. W. Y. Lam, and B. Z. Tang, Chem. Commun., 2009, 4332.
30. Photoluminescence Spectroscopyand its Applications, Ruquan Ye, Andrew R. Barron, OpenStaxCNX module: m38357.
31. M. Anpo, M. Kondo, S. Coluccia, C. Louis, and M. Che, J. Am. Chem. Soc., 1989, 111, 8791.

CHAPTER :8

RESULTS AND DISCUSSIONS

This thesis investigates the characterization procedure of low hydrothermally prepared ZnO nanostructures. The characterization procedure generally includes the investigation of optical properties, morphological properties and ohmic contact properties for the development of photodetector. The optical properties include FTIR characterization, PL characterization and DRS characterization. The morphological properties include FESEM characterization. The ohmic characterization is the basis of the photodetector investigation that basically consist the CURRENT- VOLTAGE characterization or the I-V characterization.

OPTICAL CHARACTERIZATION

8.1 FTIR ANALYSIS

FTIR To confirm the nature of the reaction intermediate and identification of various functional groups which participate in the formation of ZnO NPs, FTIR analysis was carried out in the wavenumber range 400 cm^{-1} to 4000 cm^{-1} at room temperature. The peaks below 500 cm^{-1} was assigned to the stretching vibration of Zn–O. A sharp absorption band at 1623 cm^{-1} in the higher energy region was ascribed to O–H bending vibration. The ZnO surface contains hydroxyl groups and water molecules either chemisorbed or physiosorbed as confirmed by the broad absorption band at around 3427 cm^{-1} -3440 cm^{-1} [1,2]. Here we have measured the FTIR spectra of different samples by using- Shimadzu IR Prestige, (Japan) in the wave number range of: 500 -5000 cm-1.

8.1.1: For the sample of 0.75 M concentration of NaOH.

Here as the graphs listed below, Zn-O bond happens to be formed between the wavenumber of 443.62 cm^{-1} to 447.48 cm^{-1}, the bond of hydroxyl bond found at the wavenumber of 3431.36 cm^{-1}, then the bond of N-H formed at the wavenumber 1546.91 cm^{-1} and the vacancy or deficiency of O_2 happens at the wavenumber 509.20 cm^{-1}.

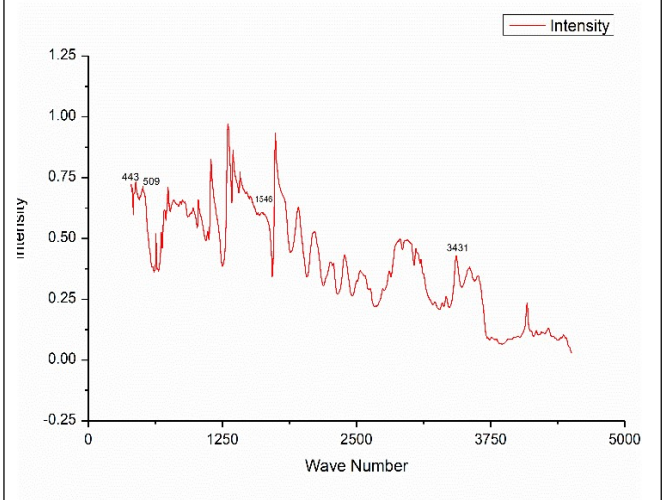

Figure 8.39: Intensity vs. wave number curve of 0.75 M concentration of NaOH applied.

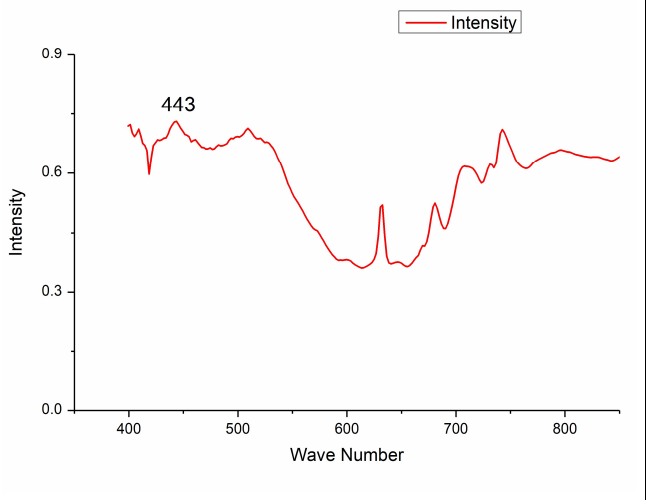

Figure 8.40: Intensity vs. wave number curve of ZnO formed using 0.75 M of NaOH.

8.1.2: For the sample of 1.00 M concentration of NaOH.

Here as the graphs listed below, Zn-O bond happens to be formed between the wavenumber of 447.48 cm^{-1}, the bond of hydroxyl bond found at the wavenumber of 3427.50 cm^{-1}, then the bond of N-H formed at the wavenumber 1556.55 cm^{-1} and the vacancy or deficiency of O_2 happens at the wavenumber 507.278 cm^{-1}.

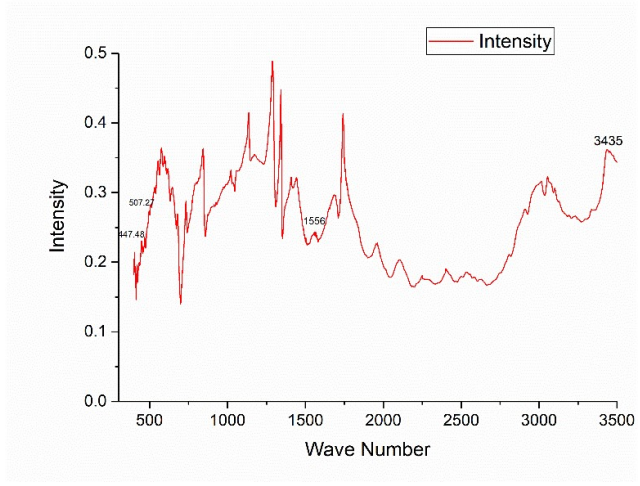

Figure 8.41: Intensity vs. wave number curve of 1.00 M concentration of NaOH applied.

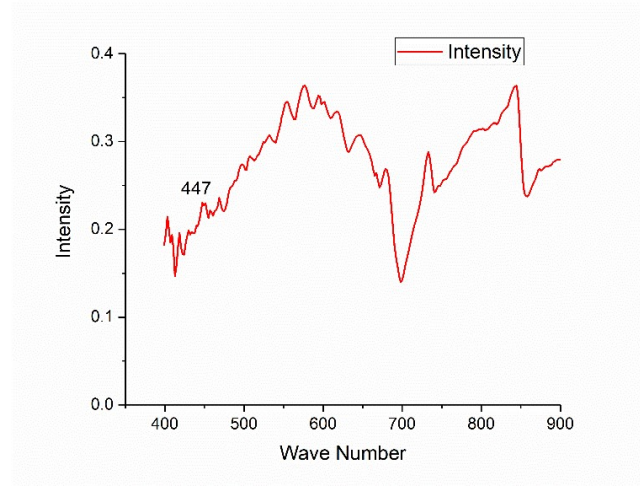

Figure 8.42: Intensity vs. wave number curve of ZnO formed using 1.00 M of NaOH.

8.1.3: For the sample of 1.25 M concentration of NaOH.

Here as the graphs listed below, Zn-O bond happens to be formed between the wavenumber of 447.48 cm^{-1}, the bond of hydroxyl bond found at the wavenumber of 3429 cm^{-1}, then the bond of N-H formed at the wavenumber 1537.26 cm^{-1} and the vacancy or deficiency of O_2 happens at the wavenumber 505 cm^{-1}.

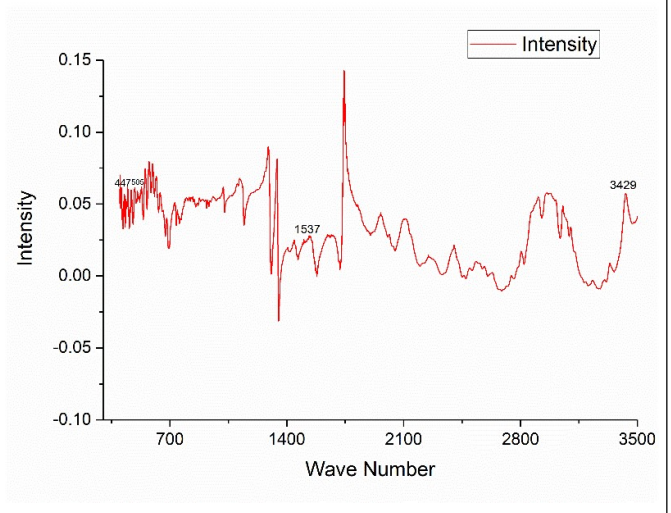

Figure 8.43: Intensity vs. wave number curve of 1.25 M concentration of NaOH applied.

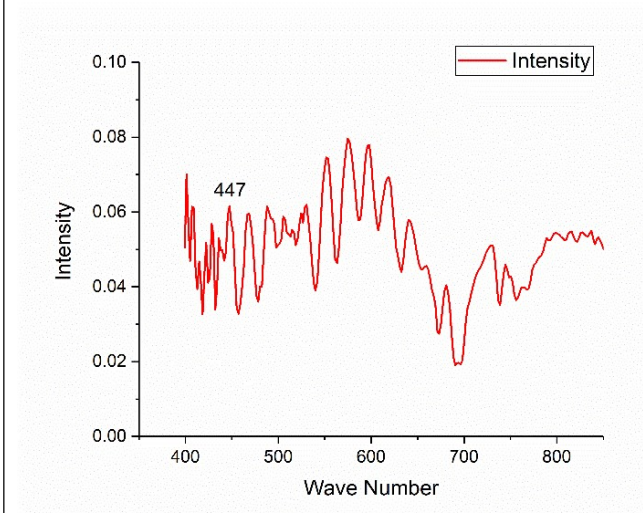

Figure 8.44: Intensity vs. wave number curve of ZnO formed using 1.25 M of NaOH.

From graphs it can be observed that as we more from lower concentration to higher concentration, the sharpness of the peak is much more intense. The bond of Zn-O can be observed better for the concentration of 1.25M than 1.00M and 0.75M and the is for 0.75M.

8.2 DIFFUSE REFLECTANCE SPECTROPHOTOMETER (DRS)

The optical characterization of the synthesized material was done using UV-Vis diffuse reflectance spectroscopy (DRS). DRS is a good technique for examining the light harvesting ability of synthesized semiconductor photocatalysts [3].

A strong absorption at 372 nm in the UV region corresponding to ZnO may be due to band-to-band transitions. A higher defect makes the electronic transitions from the filled valence band to the energy level of the defect more probable than the transitions to the conduction band. [4-7]. The diffuse reflectance spectra (DRS) for all the samples were recorded over a range of 200−800 nm.

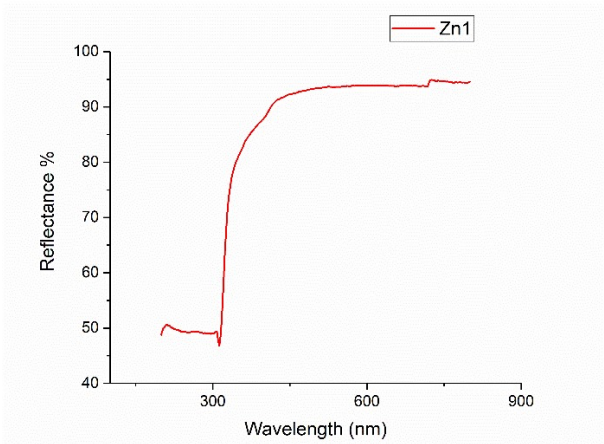

Figure 8.45: Reflectance percentage with wave length curve of ZnO with 0.75 M NaOH.

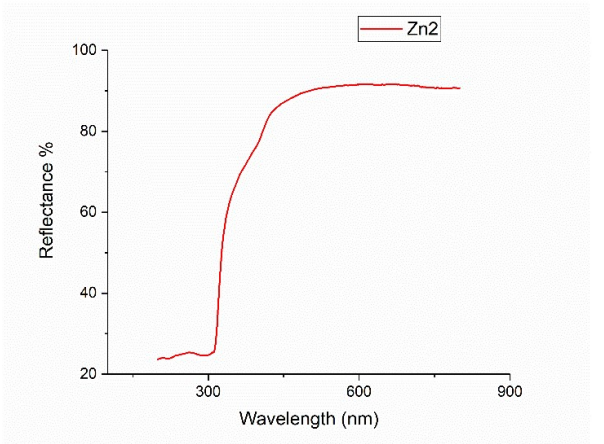

Figure 8.46: Reflectance percentage with wavelength curve of ZnO with 1.00 M NaOH.

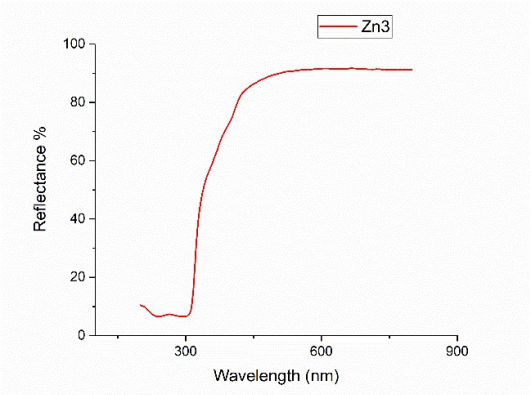

Figure 8.47: Reflectance percentage with wave length curve of ZnO with 1.25 M NaOH.

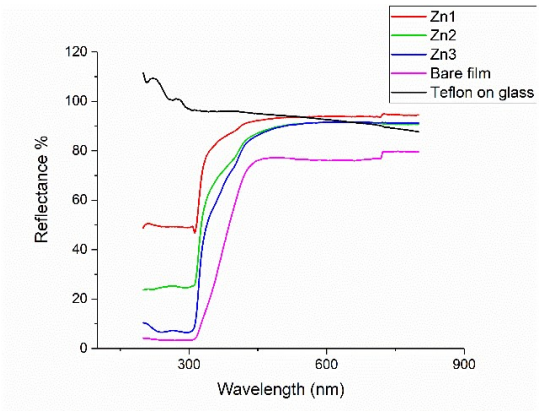

Figure 8.48: Comparison graph for all the samples with Teflon coating and bare substrate film.

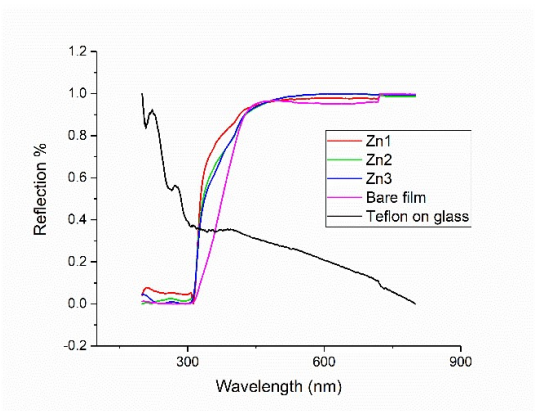

Figure 8.49: Normalized comparison graph for the samples with Teflon coating and bare substrate film.

8.3 PHOTOLUMINESCENCE (PL)

The process of photoluminescence (PL) occurs when light energy or photons excite any matter, resulting in the emission of a photon. This method of probing materials is non-contact and non-disturbing. The process is summarised as follows: light is directed onto a sample, where it is absorbed and a process known as photo-excitation takes place. The electron jumps to a higher energy state as a result of photo-excitation, and then relaxes to its lower energy state, releasing energy as photons.

Photoluminescence is the name for the light that is emitted as a result of this process (PL). Nanomaterials, semiconductors, and photovoltaics/solar cells all benefit from these. Band gap determination, impurity levels and defect detection, recombination mechanism, material quality, and molecular structure and crystallinity are all properties that can be determined using PL.

In this section, first, an excitation energy is provided to the samples and the resultant emission spectrum is observed. In both sample S1, S2 and S3, the excitation energy is provided with wavelengths 360 nm, and the resultant emission wavelength starts at 370 nm and ends at 800 nm. This emission spectrum is tallied with the excitation spectrum of the samples when the same amount of emission spectrum is provided to receive the former excitation energy.

In order to verify the above emission spectrum, an emission spectrum of 390 nm is provided in response to which an excitation wavelength of 360nm is received, which is same as that of the previous result of sample S1 This process verifies the stability of the band gap.

Similarly for sample S2, an emission spectrum of 391 nm is provided in response to which an excitation wavelength of 360nm is received, which is same as that of the previous result.

Similarly for sample S3, an emission spectrum of 390 nm is provided in response to which an excitation wavelength of 360nm is received, which is same as that of the previous result.

In the last, the calculation of intensity verses energy has been plotted that represents the band gap of zinc oxide for different concentrations of sodium hydroxide. From the plot it can be observed that the bandgap of zinc oxide for different concentrations is 3.27 eV, but due to variations in concentration the sample with higher concentration of NaOH produces sharp peak spectra than the other concentrations and as we move to lesser concentration the sharpness of the peak decreases.

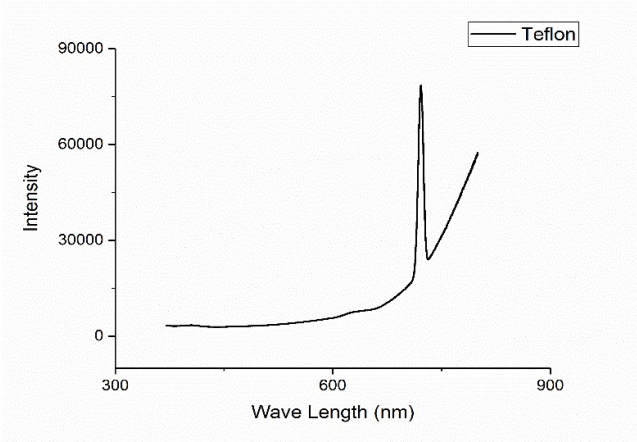

Figure 8.50: Intensity vs. wave length curve of Teflon

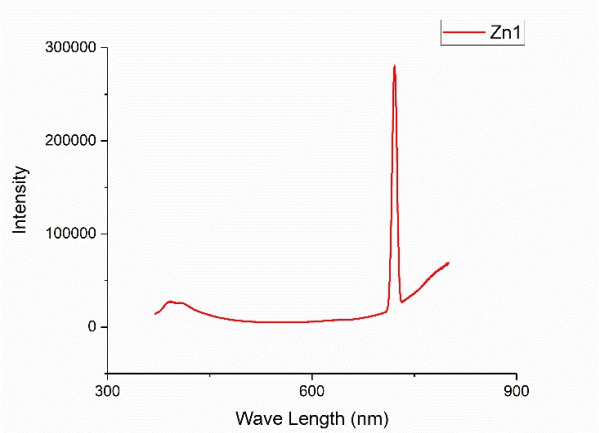

Figure 8.51: Intensity vs. wave length curve of ZnO with concentration of 0.75 M of NaOH

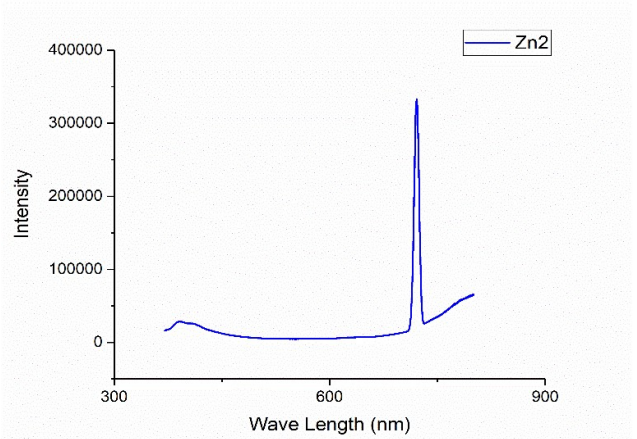

Figure 8.52: Intensity vs. wave length curve of ZnO with concentration of 1.00 M of NaOH.

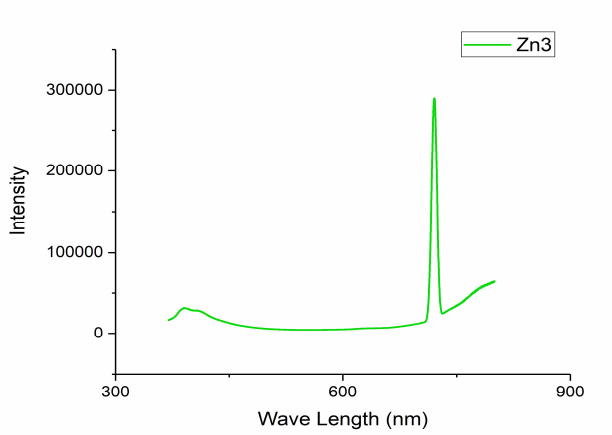

Figure 8.53: Intensity vs. wave length curve of ZnO with concentration of 1.25 M of NaOH.

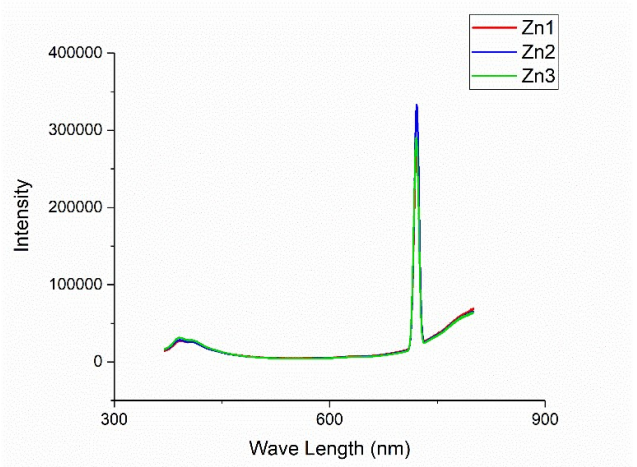

Figure 8.54: Comparison curves of intensity vs. wave length of ZnO with concentrations of 0.75 M, 1.00 M and 1.25 M of NaOH.

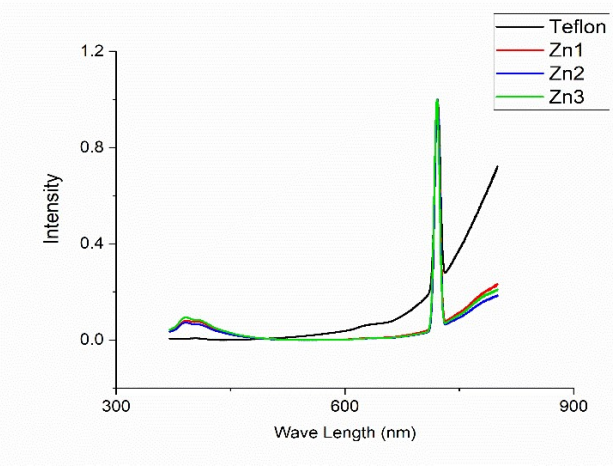

Figure 8.55: Normalized Comparison curves of intensity vs. wave length of ZnO with concentrations of 0.75 M, 1.00 M and 1.25 M of NaOH.

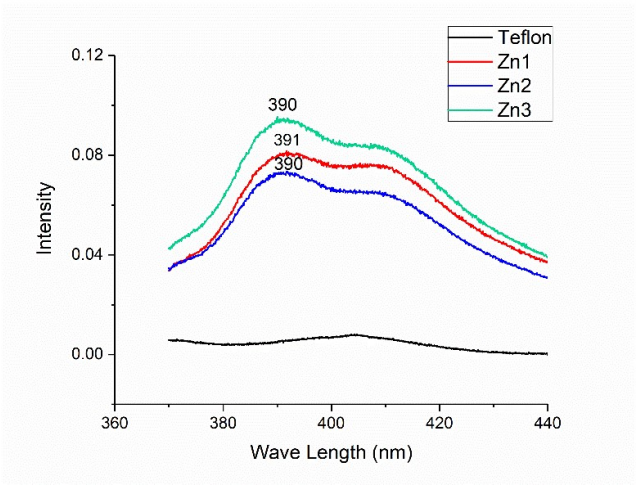

Figure 8.56: Emission peak of ZnO for all the concentrations of 0.75 M, 1.00 M and 1.25 M of NaOH.

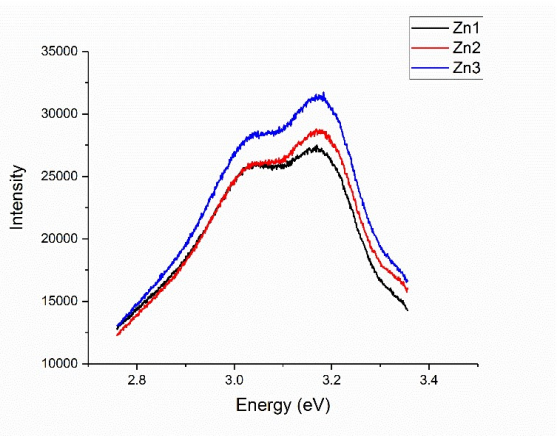

Figure 8.57: Comparison curves of intensity vs. energy of ZnO with concentrations of 0.75 M, 1.00 M and 1.25 M of NaOH.

MORPHOLOGICAL CHARACTERIZATION

8.4 FIELD EMISSION SCANNING ELECTRON MICROSCOPE (FESEM)

The surface morphology and structure of the pure ZnO nanostructures has been by the field emission scanning electron microscope (FESEM) images as displayed in Figure given below:

The images depicted here shows the roughly spherical nanoparticles structure formed from the synthesis process at a resolution of 5 micro-meter.

Moreover, we also found out that as we proceed from lower concentration to higher concentration of NaOH the particle formation is much more observable than the lower concentration of the sample content.

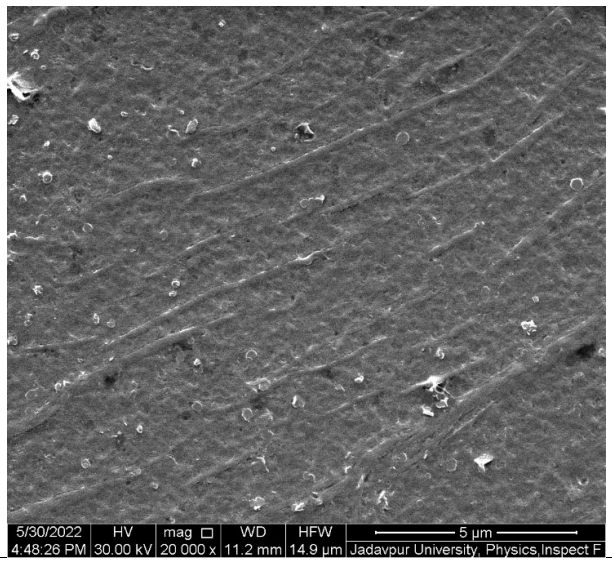

Figure 8.58: FESEM image of ZnO with 0.75 M concentration of NaOH

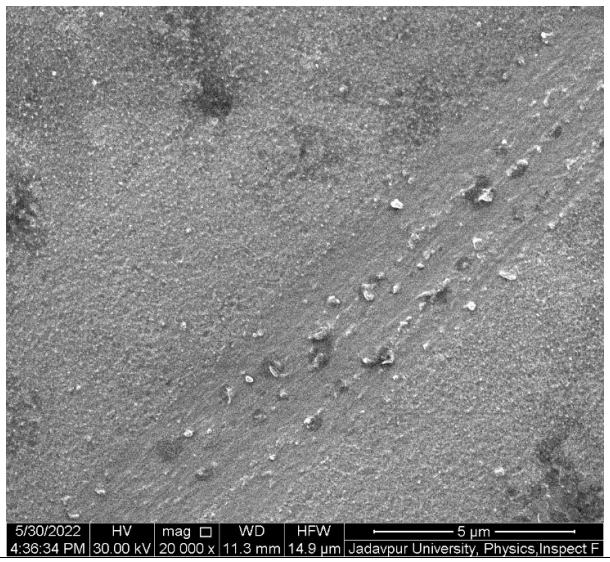

Figure 8.59: FESEM image of ZnO with 1.00 M concentration of NaOH

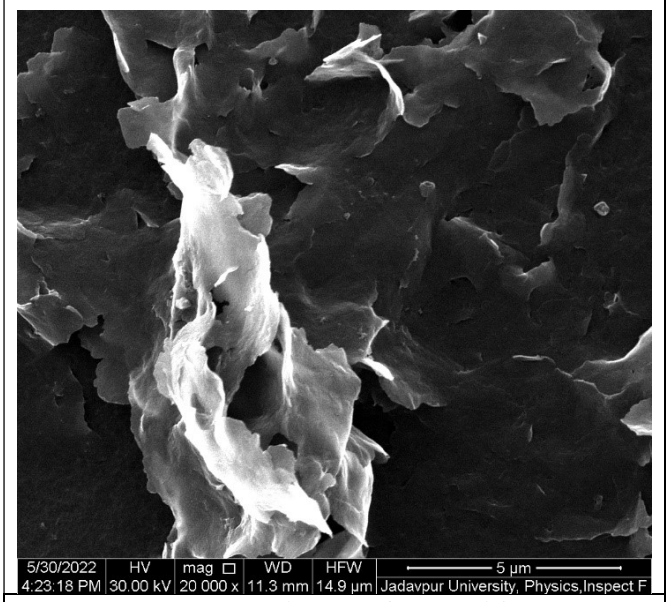

Figure 8.60: FESEM image of ZnO with 1.25 M concentration of NaOH

ELECTRICAL CHARACTERIZATION

8.5 I-V CHARACTERIZATION

At room temperature (27 °C), the (I–V) characteristics were measured for applied voltages ranging from 12 V to +12 V in both dark and light conditions. A UV lamp with a wavelength of 365 nm is used to obtain the photo characteristics. The above findings can be used to explain the UV light detection mechanism. Due to band-to-band excitation, the photo-generated carriers were formed as electrons in the conduction band and holes in the valence band when high-energy photons ($h\upsilon > E_g$) of UV light (365 nm) exposed on the sample. [8, 9].

The holes (h^+) produced then combine with the negatively charged adsorbed oxygen species O_2^- to release oxygen molecules from the surface. As a result, the free carrier concentration rises, resulting in an increase in photocurrent during photo illumination. Furthermore, when UV illumination is turned off, the carrier concentration is reduced due to electron–hole recombination and re-adsorption of atmospheric oxygen molecules on the film surface, resulting in photocurrent decay [10].

Electron–hole pairs are formed when incident photons are absorbed inside a ZnO thin film. Desorption and adsorption of oxygen at the ZnO surface control photogeneration. The photo-response in ZnO thin films is thought to be governed by the following trapping mechanism. Under dark conditions, oxygen is adsorbed by capturing a free electron from the surface of n-type ZnO, forming a depletion layer near the film's surface, lowering its conductivity. The following is a description of the surface-related process [11, 12, 14]:

$$O_2\,(g) + e^- = O_2^-\,(ad)$$

Under UV illumination the electron–hole pairs are photogenerated,

$$h\upsilon \Rightarrow h^+ + e^-$$

Where h^+ and e^- represent electron and hole respectively. As a result, photogenerated holes will be drifted in the direction of the field extending depletion layer by the electric field. These

carriers move to the surface and neutralise the adsorbed oxygen, resulting in an increase in surface conductivity.

$O_2^-(ad) + h^+ = O_2(g)$

In ZnO thin films deposited on PET substrates, this hole-trapping mechanism via oxygen adsorption and desorption was found to be the dominant process. The high density of trap states found at the surface of ZnO thin films enhances the photo-response of ZnO [11, 12, 13, 14].

According to the simple model of photo-generation and collection, the proportionate linear correlations between the collected carriers and external electrical field produce the linear I-V characteristics [15].

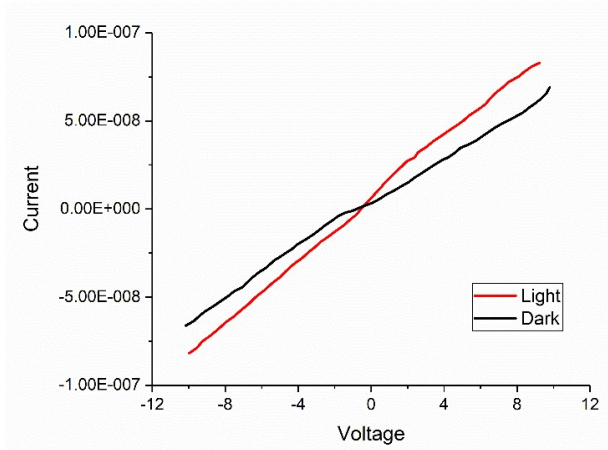

Figure 8.61: Comparison graph of current vs. voltage of ZnO with concentration of 0.75 M NaOH in Light and Dark conditions.

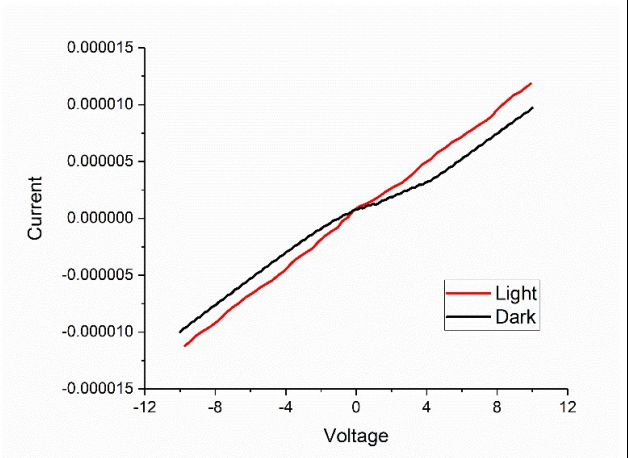

Figure 8.62: Comparison graph of current vs. voltage of ZnO with concentration of 1.00 M NaOH in Light and Dark conditions.

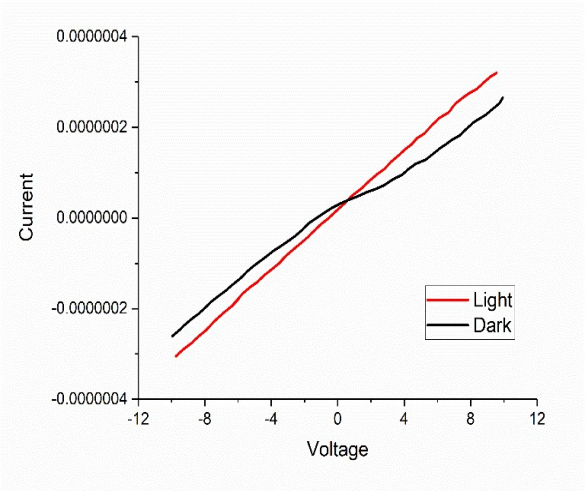

Figure 8.63: Comparison graph of current vs. voltage of ZnO with concentration of 1.25 M NaOH in Light and Dark conditions.

References

1. J. Rao, A. Yu, C. Shao and X. Zhou, *ACS Appl. Mater. Interfaces*, 2012, **4**, 5346–5352.
2. L. Loh, J. Briscoe and S. Dunn, ACS Appl. Mater. Interfaces, 2015, 7, 152–157.
3. S. K. Chaturvedi, E. Ahmad, J. M. Khan, P. Alam, M. Ishtikhar and R. H. Khan, Mol. Biosyst., 2015, 11, 307– 316.
4. D. Barpuzary and M. Qureshi, ACS Appl. Mater. Interfaces, 2013, 5, 11673–11682.
5. H. Qin, W. Li, Y. Xia and T. He, ACS Appl. Mater. Interfaces, 2011, 3, 3152–3156.
6. N. Udawatte, M. Lee, J. Kim and D. Lee, ACS Appl. Mater. Interfaces, 2011, 3, 4531–4538
7. S. D. Senol, J. Mater. Sci.: Mater. Electron., 2016, 27(8), 7767– 7775.
8. M.H. Mamat, Z. Khusaimi, M.Z. Musa, M.F. Malek, M. Rusop, Fabrication of ultraviolet photoconductive sensor using a novel aluminium-doped zinc oxide nanorod–nanoflake network thin film prepared via ultrasonic-assisted sol–gel and immersion methods, Sensors and Actuators A: Physical 171 (2011) 241–247.
9. J.M. Kim, S.J. Lim, T. Nam, D. Kim, H. Kim, The effects of ultraviolet exposure on the device characteristics of atomic layer deposited-ZnO: N thin film transistors, Journal of the Electrochemical Society158 (2011) 150–154.
10. D. Yuvaraj, M. Sathyanarayanan, K.N. Rao, Deposition of ZnO nanostructured film at room temperature on glass substrates by activated reactive evaporation, Applied Nanoscience 4 (2014) 801-808.
11. P.Sharma, K.Sreenivas, and K.V.Rao, J. Appl. Phys. 93, 3963 (2003
12. Y.Liu, C.R.Gorla, S.Liang, N.Emanetoglu, Y.Lu, H.Shen, and M.Wraback, J. Electronic Materials 29 (2000).
13. C.Soci, A.Zhang, B.Xiang, S.A.Dayeh, D.P.R.Aplin, J.Park, X.Y.Bao, Y.H.Lo, and D.Wang, Nano Lett. 7, 1003 (2007
14. D.H.Zhangt, J. Phys. D 28, 1273 (1995)
15. S. Salvatori, E. Pace, M.C. Rossi, F. Galluzzi, Photoelectrical characteristics of diamond UV detectors: dependence on device design and film quality, Diamond and Related Materials 6 (1997) 361–366.

CHAPTER :9

CONCLUSION AND FUTURE SCOPE

9.1 CONCLUSION

Zinc oxide is a multifunctional material with a wide range of UV absorption, biocompatibility, high photostability and biodegradability among the other properties. ZnO is also available in a variety of particle structures, which influence its use in new materials and potential applications in a wide range of fields. As a result, the development of a method for synthesising crystalline zinc oxide that can be used on an industrial scale has generated the interests of scientists' and industry.

The use of reactants was statistically presented. From the results depicted through characterization investigation it may be concluded that with the change of precursor concentrations we get optical data, morphological data as well as electrical data variation. Overall, the hydrothermal synthesis of ZnO nanoparticles has a lot of potential because it allows for a wide range of product morphologies that improve thin films on substrates. Hydrothermal growth has made it simple to synthesise various desirable morphologies of nanomaterials quickly and with high purity. Because the reaction mechanism can be controlled, this technique is used to achieve desired morphologies.

Other factors, such as the type of alkaline source, temperature, and pH concentration, affect the morphological structure in addition to the heating mechanism. Not only that the variations in NaOH concentration resulted in the development of new comparable properties that are completely new in these fields. In addition, the discovery and explanation of some of ZnO's distinguishing properties allowed it to be described as a potential photodetection material. The thesis primarily focuses on the analysis of ZnO-based UV photodetectors in order to demonstrate that they are a viable contender in the photodetector race. Both UV and visible light can be detected by the ZnO photodetector. Simple solution phase synthesis of high quality ZnO thin films, as well as rational control over optical and electrical properties, provide significant benefits in large-scale and low-cost ZnO thin film production for electronic, optoelectronic, sensing, and renewable energy applications. It is expected that interest in zinc oxide will continue to grow, resulting in the development of new applications for the material.

9.2. FUTURE SCOPES

- In future attempts, this method could lead to the development of a synthesis procedure to obtain nanostructures with different time and temperature variation.
- The present work focussed on thin film production of ZnO. In near future, it can be made into powder form and accordingly different characterization can be done comparing with the present data.
- This synthesis method can be used for the formation of nanostructures of other metal oxide such as Fe_2O_3, NiO, Ce_2O_3 etc and their properties can be controlled by changing the synthesis parameters.
- Further, the luminescence properties suggest that the visible emissions in ZnO nanostructures expand their use in visible region for the environmental and optoelectronics application.
- Since ZnO thin film and its nanostructures have great application in lithium-ion batteries, sensors and in water purification, the as prepared pure ZnO nanostructures can be further studied for these applications. Also, due to their more surface area and visible emissions they can be used for Solar cell, LED, LASER applications etc.